

Copyright is owned by the Author of the thesis. Permission is given for a copy to be downloaded by an individual for the purpose of research and private study only. The thesis may not be reproduced elsewhere without the permission of the Author.

RISK ANALYSIS OF A FLATFISH STOCK COMPLEX

K. McLeod

2010

RISK ANALYSIS OF A FLATFISH STOCK COMPLEX

A thesis presented in partial fulfilment of the
requirements for the degree
of
Master of Science
in
Mathematics
at Massey University

Kristin McLeod

2010

ABSTRACT

The New Zealand Ministry of Fisheries relies on fishery assessments to determine suitable catch quotas for exploited fisheries. Currently, 628 fish stocks are managed in New Zealand using the Quote Management System, which includes the 8 commercial flatfish species caught within the Exclusive Economic Zone. These eight species of flatfish, which includes four species of flounder, two species of sole, brill and turbot, are currently managed using a combined catch quota. Since these eight species are managed using a common catch quota, there is concern that some of the individual species may be under or over-fished.

This thesis describes work involving the flatfish species caught in the FLA3 management area, around the south island of New Zealand. The FLA3 management area contains three key species: New Zealand sole, lemon sole, and sand flounder. Due to the nature and limitations of the data available, simple biomass dynamic models were applied to these species. The maximum likelihood and Bayesian goodness of fit techniques were used to estimate the model parameters. Three models were used: the Fox model, the Schaefer model and the Pella-Tomlinson model with $m = 3$. As a mathematical/statistical exercise, these models were used to conduct a risk analysis to analyse the advantages and disadvantages of six management options for setting a TACC. However, because of issues over the way that the parameter K has been modelled (due to necessity caused by the lack of data), this should not be seen as an appropriate method for estimating the fish stock. Conclusions were drawn from the results regarding suitable future action for the assessment and management of flatfish stock in FLA3.

ACKNOWLEDGEMENTS

Firstly, I would like to thank the Ministry of Fisheries, for sponsoring this project and providing me with excellent supervision and contacts within the Ministry and NIWA.

A big thanks to Dr. Matthew Dunn, my fisheries supervisor from NIWA, for giving me the starting points to begin this project, and for taking the time to meet with me and guide me through the project. In particular, thank you for making time for me around your busy schedule, much appreciated! I have thoroughly enjoyed our meetings and finding solutions which resulted in the completion of this thesis.

I would also like to thank Dr. Tammy Smith, from Massey University, for supervising me through this project and supporting me through my chosen subject.

Thanks also to Dr. Geoff Jones, from Massey University, for guiding me through the world of statistics, and making it not only understandable but also enjoyable.

Thank you to the staff at NIWA - in particular, thank you to Alistair Dunn for aiding me with the initial statistics, and giving me a guideline of my project. Thank you also to Murray Smith for the statistical help and guiding me through computer coding in R and for providing great feedback.

Thank you all.

DEDICATION

I would like to dedicate this thesis to my family, for all their love, support, guidance, and advice. In particular, thank you to my Mum, for the constant love and support, for always believing in me, and in particular for always pushing me to strive for the best. A special thank you to my partner Remi for being kind and supportive and for providing a happy workplace. And finally, thanks to Nan, Ria and Kelv, for their continuous encouragement, love and support.

Contents

1	BACKGROUND	1
1.1	Flatfish Data	1
1.1.1	Introduction	1
1.1.2	Flatfish Biology	3
1.2	Fishery Summary	6
2	PROBLEM	9
2.1	Background	9
2.1.1	Previous Research	9
2.2	Mathematical Models	13
2.2.1	Schaefer Model	16
2.2.2	Pella-Tomlinson Model	17
2.2.3	Fox Model	17
2.2.4	Assumptions	18
2.3	Review of Previous Research	19
2.4	Concerns and Limitations	20
2.5	Project Objectives	22
3	SIMULATION MODEL	25
3.1	Introduction	25
3.2	Model Analysis	26
3.2.1	Schaefer Model	26
3.2.2	Pella-Tomlinson Model with $m = 3$	28
3.2.3	Fox Model	29
3.3	Simulation Models	30

3.3.1	Model 1	30
3.3.2	Model 2	31
4	PARAMETER ESTIMATION	33
4.1	Introduction	33
4.1.1	Model Choice	33
4.1.2	Data for Flatfish	34
4.1.3	Goodness of Fit	34
4.2	Maximum Likelihood Calculation	35
4.2.1	Introduction	35
4.2.2	Implementation	37
4.3	Maximum Likelihood for FLA 3	41
4.3.1	Maximum Likelihood using Schaefer Model	41
4.3.2	Likelihood Profile	44
4.3.3	Maximum Likelihood using Pella-Tomlinson Model with $m = 3$	48
4.3.4	Maximum Likelihood using Fox Model	48
4.3.5	Summary of Maximum Likelihood Estimates	49
4.4	Bayesian Goodness of Fit	51
4.4.1	Introduction	51
4.4.2	Biological Parameters from Fish Base	52
4.4.3	Regression Analysis	53
4.4.4	Implementation	56
4.4.5	Bayesian Method using Schaefer Model	57
4.4.6	Bayesian Method using Pella-Tomlinson Model with $m = 3$	58
4.4.7	Bayesian Method using Fox model	62
4.5	Concluding Remarks	66
5	MANAGEMENT STRATEGY OPTIONS	69
5.1	Introduction	69
5.2	Option 1	70
5.3	Option 2	70
5.4	Option 3	70
5.5	Option 4	70

5.6	Option 5	71
5.7	Option 6	72
6	RISK ASSESSMENT	73
6.1	Introduction	73
6.2	Option 1	73
6.2.1	Schaefer Model	74
6.2.2	Fox Model	74
6.3	Option 2	79
6.3.1	Schaefer Model	79
6.3.2	Fox Model	79
6.4	Option 3	84
6.4.1	Schaefer Model	84
6.4.2	Fox Model	84
6.5	Option 4	89
6.5.1	Schaefer Model	89
6.5.2	Fox Model	89
6.6	Option 5	94
6.6.1	Schaefer Model	94
6.6.2	Fox Model	94
6.7	Option 6	99
6.7.1	Schaefer Model	99
6.7.2	Fox Model	99
7	CONCLUSION	105
8	DISCUSSION	109
9	FURTHER RESEARCH	111

List of Figures

1.1	New Zealand lemon sole (image obtained from [19] with permission from NIWA).	4
1.2	New Zealand sole (image obtained from Peter McMillan with permission from NIWA).	5
1.3	Sand flounder (image obtained from [18] with permission from NIWA).	6
1.4	Map of the five key flatfish management areas (obtained from www.fish.govt.nz)	8
2.1	Catch for individual species in the FLA 3 stock area	11
2.2	Catch (solid line) and CPUE (dotted line).	14
2.3	Catch (solid line) and CPUE (dotted line).	14
2.4	Catch (solid line) and CPUE (dotted line).	15
2.5	Catch (solid line) and CPUE (dotted line).	16
2.6	Surplus production curve for different m	18
2.7	Catch and TACC for all stock areas	21
2.8	Catch and TACC for the FLA 3 stock area.	22
4.1	Catch and CPUE for Namibia Hake.	38
4.2	The observed CPUE (dots) and the line of best fit for the Namibia Hake.	39
4.3	Likelihood profile for Namibia Hake for r .	40
4.4	Likelihood profile for Namibia Hake for K .	40
4.5	The observed CPUE (dots) and the line of best fit for FLA3 - All.	42
4.6	The observed CPUE (dots) and the line of best fit for New Zealand sole (ESO).	42

4.7	The observed CPUE (dots) and the line of best fit for lemon sole (LSO).	43
4.8	The observed CPUE (dots) and the line of best fit for sand flounder (SFL).	43
4.9	Likelihood profile associated with r for New Zealand sole (ESO).	45
4.10	Likelihood profile associated with K for New Zealand sole (ESO).	45
4.11	Likelihood profile associated with r for lemon sole (LSO).	46
4.12	Likelihood profile associated with K for lemon sole (LSO).	46
4.13	Likelihood profile associated with r for sand flounder (SFL).	47
4.14	Likelihood profile associated with K for sand flounder (SFL).	47
4.15	The observed CPUE (dots) and the line of best fit for FLA3 - All.	49
4.16	The observed CPUE (dots) and the line of best fit for New Zealand sole (ESO).	50
4.17	The observed CPUE (dots) and the line of best fit for lemon sole (LSO).	50
4.18	The observed CPUE (dots) and the line of best fit for sand flounder (SFL).	51
4.19	Log-normal fit of r from the data obtained from Fish Base	54
4.20	The relationship between the parameters of interest	56
4.21	Graphs for ESO parameter estimates from WinBUGS	59
4.22	Graphs for LSO parameter estimates from WinBUGS	60
4.23	Graphs for SFL parameter estimates from WinBUGS	61
4.24	Graphs for ESO parameter estimates from WinBUGS	63
4.25	Graphs for LSO parameter estimates from WinBUGS	64
4.26	Graphs for SFL parameter estimates from WinBUGS	65
5.1	Landed Catch plotted with proposed TACC for management options 1,2 and 3 from recommendations from [7]	71
5.2	Landed Catch plotted with proposed TACC for management options 4, 5 and 6 from bayesian estimates calculated in previous chapter	72
6.1	Option 1 - Simulation Model 1 (green line: stable converging, blue: decreasing towards zero, red: oscillating)	75

6.2	Option 1 - Simulation Model 1 (green line: stable converging, blue: decreasing towards zero, red: oscillating)	76
6.3	Option 1 - Simulation Model 2 (green line: stable converging, blue: decreasing towards zero, red: oscillating)	77
6.4	Option 1 - Simulation Model 2 (green line: stable converging, blue: decreasing towards zero, red: oscillating)	78
6.5	Option 2 - Simulation Model 1 (green line: stable converging, blue: decreasing towards zero, red: oscillating)	80
6.6	Option 2 - Simulation Model 1 (green line: stable converging, blue: decreasing towards zero, red: oscillating)	81
6.7	Option 2 - Simulation Model 2 (green line: stable converging, blue: decreasing towards zero, red: oscillating)	82
6.8	Option 2 - Simulation Model 2 (green line: stable converging, blue: decreasing towards zero, red: oscillating)	83
6.9	Option 3 - Simulation Model 1 (green line: stable converging, blue: decreasing towards zero, red: oscillating)	85
6.10	Option 3 - Simulation Model 1 (green line: stable converging, blue: decreasing towards zero, red: oscillating)	86
6.11	Option 3 - Simulation Model 2 (green line: stable converging, blue: decreasing towards zero, red: oscillating)	87
6.12	Option 3 - Simulation Model 2 (green line: stable converging, blue: decreasing towards zero, red: oscillating)	88
6.13	Option 4 - Simulation Model 1 (green line: stable converging, blue: decreasing towards zero, red: oscillating)	90
6.14	Option 4 - Simulation Model 1 (green line: stable converging, blue: decreasing towards zero, red: oscillating)	91
6.15	Option 4 - Simulation Model 2 (green line: stable converging, blue: decreasing towards zero, red: oscillating)	92
6.16	Option 4 - Simulation Model 2 (green line: stable converging, blue: decreasing towards zero, red: oscillating)	93
6.17	Option 5 - Simulation Model 1 (green line: stable converging, blue: decreasing towards zero, red: oscillating)	95

6.18	Option 5 - Simulation Model 1 (green line: stable converging, blue: decreasing towards zero, red: oscillating)	96
6.19	Option 5 - Simulation Model 2 (green line: stable converging, blue: decreasing towards zero, red: oscillating)	97
6.20	Option 5 - Simulation Model 2 (green line: stable converging, blue: decreasing towards zero, red: oscillating)	98
6.21	Option 6 - Simulation Model 1 (green line: stable converging, blue: decreasing towards zero, red: oscillating)	100
6.22	Option 6 - Simulation Model 1 (green line: stable converging, blue: decreasing towards zero, red: oscillating)	101
6.23	Option 6 - Simulation Model 2 (green line: stable converging, blue: decreasing towards zero, red: oscillating)	102
6.24	Option 6 - Simulation Model 2 (green line: stable converging, blue: decreasing towards zero, red: oscillating)	103

List of Tables

3.1	Parameters for MSY	28
4.1	Catch and CPUE for FLA, ESO, LSO and SFL	35
4.2	Catch and CPUE for Namibia Hake	38
4.3	Optimal parameter values for each of the three key species using maximum likelihood method for Schaefer model	42
4.4	Optimal parameter values for each of the three key species using maximum likelihood method for Fox model	48
4.5	Estimate of r for each of the three key species	53
4.6	Estimated r data for sole and flounder from Fish Base	55
4.7	Optimal parameter values for each of the three key species using Bayesian statistical methods with the Schaefer model.	57
4.8	Optimal parameter values for each of the three key species using Bayesian statistical methods with the Fox model.	62
5.1	Management Options with recommended TACC's	72
6.1	Summary of results for option 1	74
6.2	Summary of results for option 2	79
6.3	Summary of results for option 3	84
6.4	Summary of results for option 4	89
6.5	Summary of results for option 5	94
6.6	Summary of results for option 6	99

Chapter 1

BACKGROUND

1.1 Flatfish Data

1.1.1 Introduction

The population dynamics of flatfish (FLA) is of interest in New Zealand for a number of reasons, including the fact that the average amount of yearly catch during the twenty year period between 1987 and 2007 was more than 3000 tonnes per year [3]. The commercial flatfish stock in New Zealand consists of eight individual species: black flounder, *Rhombosolea retiaria* (BFL); greenback flounder, *Rhombosolea taparina* (GFL); sand flounder, *Rhombosolea plebeia* (SFL); yellowbelly flounder, *Rhombosolea leporine* (YBF); lemon sole, *Pelotretis flavilatus* (LSO); New Zealand sole, *Peltorhamphus novaezeelandiae* (ESO); brill, *Colistium gunetheri* (BRI); and turbot, *Colistium nudipinnis* (TUR). Witch (WIT) can also be found, though the numbers are small and therefore not commercially important.

Stock assessment provides fishery managers with scientific information about the size and productivity of a fish stock, and is used to help fishery managers make decisions. Information on flatfish comes from a variety of sources. The key sources of information used for stock assessment include biological information gathered by fishery biologists, catch and fishing effort information provided by fishers in their logbooks, as well as landings data provided by licensed fishing processors.

Fishery biologists provide information regarding biological factors such as age structure, size at maturity, movements of fish, spawning, and fecundity. The New

Zealand Ministry of Fisheries commission relevant studies to be conducted in order to provide needed biological information for stock assessment. Fishery biologists can obtain data using direct observations, fishing surveys, tagging studies, as well as other methods. Biologists can estimate the age of fish by studying the scales and otoliths of captured fish. To date there have been no tagging studies or fishing surveys aimed specifically at flatfish, as these studies can be time consuming and so costly.

Commercial fishermen also provide important information relevant for fishery assessment. Commercial fishers are required to fill out forms detailing the catch and effort made each day. Effort can mean the amount of time spent trawling, or the amount of gill net used. For fishermen targeting flatfish this may include the Catch Effort Landing Returns (CELR). The forms used are the Trawl Catch Effort Processing Returns (TCEPR) or, more frequently, the Catch Landing Returns (CLR). For flatfish, fishermen can record the catch under individual species codes (BRI, BFL, ESO, GFL, LSO, SFL, TUR, and YBF) in the CELR and CLR forms, however in practice the catch is not always recorded using these codes and is generally reported using the generic flatfish code FLA [4].

All fish intended for commercial sale must be handled by licensed fish receivers, who are required to comply with fisheries regulations. Licensed fish receivers must fill in a Licensed Fish Receiver Returns (LFRR) form which records the landed catch for each month. The information provided by licensed fish receivers can be used to verify the information provided by commercial fishermen.

The data used in this study come from a combination of biological data, data from fishermen, and data from landings. Though there are 8 individual species in the flatfish stock, the key biological information used in this project were based on general flatfish data from around New Zealand, due to a lacking of information on all of the individual species. The majority of information used to conduct this study comes from work conducted by/for the Ministry of Fisheries and the National Institute of Water and Atmospheric Research (NIWA).

1.1.2 Flatfish Biology

There are more than 400 known species of flatfish found throughout the world. Eleven of these can be found in New Zealand waters. Eight of the eleven flatfish species found in New Zealand are combined to form the commercial fishing group 'flatfish'. All of the eight species included in the flatfish commercial stock are unique to New Zealand waters. These fish share some common characteristics, such as depth and benthic lifestyle, asymmetry of the body, as well as other similarities such as feeding habits, spawning, and fecundity.

With respect to flatfish biology, there is some variability in the expected life spans of the different species. However, for the commercially exploited New Zealand species, most generally survive to 3 – 4 years of age with a small number reaching 5 or 6 years. The flatfish species caught in New Zealand are fast growing, with females reaching maturity at 2 or 3 years of age, and males reaching maturity earlier [8]. The commercial size for flatfish is between 23 – 25cm, which is about the same size that females reach maturity. This indicates that females have a chance to spawn at least once before being fished, and since males mature earlier they have more chance of spawning before reaching commercially fished size [8].

The survival rate for juvenile flatfish is variable from year to year. Mortality rates for adult flatfish are relatively high because of natural mortality (e.g. predation) and fishing mortalities, which includes by-catch mortality, grading mortality and mortality of fish escaping from nets but dying because of wounds sustained while escaping.

Flatfish are shallow water fish living mostly in waters less than 50 metres deep [3]. They are all bottom dwelling fish which lay on their side resting on the sea floor. The fact that they lie on one side differentiates them from other bottom dwelling fish which lie on their abdomen, such as stingrays. They can move along the seabed on their side aided by extended anal and dorsal fins.

The defining feature that distinguishes flatfish from other fish is the asymmetry in the body of the fish. While flatfish are born resembling other typical fish with one eye on each side of the body, they undergo a process of metamorphosis after the planktonic stage whereby one eye migrates to the other side of the head so that both eyes are on the same side of the body. This allows them to make best use of both

eyes while laying on the sea floor. Whether the fish faces its left side or right side upwards is species dependent, and while they are born resembling other symmetric fish, their optical nerves are in fact asymmetric even before the fish is hatched [5].

Flatfish also develop other features to allow for the fact that they lay on their side. They have protrusible eyes which allows for better sight while laying on the sea floor. Most species also have pigments on the upward facing side which allow them to camouflage to blend in with the sea floor, while the side facing down is left colourless. The jaws and teeth on the bottom side are better developed than on the upwards facing side to make it easier to feed without leaving the sea floor [5].

Flatfish lay eggs which hatch into larvae. The fecundity of flatfish is high - ranging from 200,000 eggs per year to over a million eggs per year [?]. However, the mortality rates for flatfish can be high. Little is known about New Zealand flatfish reproductive behaviour.

This study focuses on flatfish caught in the FLA 3 fishing area, where the predominant species caught are the lemon sole, New Zealand sole and sand flounder, with small numbers of other species caught. Soles differ from flounders in that flounders generally have more symmetric, developed teeth which allow them to feed on small fish, whereas the soles are generally more asymmetric in the jaw and teeth structure and feed on small invertebrates and molluscs [6].



Figure 1.1: New Zealand lemon sole (image obtained from [19] with permission from NIWA).

Lemon sole is the most commonly caught species of flatfish in the FLA 3 fishing area. They are a right eye fish, which means that they face their right side upwards. In nature lemon sole can grow up to 25 - 50cm. They are usually a dark green-brown colour on the upwards facing side, and white on the seabed facing side. The body is oval in shape, with the anal and dorsal fins starting close to the mouth and running all the way to the tail (see Figure 1.1).



Figure 1.2: New Zealand sole (image obtained from Peter McMillan with permission from NIWA).

New Zealand sole is a right eye flatfish, and is also a dominant species in FLA 3. In nature they reach a length of between 25cm and 45cm. The upwards facing side is generally a green colour, duller than the lemon sole, with a pale underside. Like the lemon sole, they are oval in shape with both the anal and dorsal fins starting close to the mouth and running all the way to the tail (see Figure 1.2).

Sand flounder is a less common species caught in FLA 3. They are smaller than the soles, reaching between 25cm and 35cm in adulthood. The upside is a brown colour, and like the soles, the underside is colourless. These fish differ from the soles in shape - sand flounder are a diamond shape in contrast to the oval shape of the soles. Like the soles, sand flounder has anal and dorsal fins running from close to the mouth all the way to the tail (see Figure 1.3).



Figure 1.3: Sand flounder (image obtained from [18] with permission from NIWA).

1.2 Fishery Summary

Commercial fishing in New Zealand is controlled using the Quota Management System (QMS), which was implemented in 1986. Since individual fish species can live in separate geographical areas and have different biological characteristics, the fish species managed under the QMS are divided into separate fish stocks and managed under individual geographical areas (Quota Managements Areas or QMA's). The exclusive fishing area to New Zealand, called the Exclusive Economic Zone (EEZ), is divided into ten Fisheries Management Areas (FMA's), and these are used as a starting point for determining the QMA's. In some cases multiple species in the QMS are managed together, such as flatfish. The QMS was implemented to protect the fish stocks from overfishing, whilst maximizing catch rates in order to maximize revenue. Under the QMS, individuals or companies are allocated individual transferable quota (ITQ), which allows them to catch a fixed percentage of the total allowable catch (TAC). ITQ can be bought, sold, divided and transferred between entities. The TAC allows for recreational fishing and Maori customary fishing as well as commercial fishing. The allowance for commercial fishers is called the total allowable commercial catch (TACC). The amount of catch taken by fishermen is

monitored through fishing forms as well as through licensed fishing receivers. The catch weights caught by commercial fishers must be recorded using relevant forms, and catch is transferred to licensed fishing receivers who also record the catch weight.

The commercial flatfish fishery is divided into five management areas: FLA 1, FLA 2, FLA 3, FLA 7 and FLA 10. The current TACC for flatfish is 6670t, which is divided between the 5 areas. This study is focused on the FLA 3 management area, which is in the south island of New Zealand (see Figure 1.4). The FLA 3 fishing area accounts for about 50% of the total landed flatfish catch over the last 20 years [4]. The current TACC for the FLA 3 area is 2681t. The reason for focussing on this area is because the CPUE data needed to conduct an assessment are available only for FLA 1 and FLA 3. FLA 1 has only two dominant species while FLA 3 has three, and so FLA 3 was of more interest.

The commercial flatfish fishery is an inshore domestic fishery where most fishing occurring in waters less than 50m deep, with a small number taken from depths of 50 - 100m. The majority of flatfish caught in New Zealand are caught using inshore bottom trawling, with some taken from set netting, and a small amount by Danish Seine. In the FLA 3 stock area, 95% of targeted flatfish were caught by inshore bottom trawl, 3% by set nets and less than 1% by Danish seine [7].

Bottom trawling is a fishing method used to target bottom dwelling fish as well as some semi-pelagic fish. A trawl net is dragged behind a trawl vessel which catches the fish by initially stirring the sediments lying on the sea bed. The trawl net is held open by the trawl doors, which are connected to the net by steel wires called "sweeps". The trawl doors cause a mud cloud, and the fish don't like this, so they get herded towards the line of the net. The fish also avoid the vibrations and noise caused by the doors and the trawl sweeps. Since trawls are dragged along the sea floor there can be damage to the sea bed. Consequently, this type of fishing has been restricted in certain parts of the world, and is permitted only for commercial fishermen in New Zealand.

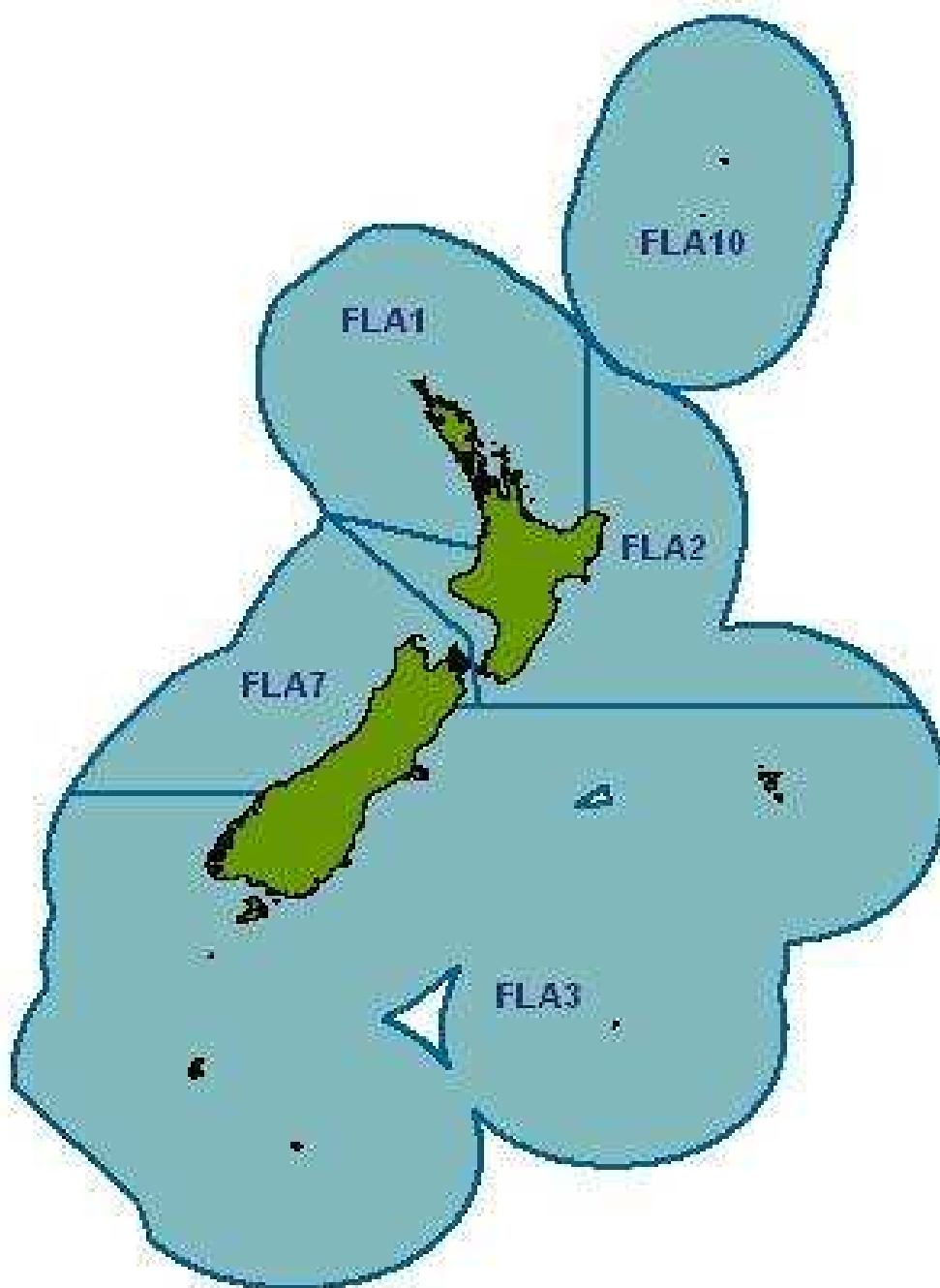


Figure 1.4: Map of the five key flatfish management areas (obtained from www.fish.govt.nz)

Chapter 2

PROBLEM

2.1 Background

2.1.1 Previous Research

Early research on flatfish was conducted by Colman in the 1970's and 1980's, [10], [11], [12]. Colman focussed his research on flounders in the Hauraki Gulf region, with studies on the biology of flounders. He studied sand flounder and yellow-belly flounder in particular, including investigations on the size at maturity [10], spawning behaviour [11], fecundity [11], and movements in the Hauraki Gulf [12].

Colman studied hundreds of males from two flounder species, and found sand flounders that were mature at as small as 12cm, and yellow-belly flounders that were mature at only 15cm length. The legal size for retaining the fish when fishing is 22.9cm and 25.4cm for the sand flounder and yellow-belly flounder respectively, so Colman's findings indicate that the male fish can probably spawn at least once before being fished. Female flatfish mature at larger sizes, and the study was focussed on the female fish. Colman was able to conclude from his study that the minimum landed sizes allow male and female sand flounder and male yellow-belly flounder to mature before being susceptible to fishing pressure, though female yellow-belly flounders are less likely to mature before being caught. Colman considers this to be a problem only if the species are heavily fished.

In his study on spawning behaviours of sand flounder and yellow-belly flounder, Colman found that these two species spawn in a similar fashion to other species

of flatfish from around the world, with sand flounder spawning during winter and spring, and yellow-belly flounder spawning during the spring months. Spawning may be related to water temperature, or salinity, though day length and light time are likely factors. The fecundity for each species was also studied, where the number of eggs produced was related to the size of the fish. The number of eggs for sand flounder ranged from 100,000 eggs to 500,000 eggs and from 250,000 to over a million eggs for yellow-belly flounder.

Colman later studied the movements of flounder in the Hauraki Gulf in 1974. Tagging studies, direct observations, acoustics, analysis of biological characteristics and fishery statistics were used to determine the movements of the fish. The study indicated that both sand flounder and yellow-belly flounder stay in shallow waters less than 5m deep during the first two summers, before moving further out to depths of 30-40m during winter. Tagging studies showed that both species remain within the stock area in which they were tagged, indicating that the populations within the management area are localized. The studies conducted by Colman have provided valuable insight into flounder biology, which has been generalized to the New Zealand flatfish group in general for subsequent studies.

In 1988, a characterisation of the flatfish fishery was conducted by Kirk [8]. The flatfish characteristics were based on the flounder studies by Colman. Kirk briefly reviewed the fishery and provided an estimate for the maximum constant yield (MCY) of flatfish, which is the maximum constant amount of catch that can be taken each year without risking a collapse in the stock. In 1985 a TAC of 4900t was recommended based on the assumption that the landings reflected the amount of available yield. This recommendation was based on the catch from the 1983 fishing year, which was the highest recorded amount to date. However, a TAC of 6050t was implemented (1150t higher than recommended) from the 1986-1987 fishing year, where this TAC was divided between the management areas. It was assumed that an annual yield of between 3000 and 5000t was sustainable under this management method. Kirk noted that the high level of the TAC can have implications for other fisheries due to incidental by-catch, whereby fishers who have ITQ for flatfish take by-catch of other species for which they have no ITQ.

The work done by Kirk was updated by Beentjes, who conducted a review of

flatfish catch data in 2003 [4]. The purpose of the report was to analyse data for flatfish from a number of sources to determine the suitability of the stock for catch per unit effort (CPUE) analyses. In this report, the individual species were described regarding main fishing areas and the percentage of flatfish catch for each of the individual species. Data from a number of sources were analysed by Beentjes to provide a better understanding of flatfish. From the sources, Beentjes concluded that the key contributors for catch in the FLA 3 fishing area are lemon sole, New Zealand sole and sand flounder. In fact, during the period 1989-2002, 40% of catch was recorded under the generic FLA stock code, 23.4% was recorded as lemon sole, 21.2% was recorded as New Zealand sole, and 7.2% as sand flounder (see Figure 2.1). The report concluded that CPUE analyses could be conducted for this stock.

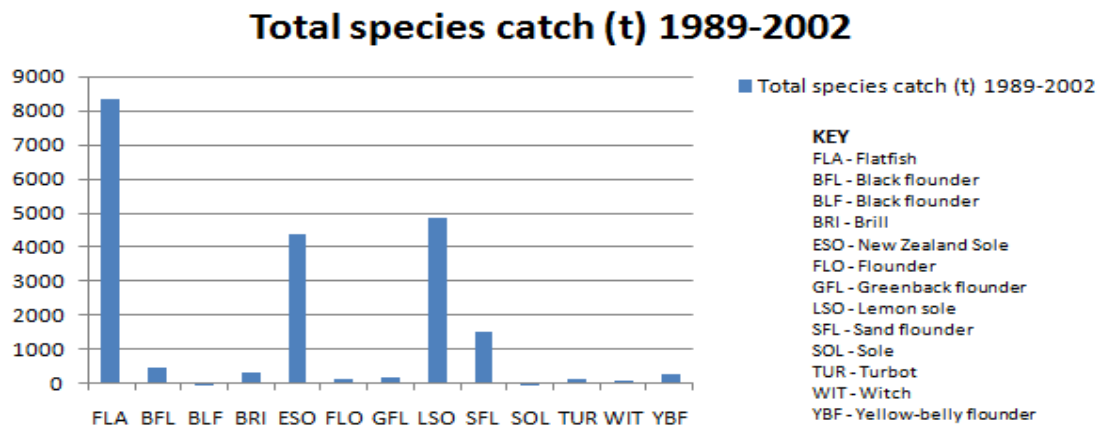


Figure 2.1: Catch for individual species in the FLA 3 stock area

In 2004, Hartill conducted a characterisation of commercial flatfish in the Kaipara Harbour, which is in the FLA 1 stock area [13]. Flatfish is the predominantly targeted stock in the Kaipara Harbour. Data from CELR forms filled out by fishermen between the 1989-1990 fishing year to the 2000-2001 fishing year in this area were analysed. Most catch for flatfish was during autumn, when effort was at its highest, however there was only a small increase in effort during this period compared with other times. There was a noted increase in the amount of effort employed by fishermen from year to year, but the total catch had declined, which may indicate the number of flatfish was declining. This is a concern for the flatfish stock, as it suggests the catches being taken were not sustainable, which indicates the need for stock assessment.

The work in the FLA 1 area was extended a year later by Coburn and Beentjes, who conducted a review of the current TACC for flatfish using CPUE analyses for the FLA 1 stock area [27]. Data from the CELR records were used as an indicator of catch, and information from fishing vessel was used as an indicator of effort. The analysis was focused on the set net fishery which accounts for 90% of the total fished catch in FLA 1. The data was extracted and then groomed to discard any data with missing information. For the CPUE analysis 88% of the original data from FLA 1 was used. Since flatfish are generally a localized population, with little migration between areas, the analysis was divided into seven subareas to account for the differences in effort for each subarea. The behaviour of the fishing vessels was also examined to determine the movements of fleets and the time spent fishing in each subarea. The standardised CPUE analyses were based on kilograms of stock per kilometre of set net as the index of abundance. The key species in FLA 1 are sand flounder and yellow-belly flounder and the results were analysed for each of these species. The analyses outlined the need for study of the individual species, since the CPUE declined, presumably due to declining numbers of sand flounder catch. From the study the authors were able to estimate CPUE index for each year analysed.

More recently, a similar CPUE analysis has been conducted by Beentjes and Manning for the FLA 3 stock area (Beentjes pers. com.; presented to the Ministry of Fisheries but currently unpublished). From the work conducted in this study, standardised values for CPUE were obtained for each of the three individual species as well as for the combined species. These values are plotted in Figures 2.2, 2.3, 2.4 and 2.5 with the catch for each year. Since effort can differ from year-to-year and between different areas, CPUE is used as a way to standardize catch data with respect to the amount of effort employed at each time.

CPUE was used as an index of abundance in this study, based on the assumption that the CPUE is proportional to abundance [20]. This assumption may be too strong and several studies have shown that CPUE can be a poor index of abundance, and can consequently result in the population being overestimated [20]. CPUE is used as an index of abundance when there are no independent abundance data available. The reliability of CPUE as a measure of abundance can depend on whether

the fish remain largely in schools or not since high schooling fish have high CPUE regardless of the size of the population. Hence, we assume that CPUE is a good measure of abundance for flatfish since they are not considered to be a largely schooling fish.

The assumed relationship between the index of abundance (in this case CPUE) and the catch amount is that as catch increases, CPUE decreases since catch decreases population size. After a time the catch should begin to decrease as the abundance of fish is low (the catch can no longer be taken). CPUE will increase when the catch becomes less than the amount of fish which are entering the fishery (recruitment) and the stock gets bigger. In some fisheries, such as those with high schooling behaviour, the fish may continue grouping as the population decreases, and fishers can continue to maintain high CPUE until the population is fished out of the fishery. The following figures show that the CPUE and catch show unexpected behaviour. For each of the figures the CPUE and catch follow similar trends. This type of behaviour indicates that the fishing has little effect on the population size or CPUE is not an index of abundance. In some cases, CPUE can be an index of something other than the population abundance, such as an index of fishing behaviour, in which case high CPUE simply reflect high levels of catch because of a fisher choice, rather than a large abundance of the population.

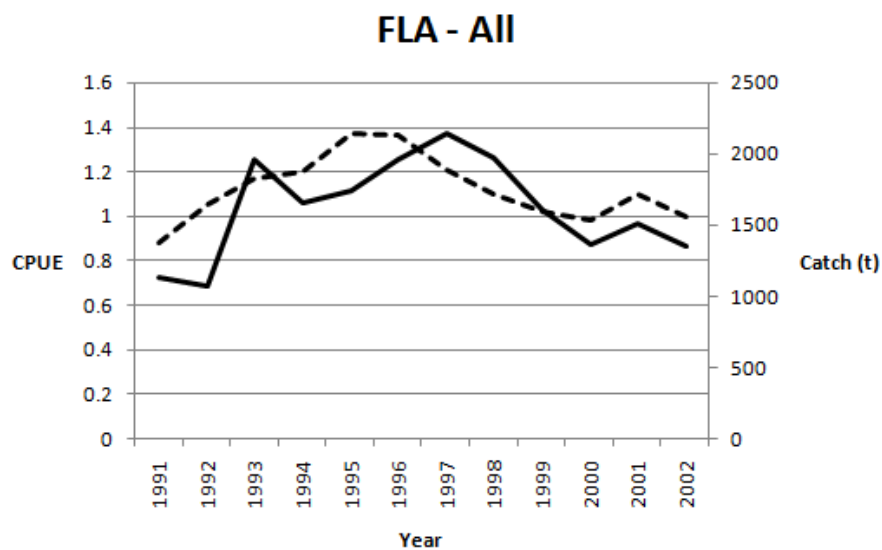


Figure 2.2: Catch (solid line) and CPUE (dotted line).

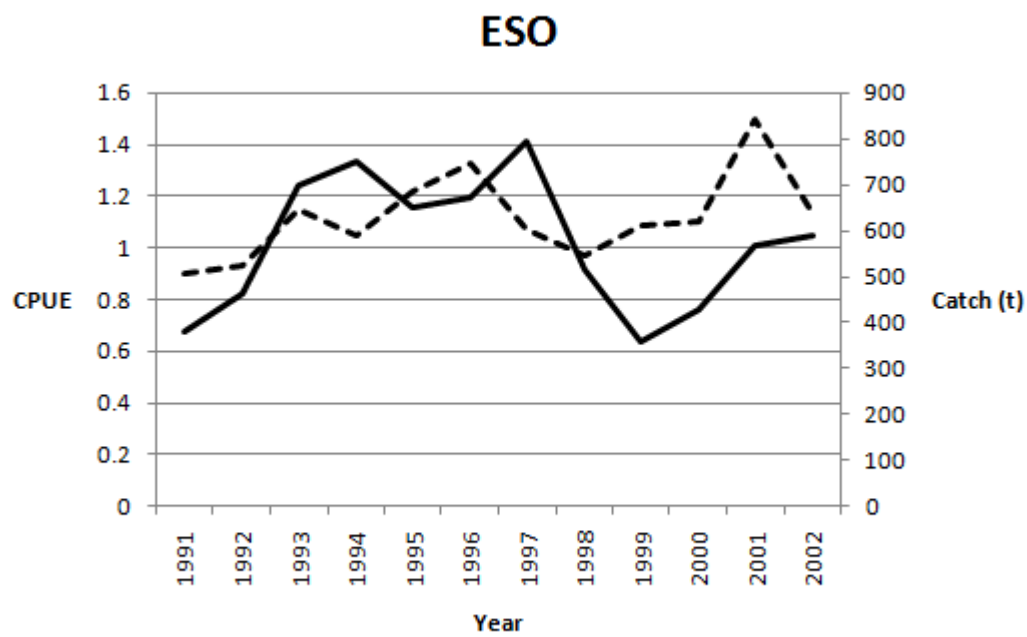


Figure 2.3: Catch (solid line) and CPUE (dotted line).

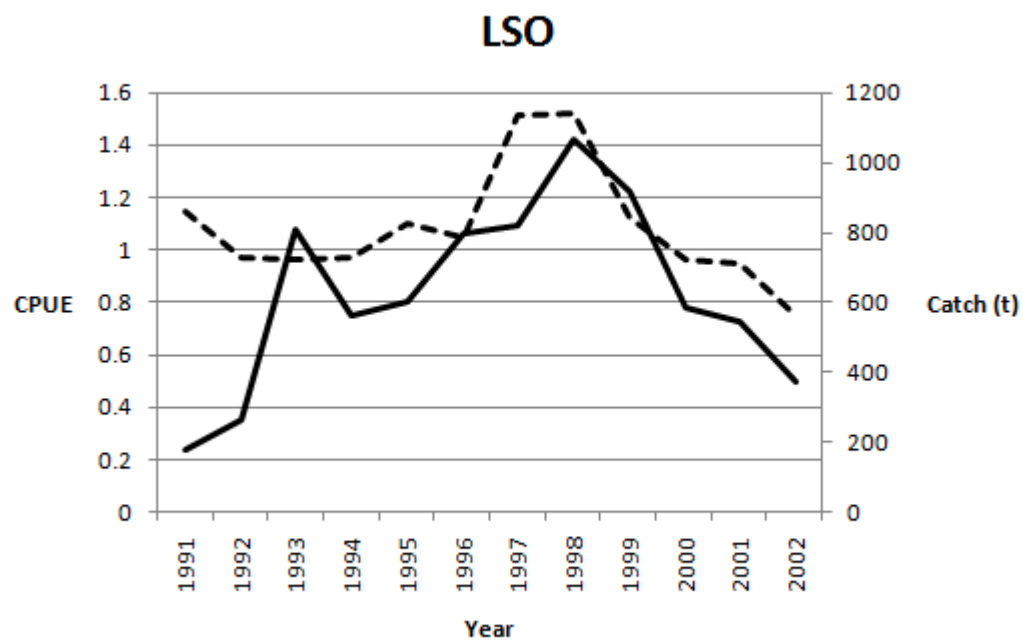


Figure 2.4: Catch (solid line) and CPUE (dotted line).

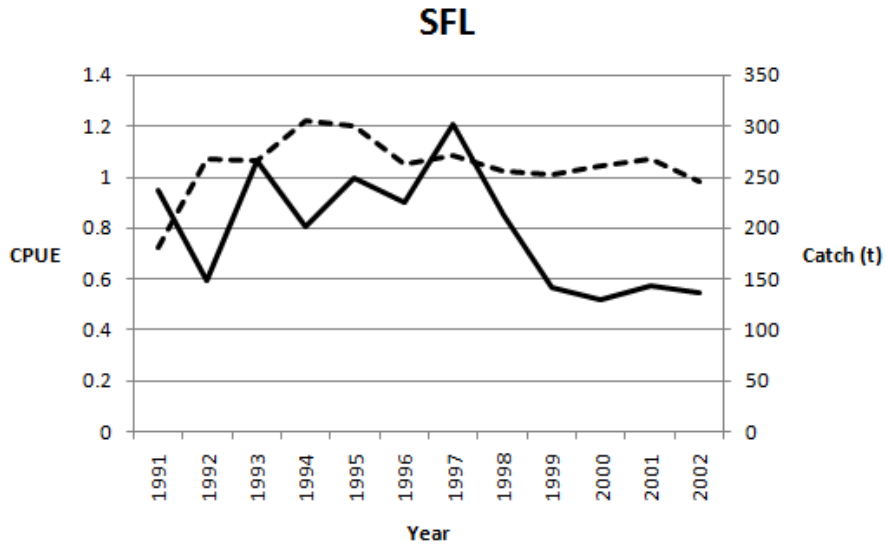


Figure 2.5: Catch (solid line) and CPUE (dotted line).

2.2 Mathematical Models

Mathematical models are often applied to fish populations to estimate the size of the population. Fisheries managers use these models to determine the best way to manage individual stocks to ensure that populations remain at long term sustainable levels.

The types of models used in this project are biomass dynamic models (also called surplus production models). These models use changes in biomass as a measure of the population. The basis for this type of model is

$$NewBiomass = OldBiomass + NewProduction - Catch. \quad (2.1)$$

Here biomass is used as the measure of a population (it is much easier to weigh fish than to count them). These models are simple due to the fact that individual differences such as age, size and sex are ignored and the effects of other factors such as recruitment and mortality do not appear explicitly in the model, rather they are combined in the surplus production function [9]. Using biomass dynamic models, the behaviour of the population can be analysed with varying catch. This allows

us to vary the catch and examine how the population reacts, and therefore we can determine the best amount of catch that will maximize the catch while ensuring long term production for the stock.

The choice of model for this project was because the data available for this stock were limited to catch and CPUE, and because of the simplicity of the model [4]. Since the stocks are considered to be fairly localized, migration is assumed to be insignificant, and is excluded from the model. There are no data for this stock regarding age distributions, therefore a complete age-structured assessment for this stock could be unsuitable. Hence, without further information for this stock, a more complex model would be misleading.

2.2.1 Schaefer Model

The Schaefer model was first developed for the Pacific Halibut fish stock by Schaefer in 1954. Written formally, the model is

$$\frac{dB}{dt} = rB \left(1 - \frac{B}{K}\right) - C, \quad (2.2)$$

where B is the biomass, r is the intrinsic growth rate, K is the population fish would tend to in absence of fishing, and C is the catch. This equation says that the total biomass of the population changes at a rate proportional to the biomass at the previous time multiplied by the growth rate of the population. The term in the bracket restricts the total biomass so that when the biomass at the previous time equals the biomass that fish would tend to in absence of fishing, then the change in biomass is just minus catch. The catch C is determined from the fishing effort E employed at each time multiplied by the efficiency of the fishing q_0 (usually called “catchability”) and the current biomass B . So the equation for catch is

$$C = q_0EB. \quad (2.3)$$

Schaefer observed that the growth of fish populations show a logistic type growth, and was able to use the above model to express the expected relationship between the size of the stock and the size of catches [9]. The advantage of this model is that the biomass can be estimated at some time t with just two sets of data for the

catch and effort employed for the previous times. The maximum production for this model occurs when the biomass is half of the biomass that fish would tend to in absence of fishing, or $K/2$ [25]. The Schaefer model assumes that CPUE decreases linearly with increasing fishing effort [24].

2.2.2 Pella-Tomlinson Model

Pella and Tomlinson extended the work by Schaefer and formulated a new biomass dynamic model in 1969 which can be represented by the following equation

$$\frac{dB}{dt} = rB - \frac{r}{K}B^m - C. \quad (2.4)$$

When $m = 2$ in this equation we have the original Schaefer model from equation 2.2. The parameter m was added by Pella and Tomlinson to account for the variability in the relationship between the size of the stock and the surplus production, where surplus production is the difference between the new and the old biomass plus the catch [1]. So, varying the parameter m alters the skew of the surplus production curve in relation to stock size (see Figure 2.6). Therefore, for $m \neq 2$ the maximum production is no longer at $K/2$. In practice, the Pella-Tomlinson model is applied to a data set with different values for m which can be determined by applying the model for a range of m and establishing which provide the best fit for the data. The maximum productivity of the Pella-Tomlinson model depends on the value of m , and can be expressed using the general formula $m^{\frac{1}{1-m}} \times K$ [25].

2.2.3 Fox Model

In 1970, Fox proposed a biomass dynamic model which uses the Gompertz curve [23]. The Fox model is similar to the Schaefer model and can be expressed as

$$B_{t+1} = B_t + rB_t \left(1 - \frac{\ln(B_t)}{\ln(K)} \right) - C_t. \quad (2.5)$$

The Fox model is the same as the Pella-Tomlinson model with $m \rightarrow 1$. For this model, as fishing effort increases CPUE decreases in a curve [24]. The maximum productivity for the Fox model occurs at around 36.8% of K [25].

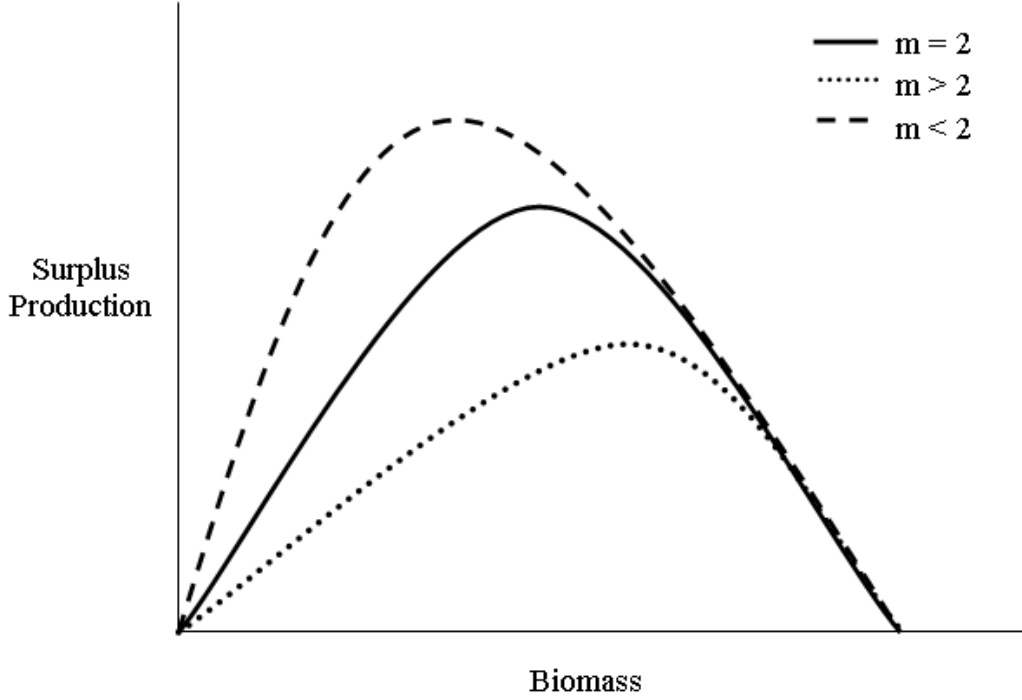


Figure 2.6: Surplus production curve for different m

2.2.4 Assumptions

A key assumption used in this particular study is that the initial biomass at time 0 equals the biomass that fish would tend to in absence of fishing. This assumption is based on the idea that the stock was un-exploited prior to 1991. However, it is known that the species were fished before 1991, though too few data are available before this time to be able to apply these models. This assumption is made to allow these models to be applied to the stock for mathematical/statistical modelling purposes, and is necessary due to the lack of data available to estimate the initial biomass independent of K . The results obtained from applying these models are meant as an academic exercise rather than for management purposes.

A number of assumptions were made to allow these models to be applied to fisheries in general. The most important assumption is that the population was at equilibrium. However in many cases the population varies naturally due to external factors such as sea surface temperature or extreme weather conditions. The mortality rate is also assumed to be relative to the amount of catch, without considering external causes of mortality like changing rates of natural mortality. The parameter K represents the biomass that fish would tend to in absence of fishing which is

the same as the carrying capacity used in the logistic model. For this project the parameter K was kept as a constant value, though the maximum population that an environment can sustain may vary from year to year based on other factors such as age structure and the populations of other species in the environment. Another important assumption for long term fisheries is that the fishing methods remain constant and so the methods are assumed to not improve with time from new technologies or improvements in the fishery. These assumptions allow the problem of applying mathematical models to fish stocks to be simplified by using a model based on the logistic growth model, which accounts for the fact that natural resources in the environment are limited.

Due to the formulation of these models, the net growth rate remains positive for all levels of the population [24]. However, in the real life context, many species require a minimum level of the population for growth (above 0). Therefore, these models can fail to capture the true dynamics of the fishery when the population is fished to low levels.

2.3 Review of Previous Research

From the background information, some conclusions can be made regarding the biological parameters of interest. Since flatfish are short-lived with high fecundity, the intrinsic growth rate r of each of the species is expected to be high, with $r > 1$. The biological parameters for fish populations can be estimated based on the behaviour of the fishery. In general, using these types of models, the population is assumed to be stable while the population is un-fished. When the population begins to be fished, the abundance is expected to decrease, and this gives information about K . If the population is not fished to zero, there will be a point where the catch rate will decrease and if catches are then reduced, the population will level off or begin to increase. When the population begins to increase, this gives some information on the rate of increase r . The strength of this estimate for r can be related to how heavily the population was fished, since heavier exploitation can give better indications for r because it gives a greater change in the population size. Following a fish population over a larger length of time can also make better inferences for the biological

parameters. Every time the fishery exhibits this decreasing-increasing behaviour, more indications for K and r can be found based on how quickly the population declines and recovers from exploitation. In the case of FLA3, the time series is short and this behaviour is weak, therefore the estimates for the biological parameters will be more uncertain than in a fishery that better exhibits this behaviour. The models also

The use of biomass dynamic models in fisheries management has been highly criticized for a number of years due to the high number of assumptions required to use these types of models. However, in the case where little data are available for a population, these methods can be useful [21].

2.4 Concerns and Limitations

There are a number of concerns for the flatfish stock. Research conducted by Hartill in 2004 on the FLA 1 area indicates that, as a unit stock, the population of flatfish may be decreasing under recent catches. Also, the fact that there are eight species managed as a unit stock could mean that some of the individual species of flatfish may be significantly under or over-fished depending on their biology (their respective r 's and K 's). The TACC for the combined management areas as well as for FLA3 has never been reached since flatfish have been managed under the Quota Management System (QMS) (see Figures 2.7 and 2.8). The high level of the TACC means that the flatfish fishery is essentially unregulated. There could also be significant habitat damage caused by fishing, and in the case of flatfish, bottom trawling can damage the sea bed and disrupt or damage other wildlife living on the sea floor.

Due to the high level of the TACC, there is concern for incidental by-catch. Since the TACC is set above reported catch amounts, fishermen can continue to fish unsuccessfully for flatfish to try to reach the allocated quota and consequently take incidental by-catch of other species.

The key limitation for this project is the lack of data available. While there are requirements for fishermen to record catch using individual species codes in the Catch-Effort section of the CELR form, about 40% of catch in FLA 3 is recorded as the generic FLA code. Therefore the proportions of each species in FLA 3 are

reasonably uncertain. There have been no biological studies applied to flatfish in the FLA 3 management area. As described earlier in this chapter, for the parameters of interest (r and K), it is likely to be difficult to find certain estimates due to the previously exhibited behaviour of the stock as well as the short time series of data available for these species. The simulations will therefore be limited since the certainty of the simulations relies on the certainty of the parameter estimates.

Due to concerns outlined by research conducted on the flatfish stock in New Zealand, further studies are required to assess the status of flatfish stock, and the long term sustainability of the stock subject to the current management strategy. As well as this, it is necessary to study the individual species managed as flatfish to determine the potential risks for the individual species. This study provides a starting point for such assessments.

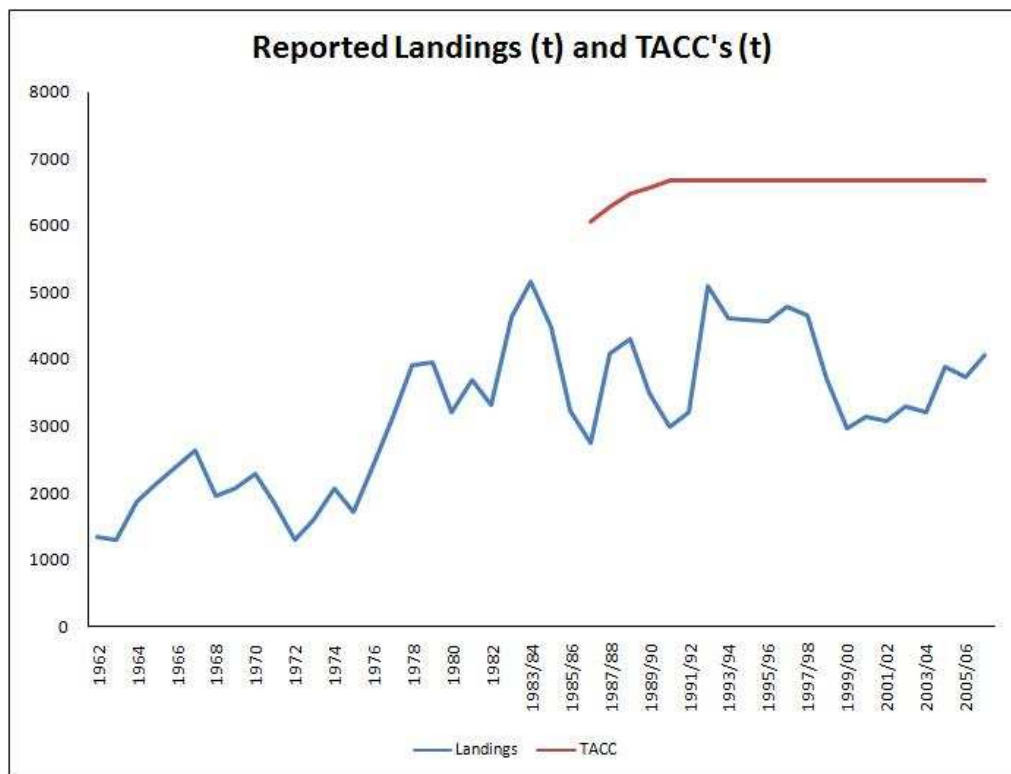


Figure 2.7: Catch and TACC for all stock areas

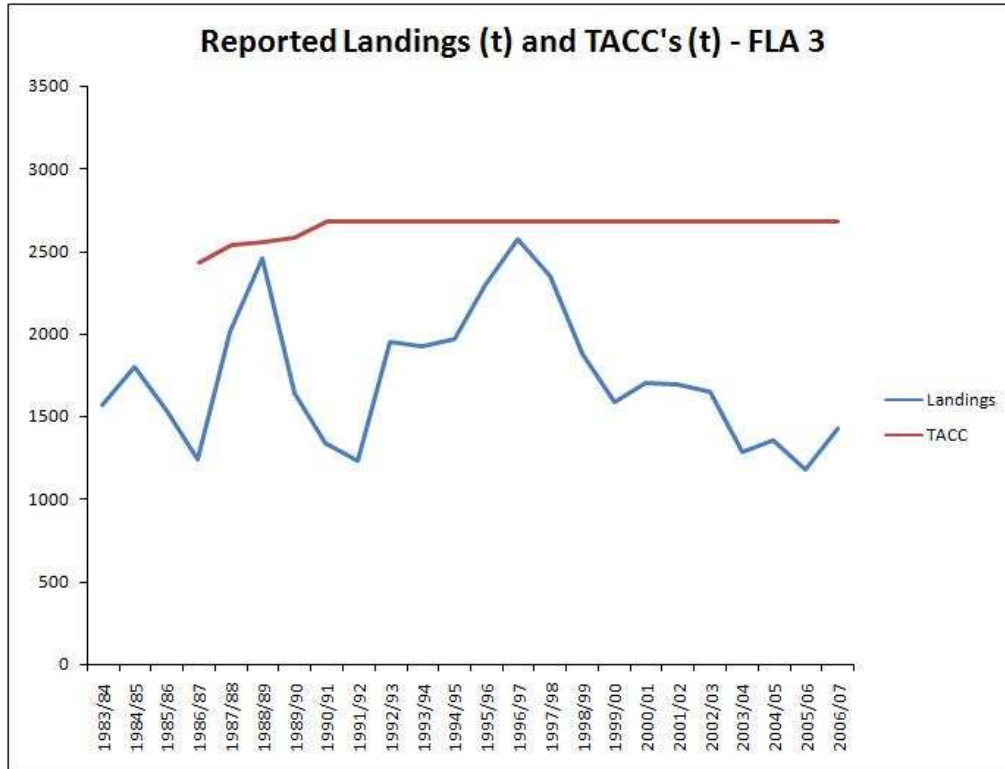


Figure 2.8: Catch and TACC for the FLA 3 stock area.

2.5 Project Objectives

The overall objective of this project is to review the current management method, and to analyse alternative management approaches (TACC's). The objectives for each chapter are outlined:

Chapter 3 This chapter provides the key information regarding the mathematical models used to determine the suitability of each of the management strategies as outlined in the previous chapter. *Objectives:*

- i. Analysis of the mathematical models used for the parameter estimations and simulation models.
- ii. Describe the simulation model applied to the flatfish stock as a single unit.
- iii. Describe the simulation model applied to each of the species individually.

Chapter 4 This chapter details the method of estimating the parameters needed to apply a model to the flatfish data. *Objectives:*

- i. Identify the optimal method to estimate the parameters required to apply the mathematical models described in Chapter 3 to the flatfish data.
- ii. Describe two goodness of fit estimations for the parameters; maximum likelihood and Bayesian methods.
- iii. Analyse the accuracy and suitability of the parameter estimates for the flatfish stock.

Chapter 5 This chapter describes an overview of some of the possible ways that the flatfish stock can be managed, including the current management strategy.

Objectives:

- i. Provide an overview of six possible management options.
- ii. Outline the advantages and disadvantages for employing each management strategy.

Chapter 6 This chapter provides a risk assessment of the different methods, where the assessment of risk is the risk of overfishing an individual species. *Objectives:*

- i. Calculate the percentage of simulations which fall below 20% and 10% of the initial biomass.
- ii. Calculate the percentage of simulations which remain above 50% and 36.8% of the initial biomass.

Chapter 7 This chapter makes concluding remarks about the project, with analyses of the results obtained from the risk analysis.

Chapter 8 A discussion of the results, the data, and the methods used in this project.

Chapter 9 Recommendations for possible further work to be conducted in the future to improve the results obtained from this study.

Chapter 3

SIMULATION MODEL

3.1 Introduction

Simulations were used to model the population of each species forward in time. This allows the dynamics of the models to be seen for each species under each of the management strategy options for the level of catch. They allow the reader to visualize the estimated outcome of each management option, based on the models and the estimated parameter values.

The model used to run the simulation is the Pella-Tomlinson model, as described in the previous chapter. The simulation was run in the Matlab student package, version 7.1.

The Pella-Tomlinson equation was used with two values for m ; $m = 2$, and $m = 3$, to test the sensitivity of the model to this parameter. The Fox model was also used (see below), which is also a form of the Pella-Tomlinson equation with $m \rightarrow 1$. Two types of simulations were used, each based on different assumptions on how the catch was taken. Parameter estimation methods were used for the three models with $m = 2$, $m = 3$ and $m \rightarrow 1$. These models are analysed in the next section to determine the fixed points (or invariant points), and the stability of these points. The stability of the fixed points is of interest as it gives an idea of the behaviour of the model around these points.

Each of the three types of model used in this study are based on the following assumptions, similar to the assumptions for the logistic equation:

- The carrying capacity K is constant.

- All members of the population are considered equal.
- Emigration and immigration are equal (effectively they are ignored).
- Factors relating to age and size structure, sex and other differences are ignored.

3.2 Model Analysis

3.2.1 Schaefer Model

For $m = 2$ we have the Schaefer model [17],

$$B_{t+1} = B_t + rB_t - \frac{r}{K}B_t^2 - C_t, \quad (3.1)$$

which was the first equation of this type applied to fish stocks. In fact the Pella-Tomlinson model was formed as an extension of the Schaefer model. To determine the fixed points of the Schaefer model, we use the fact that the catch C_t depends on the biomass B_t , using the equation

$$C_t = qB_t, \quad (3.2)$$

where $q = q_0 E_t$ is a constant value and E_t is the fishing effort at time t . Written as a function Equation 3.1 becomes

$$f(B) = B + rB - \frac{r}{K}B^2 - qB. \quad (3.3)$$

Setting $f(B) = B$ in 3.3 we get the formula for the fixed points \bar{B}

$$\bar{B} = \bar{B} + r\bar{B} \left(1 - \frac{\bar{B}}{K}\right) - q\bar{B}. \quad (3.4)$$

Rearranging and solving 3.4

$$\frac{r}{K}\bar{B}^2 + (q - r)\bar{B} = 0 \quad (3.5)$$

gives the fixed points $\bar{B} = 0$ and $\bar{B} = K \left(1 - \frac{q}{r}\right)$. Computing the derivative of $f(B)$ gives

$$f'(B) = 1 + r - \frac{2r}{K}B - q. \quad (3.6)$$

At the fixed point $\bar{B} = 0$, $f'(0) = 1 + r - q$, which is stable when

$$|1 + r - q| < 1 \quad (3.7)$$

or

$$-2 + q < r < q. \quad (3.8)$$

This means that at the fixed point $\bar{B} = 0$ the population will grow away from the fixed point for positive growth rates (provided $B \neq 0$) and when the growth rate is negative the population will move toward the fixed point. Similarly, for the fixed point at $\bar{B} = K \left(1 - \frac{q}{r}\right)$, $f'(K \left(1 - \frac{q}{r}\right)) = 1 - r + q$, and the fixed point is stable for

$$|1 - r + q| < 1 \quad (3.9)$$

which is the same as

$$q < r < 2 + q. \quad (3.10)$$

This means that the population will steadily grow (or decline) to $K \left(1 - \frac{q}{r}\right)$ and then stabilize at $K \left(1 - \frac{q}{r}\right)$ for $r < 2 + q$. When $r > 2 + q$ the behaviour of the population exhibits unstable behaviour - either periodic or chaotic depending on how large r is.

The maximum sustainable yield (MSY) of a stock; which is the maximum biomass that can be taken from a stock without significantly damaging the long term sustainability of the stock, can be derived by assuming a steady state condition of the population. From Equation 3.1, we can obtain the parameters for the MSY from the Schaefer model (see Table 3.1) [1].

Table 3.1: Parameters for MSY

MSY	$rK/4$
Stock size for MSY	$K/2$
Rate of exploitation at MSY	$r/2$
Maximum rate of exploitation	r

3.2.2 Pella-Tomlinson Model with $m = 3$

When $m = 3$ in the Pella-Tomlinson model we have

$$B_{t+1} = B_t + rB_t - \frac{r}{K}B_t^3 - C_t, \quad (3.11)$$

or written in function form

$$g(B) = B + rB - \frac{r}{K}B^3 - qB, \quad (3.12)$$

with fixed points at $\bar{B} = 0$, $\bar{B} = \frac{\sqrt{r^2K-rKq}}{r}$ and $\bar{B} = -\frac{\sqrt{r^2K-rKq}}{r}$. Using the derivative of $g(B)$

$$g'(B) = 1 + r - 3\frac{r}{K}B^2 - q, \quad (3.13)$$

we obtain $g'(0) = 1 + r - q$, $g'(\frac{\sqrt{r^2K-rKq}}{r}) = 1 - 2r + 2q$ and $g'(-\frac{\sqrt{r^2K-rKq}}{r}) = 1 - 2r + 2q$. The fixed point $\bar{B} = 0$ is stable for $|1 + r - q| < 1$, which is the same as

$$-2 + q < r < q. \quad (3.14)$$

By the same reasoning as above, this inequality is logical since the constant q is very small with $q \lll 1$. The fixed point at $\bar{B} = 0$ is unstable for positive r values and hence the population moves away from the fixed point.

The fixed point $\bar{B} = \frac{\sqrt{r^2K-rKq}}{r}$ is stable for $|1 - 2r + 2q| < 1$ or

$$q < r < q + 1. \quad (3.15)$$

Similarly the fixed point $\bar{B} = -\frac{\sqrt{r^2K-rKq}}{r}$ is stable for $q < r < q + 1$. Since $r^2K > rKq$, this fixed point is non-positive, and for this problem we are only

interested in non-negative populations. Therefore the stability of the non-zero fixed points is more restricted than in the previous model.

The MSY for this model can be calculated as

$$MSY_{Pella-Tomlinson} = rK \left(\frac{1}{m} \right)^{\left(\left(\frac{1}{m-1} \right) + 1 \right)}, \quad (3.16)$$

so for $m = 3$, the MSY is

$$MSY_{Pella-Tomlinson, m=3} = rK \left(\frac{1}{3} \right)^{\left(\left(\frac{1}{2} \right) + 1 \right)}, \quad (3.17)$$

and the biomass at the MSY is

$$B_{MSY} = m^{\left(\frac{1}{1-m} \right)} K = 3^{\left(\frac{1}{1-3} \right)} K \quad (3.18)$$

which is at 57.735% of K .

3.2.3 Fox Model

The third type of model used was the Fox model [16], which can be expressed as

$$B_{t+1} = B_t + rB_t \left(1 - \frac{\ell n(B_t)}{\ell n(K)} \right) - C_t, \quad (3.19)$$

or written in function form

$$h(B) = B + rB \left(1 - \frac{\ell n(B)}{\ell n(K)} \right) - C. \quad (3.20)$$

This has fixed points at $\bar{B} = 0$, $\bar{B} = K^{\left(1 - \frac{q}{r} \right)}$. Taking the derivative of $h(B)$ gives

$$h'(B) = 1 + r * \left(1 - \frac{\ell n(B)}{\ell n(K)} \right) - \frac{r}{\ell n(K)} - q. \quad (3.21)$$

The fixed point at $\bar{B} = 0$ is unstable due to the term in the denominator $\ell n(0)$. For the fixed point at $\bar{B} = K^{\left(1 - \frac{q}{r} \right)}$, evaluating $h'(B)$ at this point gives

$$h' \left(K^{\left(1 - \frac{q}{r} \right)} \right) = 1 + r * \left(1 - \frac{\ell n \left(K^{\left(1 - \frac{q}{r} \right)} \right)}{\ell n(K)} \right) - \frac{r}{\ell n(K)} - q. \quad (3.22)$$

The MSY for the Fox model can be calculated using the formula

$$MSY_{Fox} = \frac{rKe^{-1}}{\ln(K)}, \quad (3.23)$$

with the biomass at the MSY

$$B_{MSY} \simeq 0.368K \quad (3.24)$$

3.3 Simulation Models

3.3.1 Model 1

The first simulation model was run in Matlab 7.1 using an m-file to store the code. The code was set up to run for 50 time steps (years) to allow enough steps to see the behaviour of the model. Each of the three types of models (with $m \rightarrow 1$, $m = 2$ and $m = 3$ in the Pella-Tomlinson model) were run using the same m-file with an initial input of m in the command window (see Appendix A). For the case when $m \rightarrow 1$, $m = 1$ was inputted in the code to run the program using the Fox model.

The estimated parameters r and K from the Bayesian parameter estimates described in the following chapter were stored as a vector μ , as well as the covariance matrix (the matrix of the covariances between the vector of estimated values of r and the vector of estimated values of K) corresponding to the vector μ for each of the three species. A matrix (M) was formed for each species by applying Cholesky factorization to the covariance matrix for each μ . An initial step in the code was used to employ Monte Carlo simulation for r and K using the matrix M . The Monte Carlo simulation was run for 1000 time-steps to give 1000 estimates for r and K . This step allows for the level of uncertainty in the estimated parameters. A step was then used to calculate the biomass for each time using each of the 1000 pairs of r and K from the previous loop, with an inner step to ensure the biomass remains non-negative. The steps were run individually for each of the three key species, with fixed proportions of catch based on the average proportion of catch from 1989-2002 as reported in [4].

The fixed proportion of catch is the key difference between the first simulation

model and the second simulation model. This simulation model is based on the assumption that fishers can choose how much of each species they can take, and hence the proportions of catch remain the same regardless of the respective populations.

3.3.2 Model 2

The second simulation model was also run in Matlab 7.1 using a single m-file for each of the three models ($m \rightarrow 1, m = 2$ and $m = 3$)(see Appendix A). As with the previous simulation model, the case when $m \rightarrow 1$ was input as $m = 1$. The codes for these models were similar to the codes for the first simulation model with the initiating steps the same. The biomass for each population was calculated within the same step, again beginning with an initial step to apply Monte Carlo simulation on the parameters r and K . At the end of the step for the biomass calculations, the new proportion of each species was recorded, and this new proportion was used in the following step. This simulation model is based on the assumption that the total catch is fixed, but the proportions change depending on the ratio of biomass of each species. Therefore we are assuming that the fishers employ equal effort to catch each of the species, and what is caught depends on the abundance of the species at each time. This simulation model accounts for the fact that fishers cannot take equal amounts of a species from year to year, since low abundance levels will generally result in lower catch rates for that species.

Chapter 4

PARAMETER ESTIMATION

4.1 Introduction

A number of parameters must be estimated in order to use the mathematical models described in the previous chapters. Therefore, a large amount of work required for stock assessment of fisheries involves parameter estimation. In order to obtain parameter estimates, there are three key requirements: first a model must be formulated in which the parameters to be estimated are detailed; next real world data from observations must be obtained; finally a method for estimating the parameters based on a goodness of fit calculation calculation (where model predictions are compared against real world data).

4.1.1 Model Choice

The choice of which model to use is based on the desire to best represent or simplify the behaviour of the modelled population. However, the model that accounts for all the necessary factors may not always be possible to implement due to a lack of data. Therefore we want to formulate a model that can be implemented which best accounts for the factors related to the population such as mortality rates, growth rates, predation and so on. The choice of parameters to use to apply a model will also determine which model best suits the data. In the case of flatfish, the primary data available are catch and effort data. In the simulation model, each parameter has estimation uncertainty. Therefore, beginning with the simplest model that requires estimating the least amount of parameters reduces the total possible error

(uncertainty) and provides the best starting point for understanding the population. Since no previous models have been applied to the flatfish population, the simplest model that can account for the expected behaviour of the population is the best starting point for modelling the population.

4.1.2 Data for Flatfish

As described in the previous chapter, the model to be used in this project is the Pella-Tomlinson surplus production model. The equation used to implement this model is

$$B_{t+1} = B_t + rB_t - \frac{r}{K}B_t^m - C_t, \quad (4.1)$$

where B_t is the biomass at time t , C_t is the catch at time t , r is the intrinsic growth rate, and K is the biomass that the species would tend to in absence of fishing.

For this model, we know the catches at each time, C_t , and we have data from previous times about the amount of catch and effort (CPUE) employed by the fishing fleet in each fishing year. The catch and effort (CPUE) data were obtained from Mike Beentjes and Michael Manning (see [27] for further information on the methods used for the CPUE analysis). The data were only used for the years 1991-2002, when CPUE data are available. The parameters in this equation that we need to estimate are the growth rate r , the biomass fish would tend to in absence of fishing K , and the initial (virgin) biomass B_0 . The sensitivity of the parameter m in the Pella-Tomlinson model will be analysed in the risk assessment.

These data values were obtained from catch and effort data analysed by Mike Beentjes and Mike Manning [4]. The catch values for each of the individual species include the individual species recorded catch data, as well as a percentage of the catch recorded under the generic flatfish code, where the percentages were based on the proportion of each type of fish caught in that given year.

4.1.3 Goodness of Fit

The method for estimating the unknown parameters r and K involves using goodness of fit calculations. Two methods for calculating the goodness of fit were used in this

Table 4.1: Catch and CPUE for FLA, ESO, LSO and SFL

	FLA		ESO		LSO		SFL	
Year	Catch	CPUE	Catch	CPUE	Catch	CPUE	Catch	CPUE
1991	1136	0.88	381	0.9	177	1.15	237	0.72
1992	1069	1.05	462	0.93	264	0.97	148	1.07
1993	1964	1.17	697	1.15	808	0.96	267	1.06
1994	1659	1.2	751	1.05	563	0.97	201	1.22
1995	1738	1.37	650	1.22	605	1.1	249	1.2
1996	1962	1.36	673	1.33	795	1.05	226	1.05
1997	2148	1.21	796	1.07	824	1.51	302	1.08
1998	1979	1.1	518	0.97	1069	1.52	213	1.02
1999	1607	1.02	359	1.09	921	1.12	141	1.01
2000	1366	0.98	431	1.1	584	0.96	129	1.04
2001	1512	1.1	567	1.5	545	0.95	142	1.07
2002	1347	1	592	1.13	373	0.75	136	0.98

study - the maximum likelihood method, and the Bayesian statistical method [9].

The maximum likelihood method can be used with a normal as well as a log normal distribution. In this case it was used with the log-normal distribution, since this distribution better fits the data. This method was initially used for estimating the parameters using the negative log likelihood as the measure of best fit.

Bayesian statistics require prior distributions for the parameters. For this particular problem very little prior knowledge for the parameters of interest are known. Therefore, a combination of informative and non-informative priors are used to estimate the parameters.

4.2 Maximum Likelihood Calculation

4.2.1 Introduction

Using the previous formula for the Pella-Tomlinson equation, along with the assumption that the initial biomass equals the biomass that fish would tend to in absence of fishing (K), we have the following equations for the estimated parameters [2]:

$$B_{est,t+1} = B_{est,t} + rB_{est,t} - \frac{r}{K}B_{est,t}^2 - C_t \quad (4.2)$$

$$B_{est,0} = K. \quad (4.3)$$

Assigning I as the index of abundance, we have the equation for the estimated index of abundance:

$$I_{est,t} = qB_{est,t}, \quad (4.4)$$

where the observed index of abundance in this case is the CPUE calculated by Manning and Beentjes.

Using the log normal distribution, the negative log likelihood is given by the equation

$$\mathbf{L}_t = \log(\sigma) + \frac{1}{2}\log(2\pi) + \frac{[\log(I_{est,t}) - \log(I_t)]^2}{2\sigma^2}, \quad (4.5)$$

where σ is the standard deviation of the observation uncertainty [2]. This equation is derived from the general likelihood equation for a normal distribution of the observations:

$$\mathbf{L}\{Y|m, \sigma\} = \prod_{i=1}^n \frac{1}{\sigma\sqrt{2\pi}} \exp\left(-\frac{(Y_i - m)^2}{2\sigma^2}\right), \quad (4.6)$$

with $n = 1$ in our case. The Y_i are the observations with mean m and variance σ^2 [2]. We use the log-likelihood equation since it avoids there being a negative biomass or index of abundance, which would make no sense in this example. In the log-likelihood equation we assume there is some observation uncertainty. Assuming observation uncertainty but no process error implies that the dynamics of the fishery are deterministic. Applying this equation for the negative log likelihood means that the simulation model does not accumulate errors in the population estimates since these errors are independent of one another, and there is an equal probability of under and over estimating the population in each step. Finally, using the above equation, we can calculate the total negative log likelihood as the sum of all the negative log likelihoods. This gives the most likely estimates for the model, which are the values for r , K , q and σ that give the minimal total negative log likelihood.

4.2.2 Implementation

Using the equations for $B_{est,t+1}$, B_0 , $I_{est,t}$ and \mathbf{L}_t , the total negative log likelihood was minimized using the *R* software package. The code written to minimize the function required one step using a multi-parameter optimizer with the simulated annealing method to find an approximation for the minimum, followed by the Nelder and Mead method to give a more accurate value for the minimum (see Appendix B). The initial step using the annealing method was used to overcome the problem of local minima. Where other methods in general stop once they have found a local minimum, the annealing methods searches until it finds the global minimum. The code was designed to run starting with estimates for the parameters r , K , q and σ . Each step was limited by a maximum of 100000 iterations.

To test the minimizer, an example from Hilborn and Mangel (1997) was used to estimate the same parameters for the Namibia Hake stock using the Schaefer model. The data provided for this example is CPUE (in tons per standardized trawl hour), and catch (in thousands of tons) per year from 1965 to 1987. This example is similar to the flatfish problem in that two species of hake were managed as a single stock.

This example shows behaviour expected from exploited fisheries, where the stock begins to be overfished and consequently CPUE, and then catch decline. The Hake problem is a good example because the catch and CPUE show behaviour similar to what is assumed to occur in a fishery of this type, and indicates that in this case CPUE is related to abundance. In the 1970's, the fishery became regulated due to concerns in the decreasing CPUE. Subsequently catches were reduced and CPUE began to increase as the stock recovered (see Figure 4.1). A key concern for management is maintaining adequate levels of the CPUE, because profit may decline as CPUE declines, as more effort is required to maintain catches levels.

The optimal values of the parameters reported by Hilborn and Mangel are $r = 0.39$, $K = 2709$, $q = 0.00045$ and $\sigma = 0.12$. Using the code written in *R* gives the optimal values as $r = 0.3938579$, $K = 2708.337$, $q = 0.0004487035$ and $\sigma = 0.1230662$.

The plot of the CPUE and the line of best fit calculated from this code show that this fit is relatively good (see Figure 4.2), which indicates the model with observation uncertainty is relatively accurate at estimating the data.

Table 4.2: Catch and CPUE for Namibia Hake

Year	Catch (thousands of tons)	CPUE (tons per standardized trawl hour)
1965	94	1.78
1966	212	1.31
1967	195	0.91
1968	383	0.96
1969	320	0.88
1970	402	0.90
1971	366	0.87
1972	606	0.72
1973	378	0.57
1974	319	0.45
1975	309	0.42
1976	389	0.42
1977	277	0.49
1978	254	0.43
1979	170	0.40
1980	97	0.45
1981	91	0.55
1982	177	0.53
1983	216	0.58
1984	229	0.64
1985	211	0.66
1986	231	0.65
1987	223	0.63

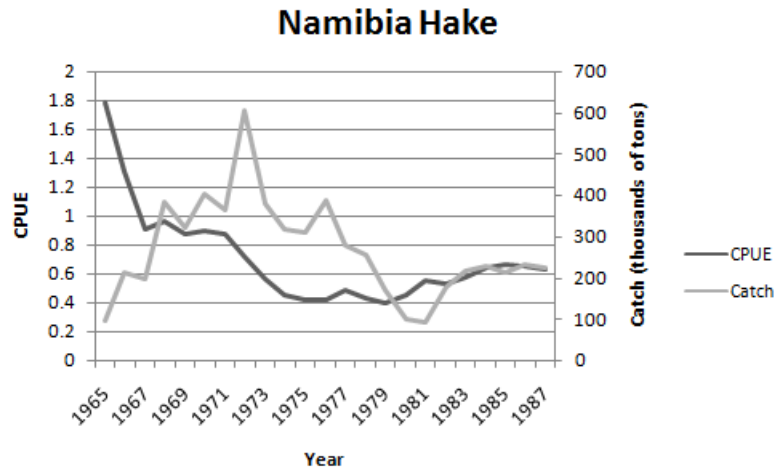


Figure 4.1: Catch and CPUE for Namibia Hake.

The same method was then used with fixed values of either r or K so that the negative log likelihood was minimized with respect to the remaining parameters

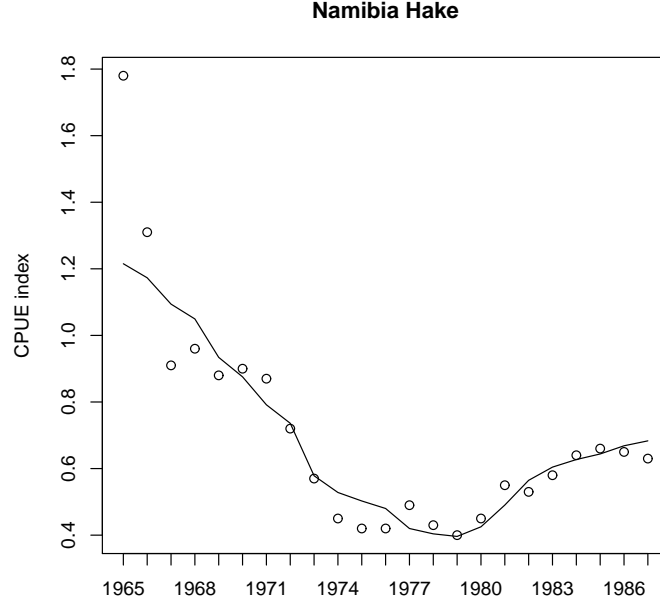


Figure 4.2: The observed CPUE (dots) and the line of best fit for the Namibia Hake.

in order to determine the level of confidence for each of r and K . By initially fixing r , the negative log likelihood was minimized with respect to the remaining three parameters K , q , and σ . The optimal values for each of the three parameters were recorded, as well as the negative log likelihood. The same procedure was then repeated for K . This method allows us to conduct a likelihood profile for r and K . The likelihood profiles are conducted for only r and K because the values of q and σ are less variable in the calculation, and in fact an analytical solution for q can be found which does not depend on σ (see [2]). Plotting the negative log likelihoods for each value of r (or K) allows us to visually represent the likelihood of each value of r (see following Figures). Ideally, the values should decrease toward the optimal value of r , and increase after the optimum. Larger differences in likelihood for different values of r indicate that the likelihood of r being at the optimum is greater. As we can see from the plotted values of the negative log likelihood for both r and K for the Namibia hake example the curves both decrease in a parabolic manner to the optimal r and K , with the differences in likelihood from other values of r and K and the optimal values being reasonably large. The 95% confidence bounds indicate that the estimated parameters are reasonably certain. Here the confidence bounds were

calculated using the formula $CI_x = \hat{x} \pm t_x \sigma_x$, where x is the parameter of interest (r, K) and t_x is the t distribution with respect to x (or more precisely, the number of degrees of freedom in the calculation of x).

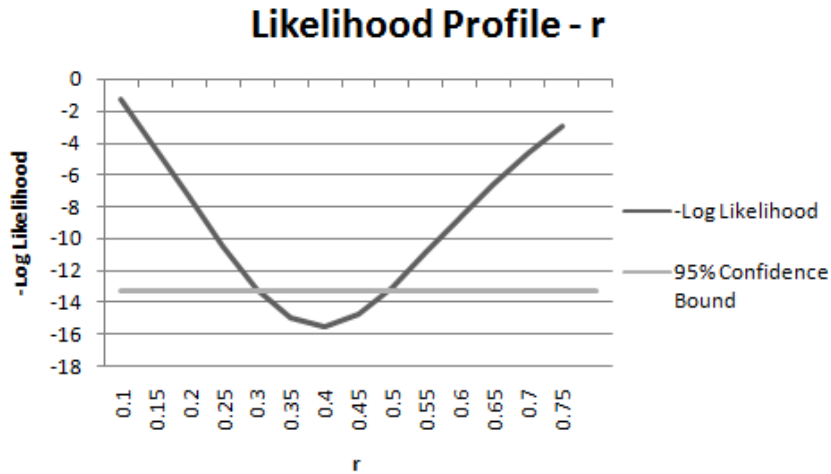


Figure 4.3: Likelihood profile for Namibia Hake for r .

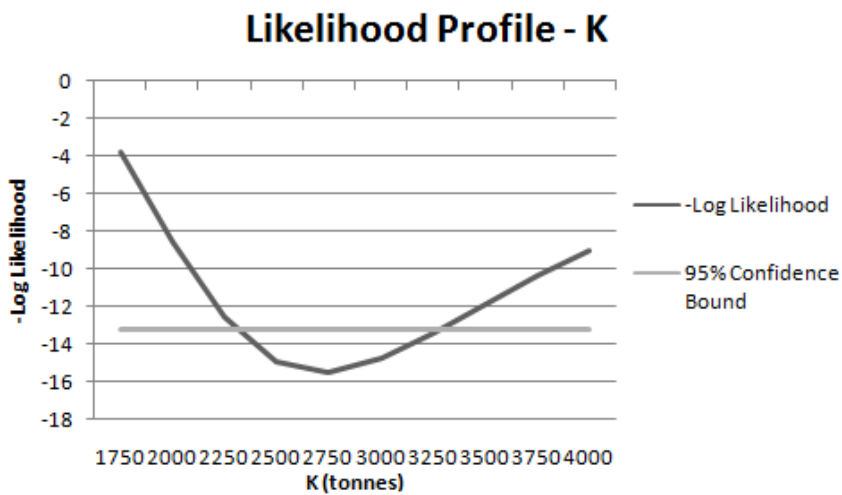


Figure 4.4: Likelihood profile for Namibia Hake for K .

4.3 Maximum Likelihood for FLA 3

The same code was then run using the data for the flatfish stock in the FLA 3 stock. Using the data from Table 3.1, the code was applied initially to the stock as a whole, and then to each of the three key species (ESO, LSO and SFL), using the three models. The remaining species caught in FLA 3 are not plotted due to the fact that they are all less than 5% of the total stock. This was done for each of the models (Schaefer, Pella-Tomlinson with $m = 3$, Fox).

4.3.1 Maximum Likelihood using Schaefer Model

The code written to estimate the parameters outputs the optimal parameter values as well as the minimum negative log-likelihood. These optimal values are summarized in Table 4.3.

For each of the four cases, the CPUE was plotted with the fit from the model, as in the Hake example (see the Figures 4.5, 4.6, 4.7, 4.8). Comparing these four plots with the plot from the Namibia Hake example, we can see that the fit is much worse than in the example. In particular for the stock as a whole, the fit is almost a straight line.

As we can see there is little variability in the optimal values for q and σ . Since ESO is the second most productive stock in FLA3 after LSO, we would have expected the virgin biomass to be higher than that of SFL, which is the third most productive stock in FLA3. In fact, the difference between the virgin biomass of LSO and SFL is much smaller than expected, due to the fact that LSO produces approximately twice as much of the total catch as SFL. These values for K do not reflect the proportions of catch in the population, based on the basic assumption that the number of catches is related to the number of fish in the population for each of the three species.

Looking at the parameter estimates for FLA3-All, the estimated value of K for FLA3-All contradicts the values of K for the three individual species since K for FLA3-All should be more than the sum of the K 's for each of the individual species. The sum of the estimated K values for the three individual species is more than 100000 above the estimated value for K for FLA3-All.

Table 4.3: Optimal parameter values for each of the three key species using maximum likelihood method for Schaefer model

Species	K	r	q	σ	-Log Likelihood
ESO	51261.53	2.314671	0.00002185303	0.1334687	-7.139348
LSO	108802.9	2.614116	0.00001	0.1691975	-4.141916
SFL	103890.1	2.326340	0.00001	0.1247933	-7.946086
FLA3-All	109508.9	1.834420	0.00001000039	0.1656193	-4.550041

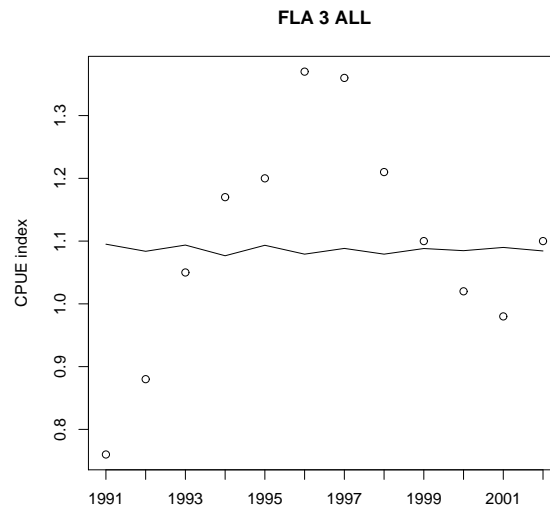


Figure 4.5: The observed CPUE (dots) and the line of best fit for FLA3 - All.

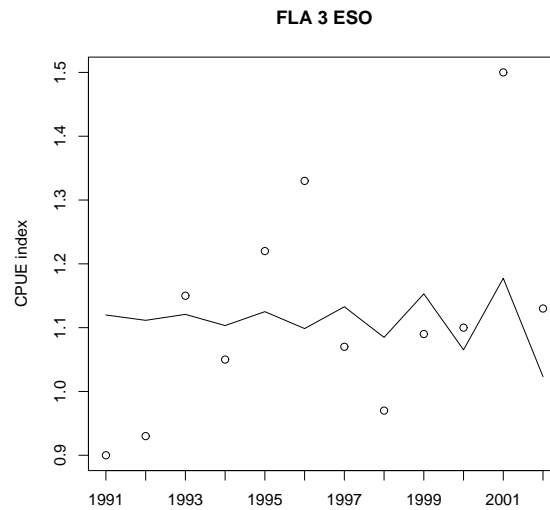


Figure 4.6: The observed CPUE (dots) and the line of best fit for New Zealand sole (ESO).

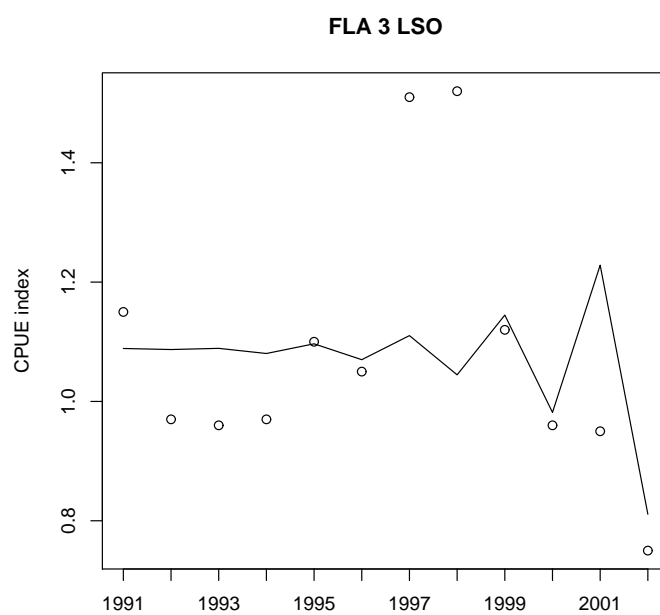


Figure 4.7: The observed CPUE (dots) and the line of best fit for lemon sole (LSO).

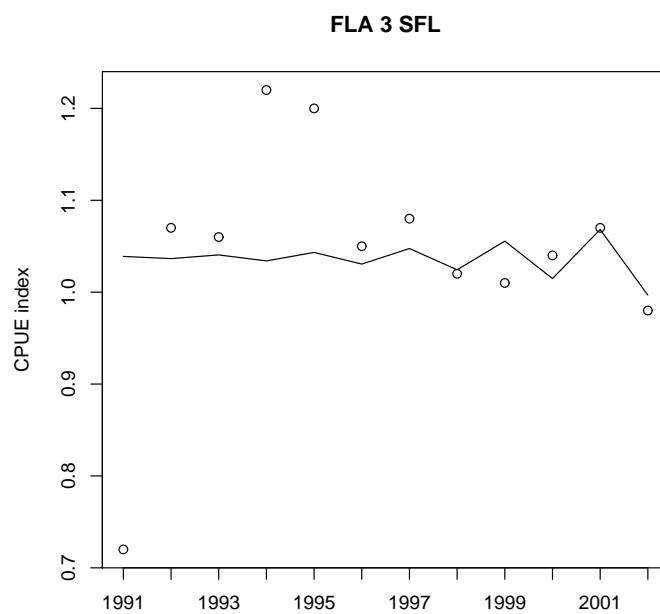


Figure 4.8: The observed CPUE (dots) and the line of best fit for sand flounder (SFL).

Based on previous assumptions of what the parameter r should be, FLA3-All seems to provide better estimates than for the individual species. However, to date there have been no biological studies which calculate the true value for r for this family of fish. Therefore it is difficult to establish whether these estimates are realistic.

4.3.2 Likelihood Profile

As described earlier, we can determine the confidence of the estimated parameters r and K by conducting a likelihood profile for each of these parameters. This was done for each of the three individual species. The values of the negative log likelihoods are plotted against the values of r and K (see the Figures 4.10, 4.9, 4.12, 4.11, 4.14 and 4.13). The 95% confidence bounds are also plotted for each of the three species. For each of the three species, the optimal values for both r and K are very uncertain. The plotted confidence bounds show that the range of possible optimal parameters is very wide and therefore the confidence of the optimal parameters is very low.

The likelihood of the above values for K for each of the individual species was discussed with Mike Beentjes, who has done a lot of work on this stock and in the stock area of interest. We considered the combined values for K for ESO, LSO and SFL, which is 263954.5. The highest level of catch taken since 1983 is 2573 tons, which was taken in the 1996-1997 fishing year. As a percentage of the estimated virgin biomass this catch is around 1%. If we assume that the amount of catch taken is 10% of the biomass at that time (a reasonable estimate according to Mike Beentjes), and that the catch in the current fishing year is 2500 tons, then that would indicate that the current biomass is 25000 tons, which is 10% of the estimated virgin biomass. This indicates that these values for the virgin biomasses are not altogether impossible, however they are much higher than expected, and at that level the fishery is being under-fished.

Fishery managers use these percentages to determine what action needs to be taken to maintain sustainable catch levels. In New Zealand under the 2009 legislation, when a fishery falls below 20% of the virgin biomass the catch must be reduced to allow the stock to rebuild, and when a fishery falls below 10% of the virgin biomass, closing the fishery should be considered.

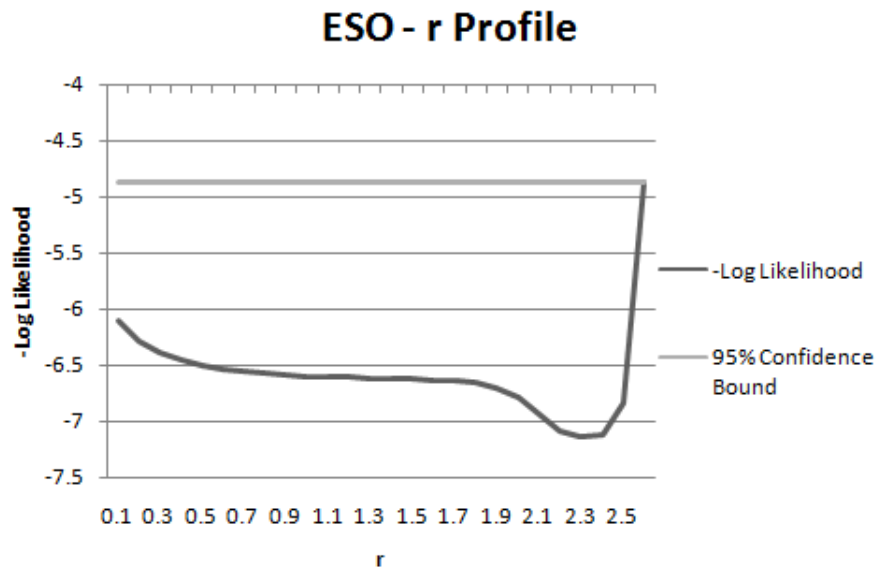


Figure 4.9: Likelihood profile associated with r for New Zealand sole (ESO).

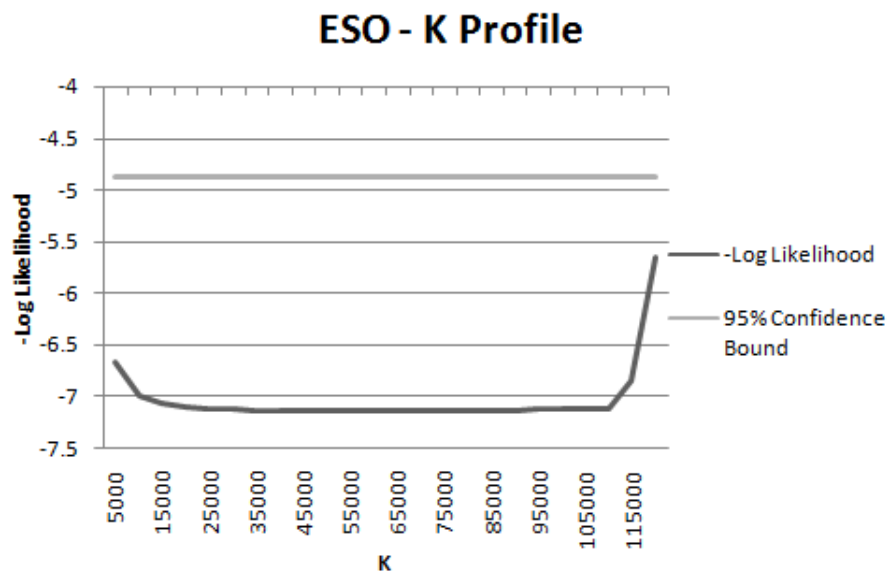


Figure 4.10: Likelihood profile associated with K for New Zealand sole (ESO).

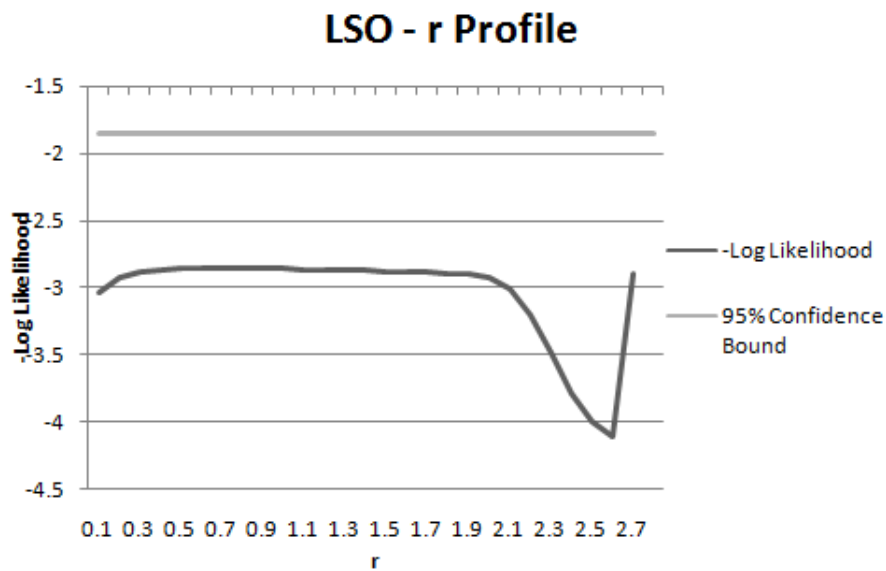


Figure 4.11: Likelihood profile associated with r for lemon sole (LSO).

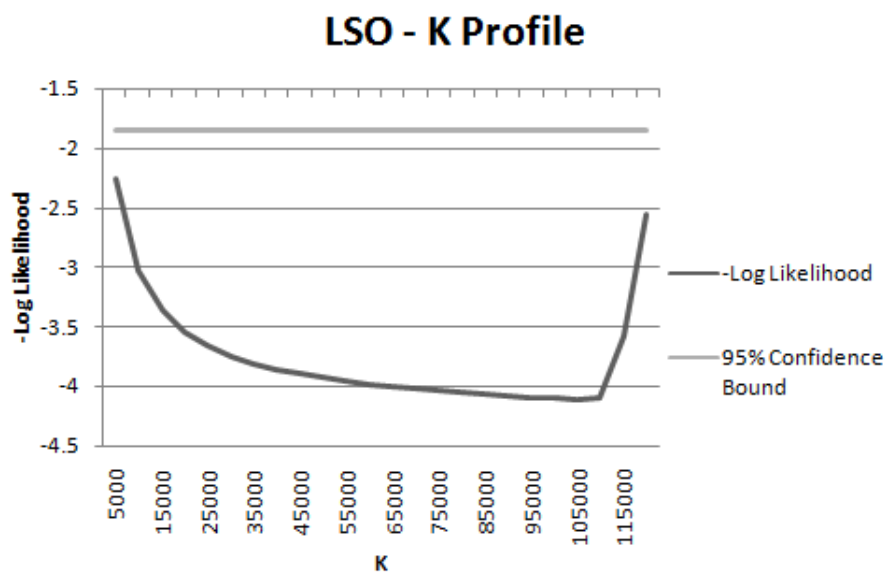


Figure 4.12: Likelihood profile associated with K for lemon sole (LSO).

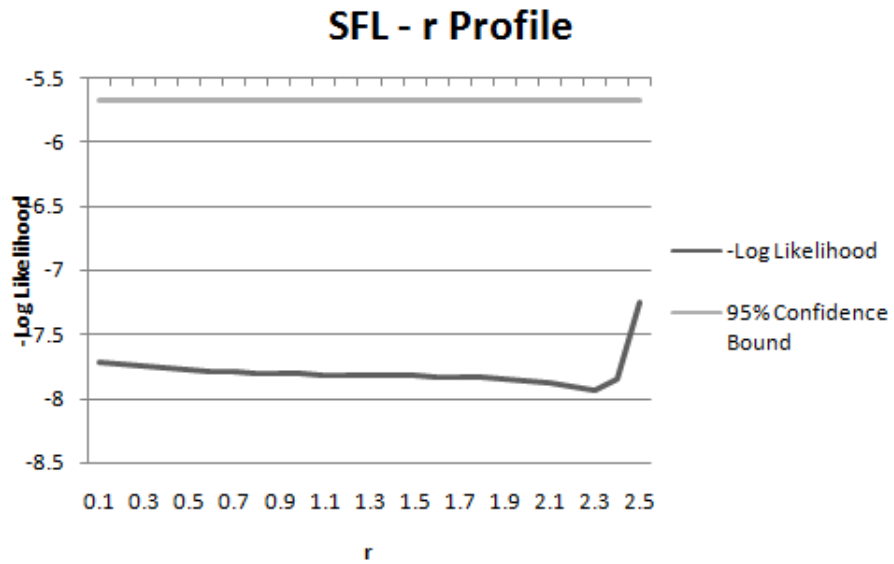


Figure 4.13: Likelihood profile associated with r for sand flounder (SFL).

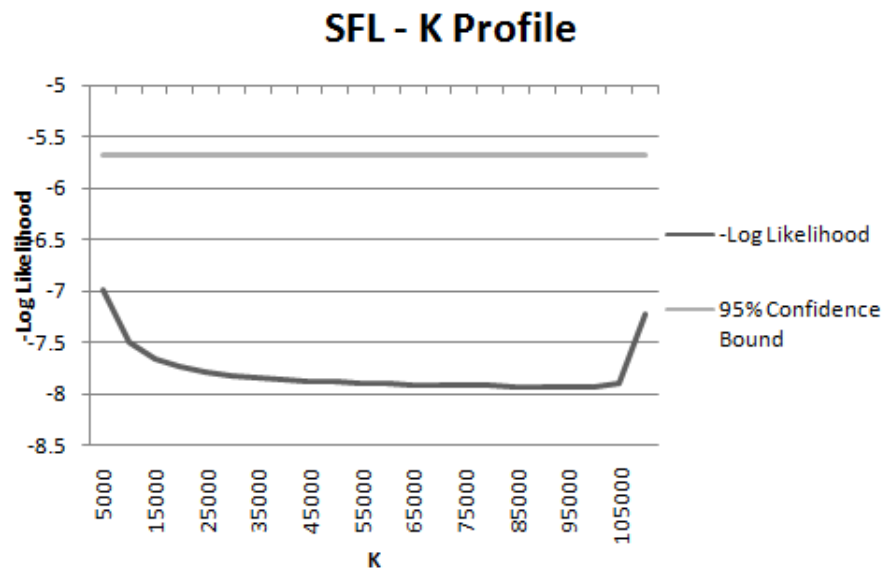


Figure 4.14: Likelihood profile associated with K for sand flounder (SFL).

4.3.3 Maximum Likelihood using Pella-Tomlinson Model with

$$m = 3$$

The same code that was used for the maximum likelihood for the Schaefer model was applied to the Pella-Tomlinson model with $m = 3$, with one difference in the line calculating the new biomass. The program outputted an error after the simulated annealing step:

```
Error in optim(y, fr, method = "SANN", control = list(maxit = 1e+05),  
: non-finite finite-difference value [1]
```

which means that the first element y ($y = (K, r, q, \sigma)$), has one or more elements that are either infinite, not a number (NaN) or not available (NA). Therefore, this program fails for the Pella-Tomlinson model.

4.3.4 Maximum Likelihood using Fox Model

Applying the same program to the Fox model was successful. The program works for the simulated annealing step as well as the Nelder and Mead step, and the output from the program indicates that the values converge. The results from the maximum likelihood method using the Fox model are summarized in Table 4.4.

Table 4.4: Optimal parameter values for each of the three key species using maximum likelihood method for Fox model

Species	K	r	q	σ	-Log Likelihood
ESO	49984.56	25.27234	0.0000224	0.1332784	-7.156673
LSO	108638.9	30.19385	0.00001	0.1725430	-4.05817
SFL	103880.7	26.84465	0.00001	0.1247861	-7.945668
FLA3-All	115959.8	1.025068	0.00001	0.1789020	-3.479238

The CPUE was plotted with the fit from the model for each of the four cases FLA-All, ESO, LSO and SFL (see Figures 4.15, 4.16, 4.17, 4.18). Comparing the hake example with the likelihood method using the Fox model shows the great uncertainty in these estimates. The optimal values for r for each of the individual species are extremely high compared with the estimated values from the Schaefer model (approximately 10 times more). The combined value of r (FLA-All) is lower

than the values obtained using the Schaefer model, and is more realistic than the individual r 's. The K values are close to those calculated using the Schaefer model. The likelihood profiles yielded wide confidence intervals like those from the maximum likelihood estimates for the Schaefer model.

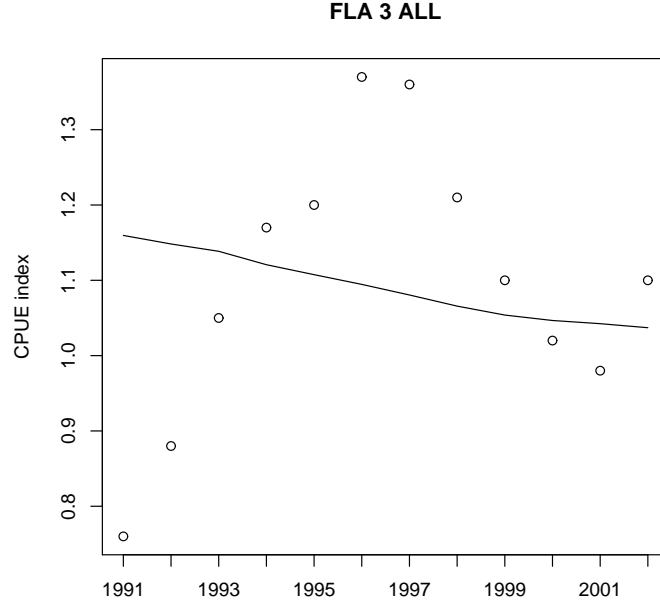


Figure 4.15: The observed CPUE (dots) and the line of best fit for FLA3 - All.

4.3.5 Summary of Maximum Likelihood Estimates

Comparing the plots for the Namibia hake example and the flatfish data outlines the difference in certainty between the two sets of estimated parameters. Therefore, further work needs to be done to obtain more certain estimates for r and K , and the uncertainty of the estimated parameters needs to be accounted for in the simulation model and also in the analysis of the results.

The great uncertainty in the parameter estimates for flatfish was expected due to the behaviour between the CPUE and catch data, as discussed in the previous chapter, where trends in CPUE do not clearly relate to trends in catch (i.e. when catch goes up CPUE goes down and vice-versa). Due to the high level of uncertainty in the parameter estimates, the Bayesian goodness of fit method was applied to attempt to estimate more certain biological parameters.

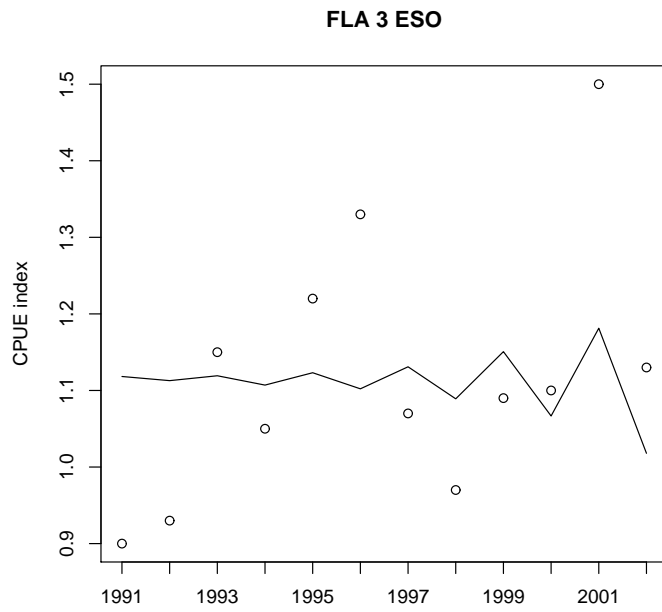


Figure 4.16: The observed CPUE (dots) and the line of best fit for New Zealand sole (ESO).

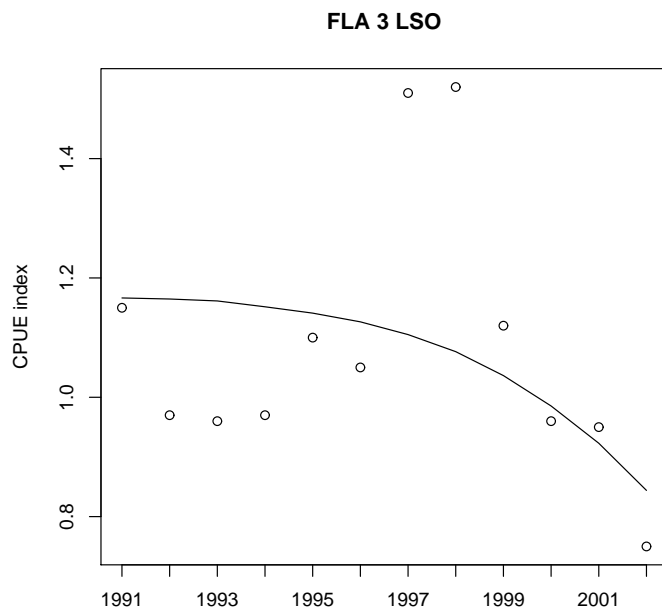


Figure 4.17: The observed CPUE (dots) and the line of best fit for lemon sole (LSO).

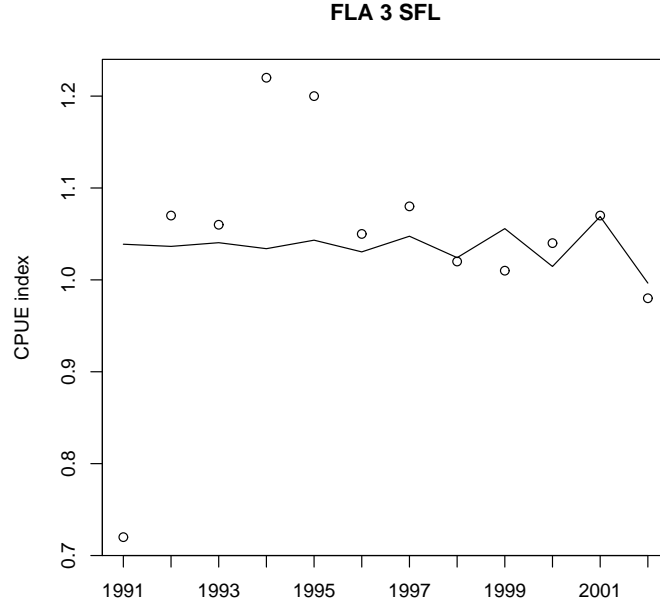


Figure 4.18: The observed CPUE (dots) and the line of best fit for sand flounder (SFL).

4.4 Bayesian Goodness of Fit

4.4.1 Introduction

Bayesian goodness of fit is based on Bayes' Theorem, which was developed and named after Thomas Bayes (for further reading on Bayes' Theorem, see [28]). The basis for use of this method in estimating parameters is that often there is some previous information available. In particular, Bayesian goodness of fit is useful when previous (but independent) studies have been conducted. This method allows the information from previous studies to be incorporated into the parameter estimation. Bayes' theorem can be written in terms of probabilities using the basic formula

$$P(H|Data) = \frac{P(Data|H)P(H)}{P(Data)}, \quad (4.7)$$

where H is the given hypothesis. $P(H)$ is known as the prior probability which is the probability of H before the data was obtained. $P(Data|H)$ is the probability of the data when the hypothesis H is true and $P(H|Data)$ is called the posterior probability, which is the probability of H given the data. The term in the denomi-

nator $P(Data)$ represents the probability of the data over all hypotheses, which can be summed over i for all possible hypotheses H_i .

Although there have been few studies conducted on flatfish species in New Zealand, information from studies conducted on flatfish species from around the world can be incorporated as prior information in the parameter estimation since many flatfish species share common biological characteristics and have similar life expectancies. Information from the Fish Base website was incorporated into the calculation to attempt to better estimate the unknown parameters.

4.4.2 Biological Parameters from Fish Base

The Fish Base website provides a catalogue of information available for more than 30000 individual fish species from around the world [15]. The site is available through the internet as well as on CD-rom, with genetic information, morphology, catch analysis, fish statistics, and more. There is also a life-history tool which makes an estimation of the value of r using the maximum length and the maximum age which the species can live to, as well as other biological parameters. The site includes references from more than 40000 sources, and has contributions from more than 1600 collaborators.

The life-history tool was developed by Eli Agbayani, a former Fish Base staff member. This tool was used to estimate the parameters for the species in this study. The tool begins with an estimate for either the maximum length, L_{max} or the asymptotic length L_{∞} (the mean length fish would grow to if allowed to grow indefinitely). In some cases, this information is published in the website, otherwise the user can enter this information. Using these values, along with available information on the length at maturity, natural mortality rate, life span, age at first maturity, relative recruit per yield, intrinsic rate of increase r , as well as the growth parameter K (from the von Bertalanffy growth function) the missing parameters are estimated. The values of the biological parameters are already on the Fish Base website, but these can all be updated if better estimates are known. This allows the user to improve the estimates when more information is gathered. The key parameter of interest from this tool in this study is the rate of increase r .

The tool was able to be used for New Zealand sole and New Zealand sand floun-

der, but not for New Zealand lemon sole (an error message was displayed). Using the life-history tool for New Zealand sole with maximum length 50cm and maximum age 5 years, the tool calculated that the growth rate r is 1.92. Similarly, using the tool for New Zealand sand flounder with $L_{\infty} = 37.4$, the value for r is given as 2.8 (the tool allows the user to enter a value for L_{∞} but not for L_{max} for the sand flounder). This value for the asymptotic length is based on data for males from the Fish Base website. If we run the tool again using $L_{\infty} = 59.9$, which is the asymptotic length for females given by Fish Base, the life-history tool gives a value for r of 1.3. Using the average of these two asymptotic lengths, 48.7, calculates r as 1.76.

4.4.3 Regression Analysis

Using the life-history tool from Fish Base, the growth rates (r) of 40 species of flatfish from around the world were estimated. These 40 species were chosen from over 600 species of sole and over 500 species of flounder at random. Only species for which there was enough information that the life-history tool was available were used, and those which led to an error message were excluded. The values for L_{max} that were used as a basis for the estimates were the original entered values set for each of the species in Fish Base (see Table 4.6).

Different trend lines were fitted to the L_{max} and r values from the 40 species from Fish Base in Microsoft Excel 2007. Linear, power, polynomial and log trend lines were fitted. Using the formulae outputted from the trend lines an estimate for r was obtained for each of the three key species in FLA3 using the mean values of L_{max} for each of the three key species (see Table 4.5).

Table 4.5: Estimate of r for each of the three key species

	ESO	LSO	SFL
Linear	1.3427	2.1827	1.9027
Power	1.259872831	1.651520634	1.651520634
Polynomial	1.0078	1.5133	1.2498
Log	1.128324337	1.852488121	1.584649498

A log-normal distribution was also fitted to the data from Fish Base using the Easy Fit 5.1 Professional statistical program. The prior for r was constructed as

a lognormal distribution with $\mu = 0.73881$, $\tau = 2.588915$ from the lognormal fit in Figure 4.19. The prior for K was a non-informative prior with a uniform distribution from 0 to 200000. From discussions with Matthew Dunn and Mike Beentjes (both from NIWA) this non-informative prior was considered to be the best prior for K at the time due to the uncertainty in K and no prior information available. The prior for q was also kept relatively uninformative, with a gamma distribution being used with $r = 1$, $\mu = 1000$ (this is a standard non-informative prior gamma distribution). The biomass was calculated for the 12 time steps that data was available for the catch and CPUE, with an error term included in this calculation to allow for the uncertainty in the biomass calculation. The biomass was assumed to follow a normal distribution and the CPUE was assumed to follow a log-normal distribution. A gamma distribution was used for the τ values for the error in the CPUE and the biomass calculation. These distributions were chosen based on the expected values for the parameters following discussions with Matthew Dunn (NIWA) and Geoff Jones (statistician, Massey University).

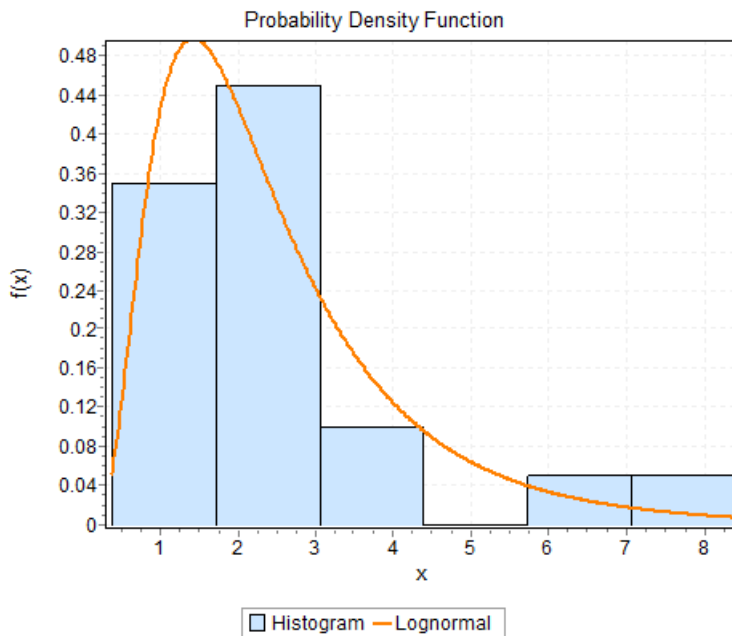


Figure 4.19: Log-normal fit of r from the data obtained from Fish Base

Table 4.6: Estimated r data for sole and flounder from Fish Base

Common Name	Country	Species	L_{max}	r
Annular sole	Australia	<i>Brachirus annularis</i>	13	6.22
Big-eyed tongue-sole	Australia	<i>Cynoglossus macrophthalmus</i>	27.7	2.64
Black sole	Australia	<i>Synaptura nigra</i>	55	1.76
Blackhand sole	UK	<i>Solea bleekeri</i>	17	3.54
Brown sole	UK	<i>Achirus klunzingeri</i>	23	3.5
Butter sole	UK	<i>Isopsetta isolepis</i>	55	1.36
Dover sole	UK	<i>Microstomus pacificus</i>	76	1.34
Eyed sole	UK	<i>Microchirus ocellatus</i>	20	2.94
Flathead sole	UK	<i>Hippoglossoides elassodon</i>	52	1.42
Freshwater sole	Australia	<i>Trinectes maculatus</i>	20	2.7
Fringed sole	UK	<i>Trinectes fimbriatus</i>	9	8.34
Guinean sole	UK	<i>Synaptura cadenati</i>	35	2.38
Klein's sole	UK	<i>Synapturichthys kleinii</i>	40	1.72
Lemon sole	Canada	<i>Parophrys vetulus</i>	49	1.34
Lemon sole	Sth. Africa	<i>Solea fulvomarginata</i>	26	2.28
Lemon sole	UK	<i>Microstomus kitt</i>	65	0.82
Long tongue sole	UK	<i>Cynoglossus lingua</i>	46.9	1.66
Long-finned sole	UK	<i>Glyptocephalus zachirus</i>	60	0.62
Marbled sole	Japan	<i>Pseudopleuronectes yokohamae</i>	45	1.72
Moses sole	Micronesia	<i>Pardachirus marmoratus</i>	26	3.26
Pacific sand sole	UK	<i>Psettichthys melanostictus</i>	63	1.24
Red tonguesole	UK	<i>Cynoglossus joyneri</i>	24	1.92
Sole	Australia	<i>Paraplagusia bilineata</i>	30	2.44
Southern sole	Australia	<i>Aseraggodes haackeanus</i>	14	4.22
Whiskered sole	UK	<i>Monochirus hispidus</i>	20	2.66
American smooth flounder	UK	<i>Liopsetta putnami</i>	30	1.44
Arctic flounder	USA	<i>Liopsetta glacialis</i>	35	0.38
Banded-fin flounder	Australia	<i>Azygopus pinnifasciatus</i>	20	2.1
Bay flounder	Australia	<i>Ammotretis rostratus</i>	30	1.44
Black flounder	NZ	<i>Rhombosolea retiaria</i>	25	2.18
Channel flounder	UK	<i>Syacium micrurum</i>	40	2.84
European flounder	UK	<i>Platichthys flesus</i>	60	1.02
Flounder	Australia	<i>Pseudorhombus arsius</i>	45	1.74
Greenback flounder	NZ	<i>Rhombosolea tapirina</i>	45	1.26
Jenyn's flounder	Australia	<i>Pseudorhombus jenynsii</i>	34	2.44
Long-fin right-eye flounder	UK	<i>Nematops macrochirus</i>	15	2.62
Mottled flounder	UK	<i>Bothus maculiferus</i>	25	2.9
Pacific eyed flounder	UK	<i>Bothus constellatus</i>	15.7	3.1
Southern flounder	UK	<i>Paralichthys lethostigma</i>	83	1.56
Yellow-dabbled flounder	UK	<i>Brachypleura novaezeelandiae</i>	14	5.92

4.4.4 Implementation

The Bayesian goodness of fit method was applied to the data for FLA3 using WinBUGS version 1.4 (a program written specifically to do Bayesian analysis using Markov chain Monte Carlo methods). Using the WinBUGS program, a model was written to estimate the parameters K , r , and q (see Appendix C). The method used to estimate the parameters using the WinBUGS program involves using Markov chain Monte Carlo (MCMC) simulation with Gibbs sampling. Using prior estimates for K , r and q , a loop was used to calculate the new biomass at each time. Probability density functions were used for the prior estimates for K , r and q . The program was run individually for each of the three species and took approximately 5 hours to run 10000000 updates with the updates thinned by every 1000. Figure 4.20 shows the relationships between the parameters. Parameters within a loop are placed within the plate with constant parameters denoted as rectangles, stochastic nodes denoted as ellipses, and the relationships between the parameters connected using solid arrows which indicate stochastic dependence, and hollow arrows which indicate logical function.

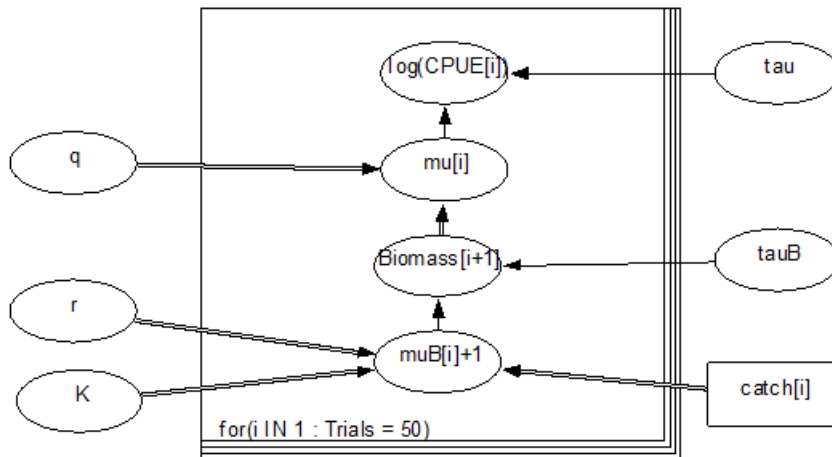


Figure 4.20: The relationship between the parameters of interest

4.4.5 Bayesian Method using Schaefer Model

The parameter estimates obtained from updating the MCMC chains 10000000 times using the Schaefer model are summarized in Table 4.7.

Table 4.7: Optimal parameter values for each of the three key species using Bayesian statistical methods with the Schaefer model.

Species	K	r	q	MSY
ESO	6528	1.647	0.0001489	2688
LSO	12160	1.634	0.00005806	4968
SFL	8079	1.442	0.0000995	2912

These values for K seem more reasonable than those obtained from the maximum likelihood estimations, based on the expected value of the initial biomass relative to the current amount of catches. The estimates for r are close in value, which is expected since these species have similar life expectancies and biological characteristics.

The following figures (4.21, 4.22, 4.23) are from the WinBUGS program for the Schaefer model with density, quantile and history graphs plotted for r and K for ESO, LSO and SFL. Each plot shows the output from 10 million iterations which were thinned by 1000.

Figure 4.21 shows the plots related to ESO. Ideally for the density plot, we would like the curve to be smooth with only one peak, similar to a normal distribution curve. The shape of the density plot for r is reasonably similar to a normal curve, though not as smooth. For K , the density plot has multiple peaks, and therefore has a number of likely values. We can see from the quantile plots that the 2.5% and 97.5% quantiles show a wide range for both r and K . The history plots show the desired behaviour for r with the estimates fluctuating consistently through time, while the history plot for K shows that the values are fluctuating inconsistently and therefore they are not converging. The history and density plots for this species show that the estimate for r is relatively certain while the estimate for K is more uncertain.

Figure 4.22 shows the plots related to LSO. Again the density plots show multiple peaks, though the shape itself is relatively normal for r and skewed for K . The

quantile plots also show a high level of uncertainty, with wide ranges for both r and K , with r between 0.5 and 2.5 and K between approximately 8000 and 30000. The history plot for r indicate that the chain is converging, however the history plot for K shows a number of uneven fluctuations which indicate that the estimate is not converging and very uncertain.

The plots related to SFL are shown in Figure 4.23. The density plot for K show that there are several peaks, with similar likelihood, which indicate that the estimate for K is extremely uncertain for this species. The density plot for r is reasonable, with one significant peak and normal-like shape.

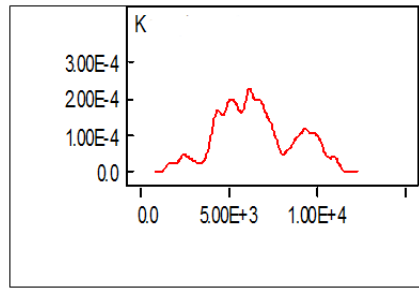
Presumably these results reflect the fact that r has an informative prior and K has an un-informative vague prior. Similar to the other species, the quantile plot for r shows the 95% confidence interval is between 0.5 and 2.2.

4.4.6 Bayesian Method using Pella-Tomlinson Model with $m = 3$

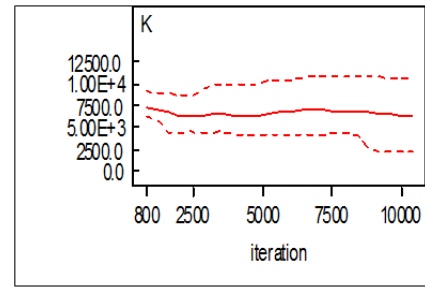
The same WinBUGS code that was used for the Bayesian parameter estimation using the Schaefer model was used for the Pella-Tomlinson model with $m = 3$, with the only difference between the two codes in the line used to calculate the biomass.

For the Pella-Tomlinson model with $m = 3$, WinBUGS was unable to generate initial values for the uninitialized parameters. WinBUGS uses forward sampling to generate initial values based on the prior distributions given in the model. The sampling continues until a feasible solution is found, however once 100 attempts have been made to generate the initial values, the sampling stops and a trap message comes up with “undefined real result” displayed. The reason the initial value generator fails can be due to a prior distribution being too vague (see WinBUGS manual). Without the generated initial values, the program cannot run the MCMC simulation. The program also rejects manually inputted initial values for the uninitialized parameters. Therefore this method fails for the Pella-Tomlinson model with $m = 3$, using these initial values and prior distributions.

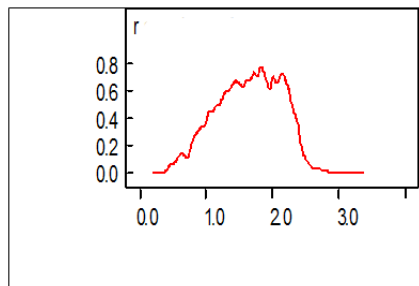
The figures below are for ESO.



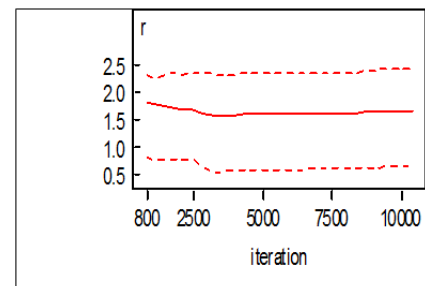
(a) ESO: Density graph for K from Bayesian parameter estimate in WinBUGS.



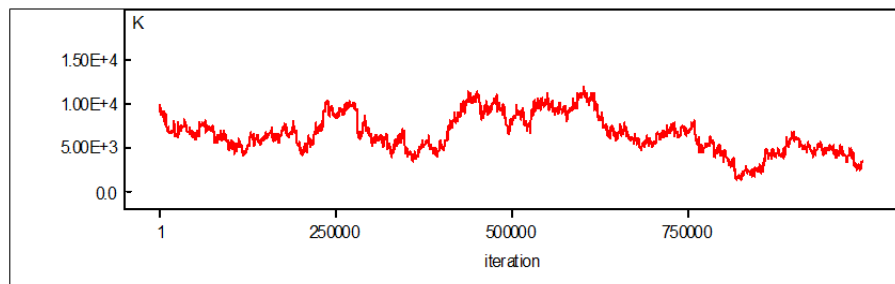
(b) ESO: Quantile graph for K with 2.5% and 97.5% percentiles.



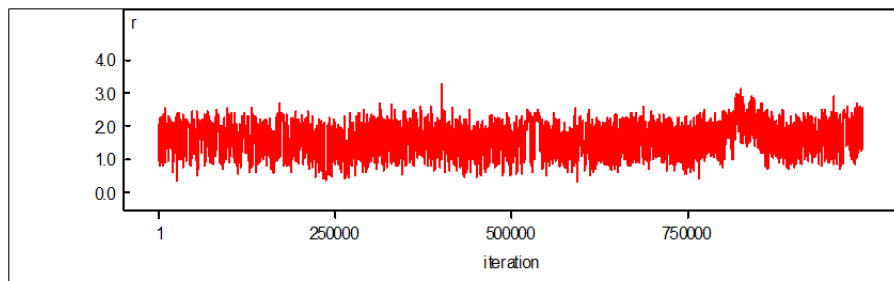
(c) ESO: Density graph for r from Bayesian parameter estimate in WinBUGS.



(d) ESO: Quantile graph for r with 2.5% and 97.5% percentiles.



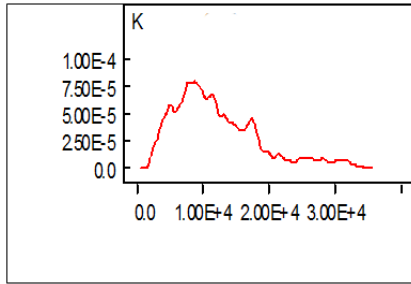
(e) ESO: History graph for K.



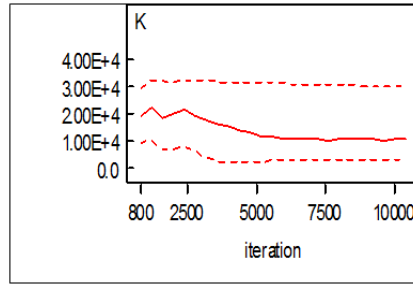
(f) ESO: History graph for r.

Figure 4.21: Graphs for ESO parameter estimates from WinBUGS

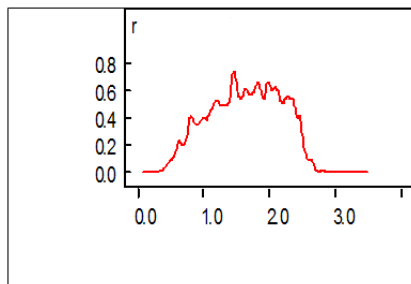
The figures below are for LSO.



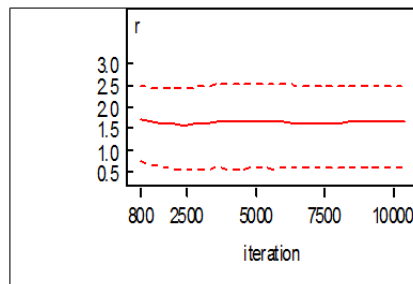
(a) LSO: Density graph for K from Bayesian parameter estimate in WinBUGS.



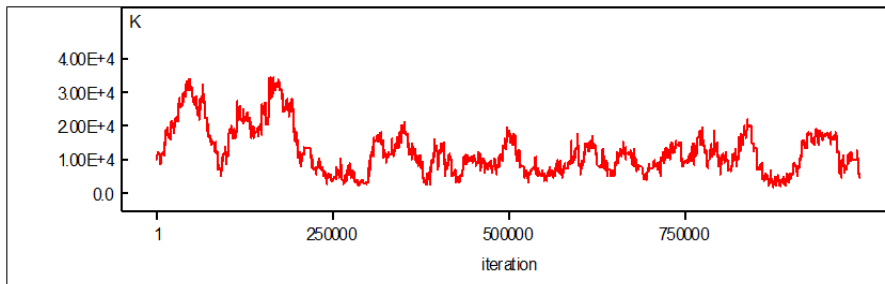
(b) LSO: Quantile graph for K with 2.5% and 97.5% percentiles.



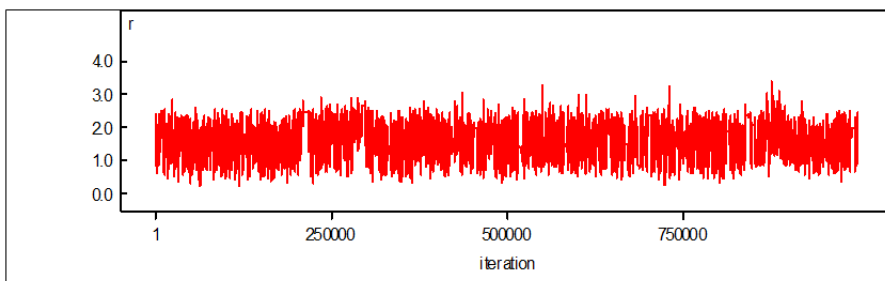
(c) LSO: Density graph for r from Bayesian parameter estimate in WinBUGS.



(d) LSO: Quantile graph for r with 2.5% and 97.5% percentiles.



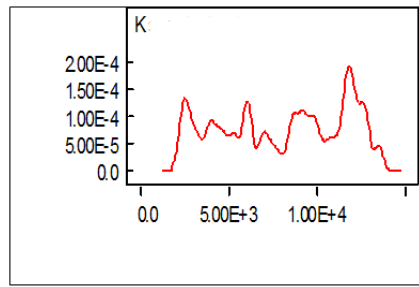
(e) LSO: History graph for K.



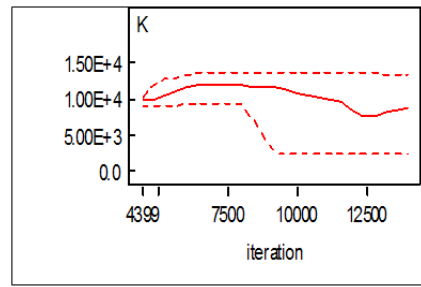
(f) LSO: History graph for r.

Figure 4.22: Graphs for LSO parameter estimates from WinBUGS

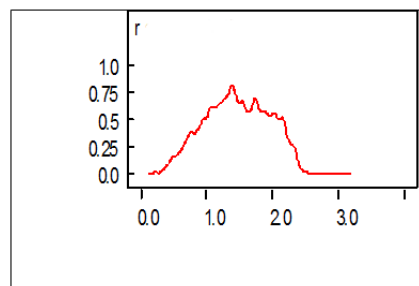
The figures below are for SFL.



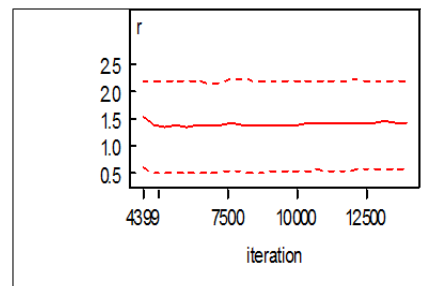
(a) SFL: Density graph for K from Bayesian parameter estimate in WinBUGS.



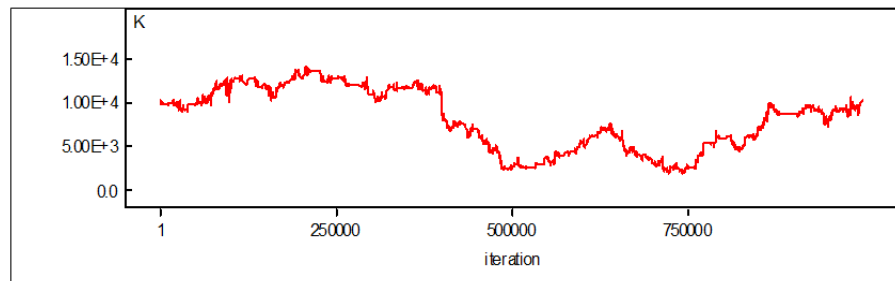
(b) SFL: Quantile graph for K with 2.5% and 97.5% percentiles.



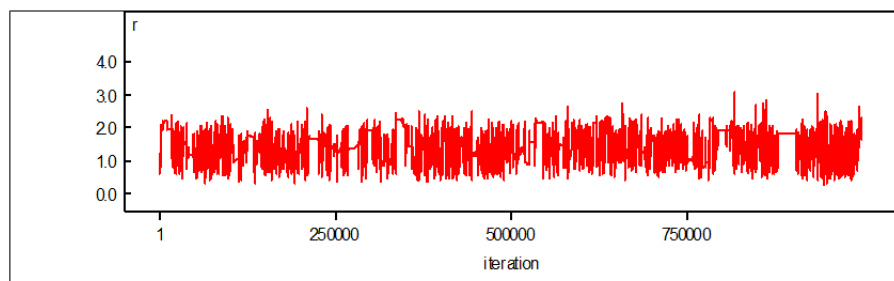
(c) SFL: Density graph for r from Bayesian parameter estimate in WinBUGS.



(d) SFL: Quantile graph for r with 2.5% and 97.5% percentiles.



(e) SFL: History graph for K.



(f) SFL: History graph for r.

Figure 4.23: Graphs for SFL parameter estimates from WinBUGS

4.4.7 Bayesian Method using Fox model

The WinBUGS code written for the Schaefer model was applied to the Fox model. The code was run for 10 million iterations, thinned by 1000. The optimal parameter values from the WinBUGS output for this model are summarized in Table 4.8, along with the MSY for each of the species.

Table 4.8: Optimal parameter values for each of the three key species using Bayesian statistical methods with the Fox model.

Species	K	r	q	MSY
ESO	9986	4.508	0.000027	1798
LSO	24355	2.6201	0.0000684	2325
SFL	25070	2.772	0.0000881	2524

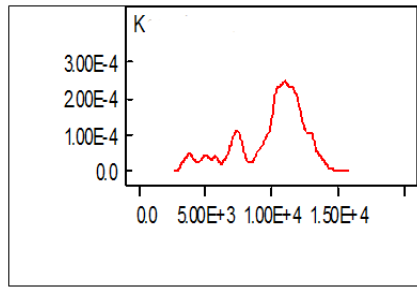
The values for K are reasonable, and quite similar to those obtained from the Schaefer model. The values for the r 's are more likely than those obtained from the maximum likelihood estimates for LSO and SFL, however the r for ESO is still very high. The r values are expected to be close in value, but the r for ESO is much higher than r 's for LSO and SFL.

Figures 4.24, 4.25 and 4.26 show the outputted density, history and quantile plots from the WinBUGS program for each of the three key species for the Bayesian estimates using the Fox model.

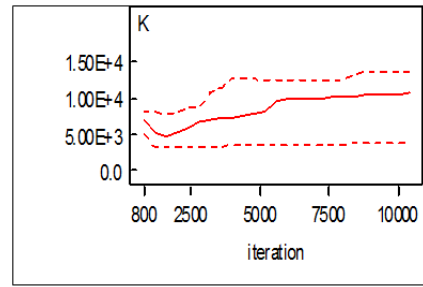
Figure 4.24 shows the plots related to ESO. The density graphs show that r and K are correlated, which can be seen by the opposing skews. The density plot for K has multiple peaks, which indicate that the estimate is uncertain, while the density plot for r is reasonably smooth. The quantile plots indicate that the confidence bounds are wide for both K and r . The history plot for K indicates that the chain is not converging, whereas the history plot for r is oscillating reasonably consistently.

The plots relating to LSO are in Figure 4.25. The density graphs for LSO also indicate that K and r are correlated. The density plot for r is very skewed, and the quantile plots for r show an extremely wide range for the confidence bounds. The history plot for r shows that the chain is oscillating between 0 and 20. The density plot for K shows high uncertainty due to the multiple peaks, and the quantile plot shows a wide range of values within the confidence bounds.

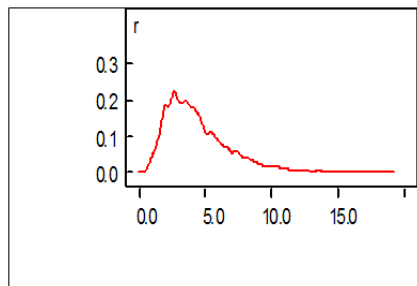
The figures below are for ESO.



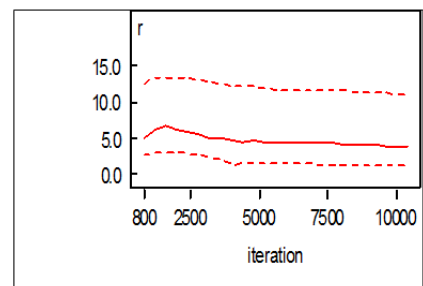
(a) ESO: Density graph for K from Bayesian parameter estimate in WinBUGS.



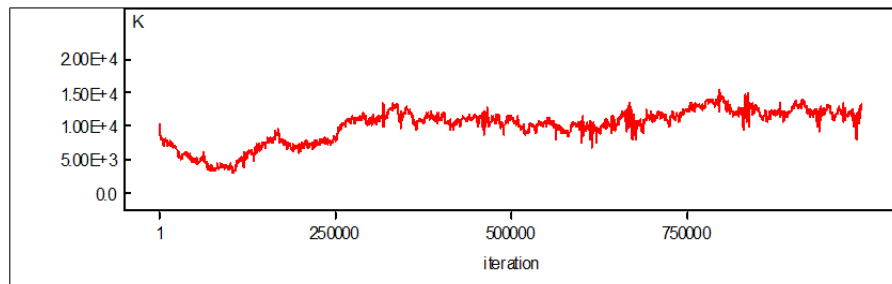
(b) ESO: Quantile graph for K with 2.5% and 97.5% percentiles.



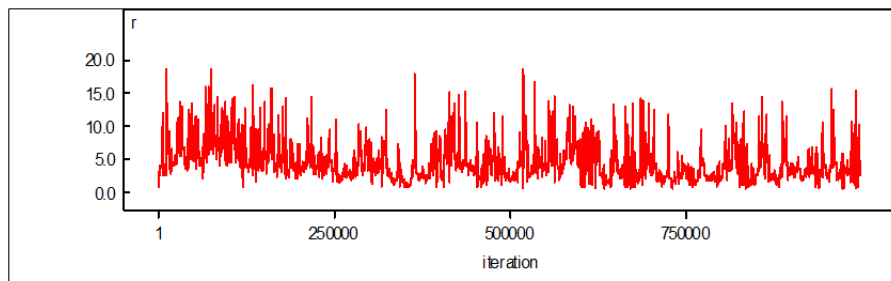
(c) ESO: Density graph for r from Bayesian parameter estimate in WinBUGS.



(d) ESO: Quantile graph for r with 2.5% and 97.5% percentiles.



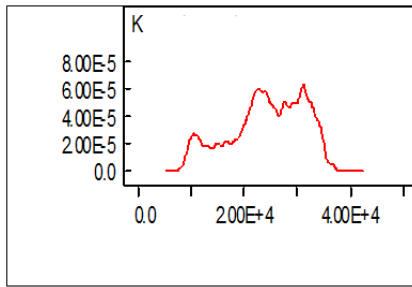
(e) ESO: History graph for K.



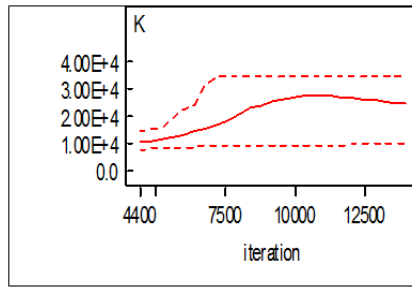
(f) ESO: History graph for r.

Figure 4.24: Graphs for ESO parameter estimates from WinBUGS

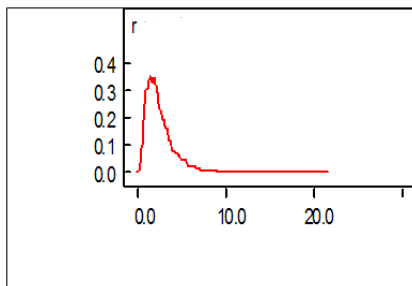
The figures below are for LSO.



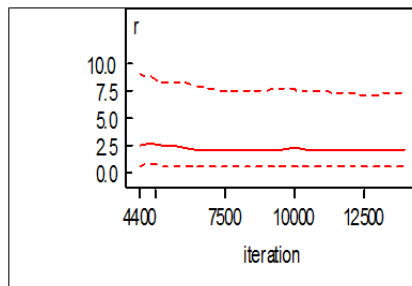
(a) LSO: Density graph for K from Bayesian parameter estimate in WinBUGS.



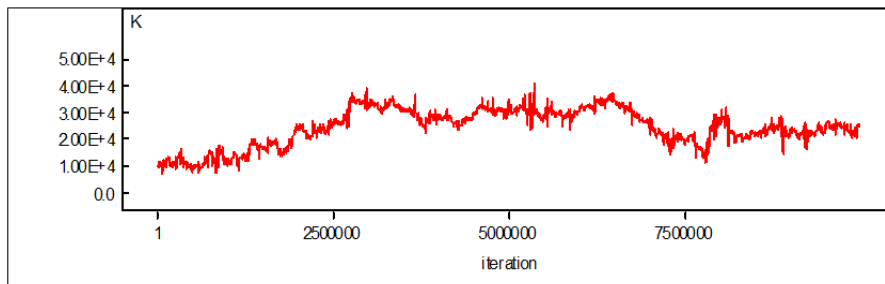
(b) LSO: Quantile graph for K with 2.5% and 97.5% percentiles.



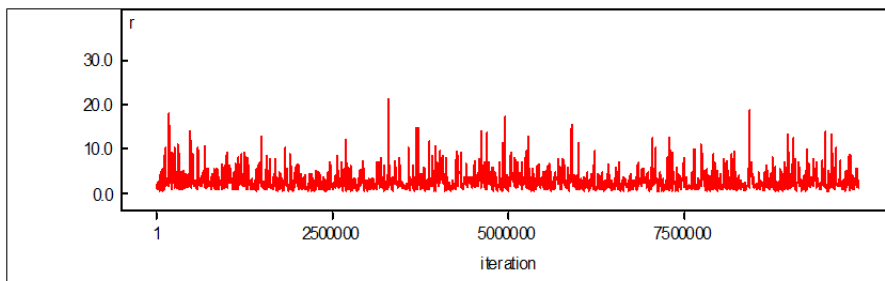
(c) LSO: Density graph for r from Bayesian parameter estimate in WinBUGS.



(d) LSO: Quantile graph for r with 2.5% and 97.5% percentiles.



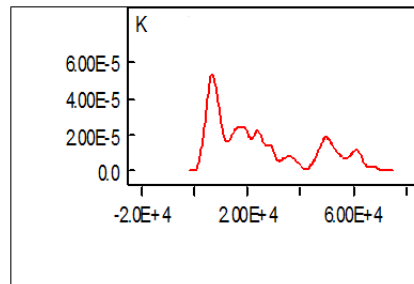
(e) LSO: History graph for K.



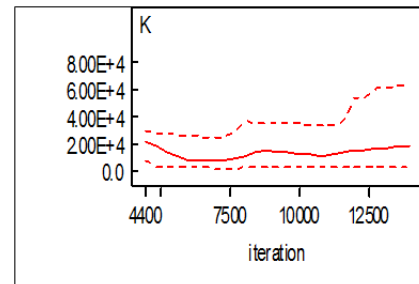
(f) LSO: History graph for r.

Figure 4.25: Graphs for LSO parameter estimates from WinBUGS

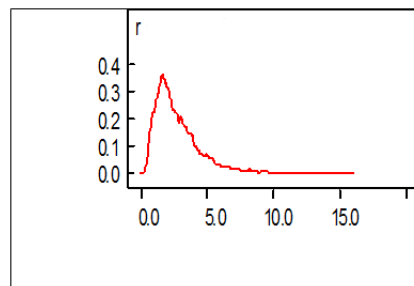
The figures below are for SFL.



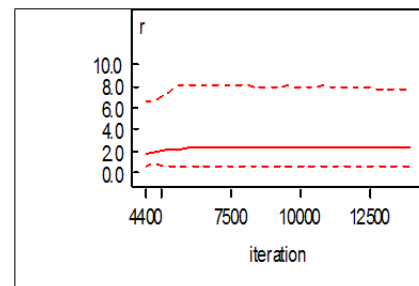
(a) SFL: Density graph for K from Bayesian parameter estimate in WinBUGS.



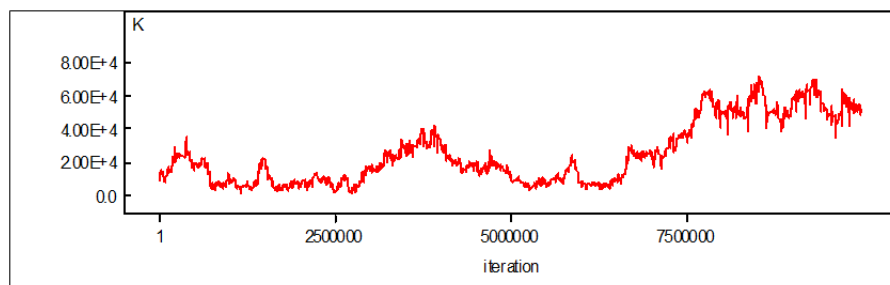
(b) SFL: Quantile graph for K with 2.5% and 97.5% percentiles.



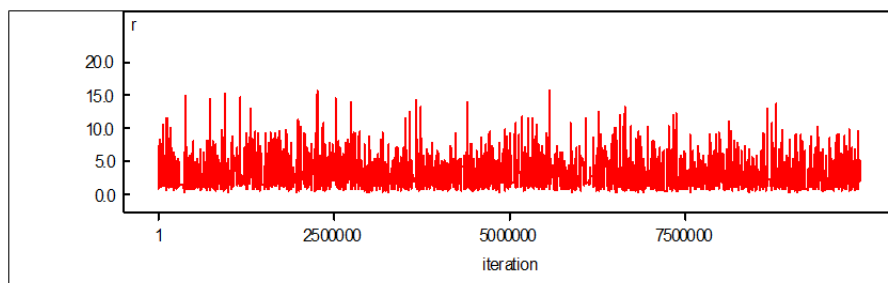
(c) SFL: Density graph for r from Bayesian parameter estimate in WinBUGS.



(d) SFL: Quantile graph for r with 2.5% and 97.5% percentiles.



(e) SFL: History graph for K.



(f) SFL: History graph for r.

Figure 4.26: Graphs for SFL parameter estimates from WinBUGS

Figure 4.26 shows the plots relating to SFL. The density plot for K show that this estimate is the least certain of the three species, with the curve least-resembling a normal curve. The density plot for r is also skewed. The quantile plots both show a wide range of values within the confidence bounds. The history plot for K shows that the chain is not converging, whereas the history plot for r is the most dense of all the species.

4.5 Concluding Remarks

The estimated values for r and K calculated using the maximum likelihood method were very uncertain for both the Schaefer model and the Fox model. This was expected since the assumption that the initial biomass equals the biomass that fish would tend to in absence of fishing is invalid in this case. The CPUE data also do not show the behaviour expected from a fishery of this kind, where the CPUE decreases as catches increase, up to a point where CPUE will begin to increase when catches decrease, as was exhibited by the Namibia Hake example.

This led to the use of the Bayesian method to attempt to increase the certainty of the parameters. These estimates were expected to have a high level uncertainty for the same reasons (the assumption that $B_0 = K$, and the poor data). However, the estimates for r for each of the three species obtained using Bayesian methods are closer to the estimated values from Fish Base and the regression described in this chapter than the estimated values from the maximum likelihood calculations. This was expected since the priors came from Fish Base. The plots from WinBUGS show that overall the estimates for r are reasonably certain compared with the estimates for K which are very uncertain. These findings were expected since the prior log normal distribution for r used in the calculation was an informed prior, while the prior for K was non-informative. In fact gave very little information about K since a uniform distribution was used between a very wide range (between 0 and 200000). Using both methods the estimated values for K for each of the species are very uncertain.

The Pella-Tomlinson model with $m = 3$ fails due to the nature of the model, and the initial values and priors used. The non-zero fixed point for this model is

stable only for $q < r < q + 1$ (see previous chapter), therefore is not suitable for these species, where r is expected to be close to 2. This fixed point is also much smaller than the non-zero fixed point for the Schaefer model,

$$\bar{B}_{Schaefer} = K \left(1 - \frac{q}{r}\right) \quad (4.8)$$

and since $q \ll 1$ then

$$\bar{B}_{Schaefer} \approx K. \quad (4.9)$$

Comparing this to the non-zero fixed point for the Pella-Tomlinson model with $m = 3$

$$\bar{B}_{m=3} = \bar{B} = \frac{\sqrt{r^2 K - r K q}}{r} \quad (4.10)$$

and again using the fact that $q \ll 1$,

$$\bar{B}_{m=3} \approx \sqrt{K}. \quad (4.11)$$

Also, due to the cubed term in the model, the biomass decreases at a much faster rate than the Schaefer and Fox models. Since the K values are expected to be reasonably high for this problem (initial value used in the estimation was $10000t$), the cubed term will then become very large. In order for this method to obtain non-zero values after the first time-step in the simulation models, the inequality

$$K + rK - rK^2 > Catch \quad (4.12)$$

must be satisfied. Since this inequality is unlikely to be satisfied for this type of data, the Pella-Tomlinson model with $m = 3$ gives no useful information for this problem.

Based on discussions with fisheries employees from NIWA, the estimated values from the Bayesian calculations are more reasonable than those calculated using maximum likelihood. Consequently, the simulation models were run with the parameter estimates obtained using the Bayesian method rather than those obtained

from the maximum likelihood method. Due to the fact that these estimates are still relatively uncertain, the simulation models were run with Monte Carlo simulation on the parameter estimates to account for this uncertainty.

Chapter 5

MANAGEMENT STRATEGY OPTIONS

5.1 Introduction

There are several different ways in which a stock can be managed. The current management method for the FLA 3 fishing area allows a total amount of commercial catch (TACC) of 2681 tonnes. As was discussed earlier, there are some concerns for this stock due to the fact that several species are managed as one stock, and the high level of the TACC means this stock shows behaviour characteristic of open fisheries due to the fact that the TACC is well above yearly catches. This document presents six different management options, which are detailed below. The first three options are based on those in [7] which include the current management strategy, a TACC based on the average commercial catch from a 15 year period, and a TACC based on the average commercial catch from a 5 year period. Three further options use the data obtained from this study; these are based on the maximum sustainable yield (MSY) for the most productive species, the MSY for the least productive species, and a MSY based on the average of all three species. Since this project is interested only on the commercial catches, the management options discussed in this chapter refer only to the commercial catches. The additional allowances for recreational and customary fishing are ignored in this study.

5.2 Option 1

The first management option is based on the current management strategy. Currently the TACC is set at 2681 tonnes. This allowance is set at a high level above yearly catch, and allows fishers to capitalize on years with high abundance. This high level for the TACC was set in 1987, based on the catch from the 1983 fishing year (which was the highest ever recorded catch from FLA 3 on record [7]).

5.3 Option 2

The second option proposed in [7] is a TACC of 1780 tonnes. This figure comes from the average catch from the 15 year period between 1991 and 2006. This period allows for the natural variability in flatfish abundance that occurs over a number of years. This option sets the allowable catch at a level greater than the reported commercial catch per year for the last 10 fishing years. This means that effectively the behaviour of the fishers can remain unchanged, but this lower level of the TACC will close the gap between the TACC and yearly catch amounts, which can reduce the incidental by-catch of other species caught when targeting flatfish.

5.4 Option 3

A TACC of 1430 tonnes is proposed as the third option in [7]. This allowance is based on the average catch from the 5-year period from 2001-2006. This TACC is lower than that of option 2 due to the fact that there was a high level of catches in the years 1995-1996 and 1997-1998, which is not in the period considered for this TACC.

5.5 Option 4

The fourth management option is based on the data found in the previous chapter. The allowance for commercial catches for this option is 14902 tonnes for the Schaefer model, and 7572 tonnes for the Fox model. This TACC recommendation is based on the MSY for the most abundant stock (which is lemon sole (LSO) for the Schaefer

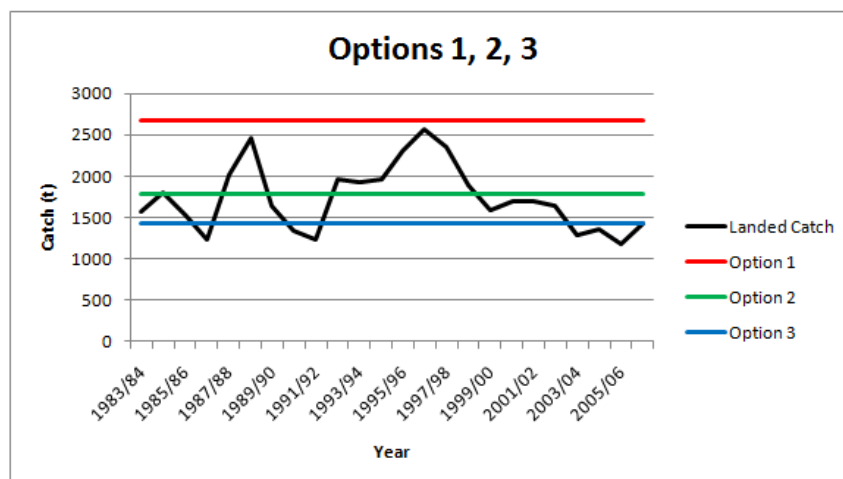


Figure 5.1: Landed Catch plotted with proposed TACC for management options 1,2 and 3 from recommendations from [7]

model and sand flounder (SFL) for the Fox model), so the catch for this option equals three times the MSY for LSO (or SFL), as calculated from the Bayesian parameter estimates from WinBUGS (see previous chapter). This option allows for the abundance in the most productive stock and allows catches to remain high for the abundant species.

5.6 Option 5

The fifth management option is based on the MSY for the least productive stock as calculated using the data from the previous chapter. The TACC recommendation for this option is 8738 tonnes for the Schaefer model and 5394 tonnes for the Fox model. This TACC recommendation is based on the MSY for the least abundant stock (which is New Zealand sole (ESO) for both models), so the catch for this option equals three times the MSY for ESO, as calculated from the Bayesian parameter estimates from WinBUGS (see previous chapter). This management strategy is a low risk option since it ensures sustainable production of the least abundant stock, and therefore the more abundant stocks as well. However, this catch is lower than that of option 4 and therefore there may potentially be a loss of profits due to decreased catches.

5.7 Option 6

The last option considered in this project is also based on the data from the previous chapter. The TACC recommendation for this option is 10568 tonnes for the Schaefer model and 6647 tonnes for the Fox model. Here the TACC is based on the MSY for the average of the three species, as calculated from the Bayesian parameter estimates from WinBUGS (see previous chapter). This method reconciles with the previous two methods in that it provides a middle ground between setting the TACC too high and setting it too low.

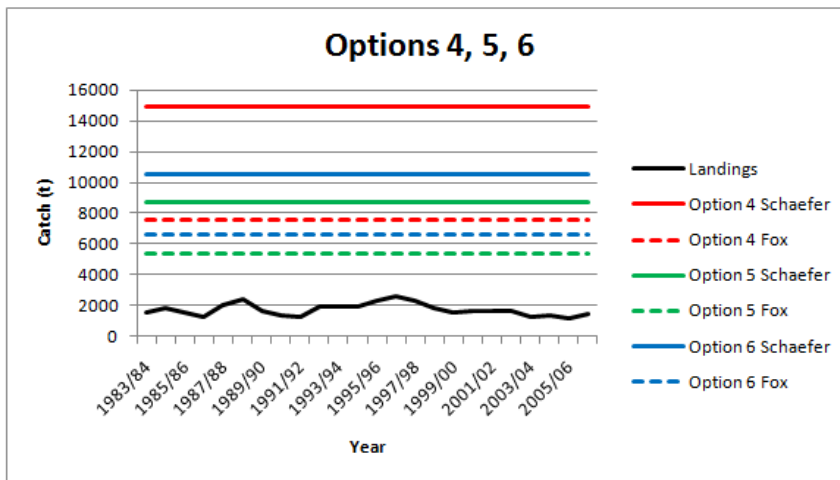


Figure 5.2: Landed Catch plotted with proposed TACC for management options 4, 5 and 6 from bayesian estimates calculated in previous chapter

Table 5.1: Management Options with recommended TACC's

	Basis for Recommendation	Recommended TACC (t)
Option 1	Status Quo	2681
Option 2	15-year average	1780
Option 3	5-year average	1430
Option 4	MSY (LSO)	14902-Schaefer, 75210-Fox
Option 5	MSY (SFL)	8738-Schaefer, 29958-Fox
Option 6	MSY (Combined)	10568-Schaefer, 59416-Fox

Chapter 6

RISK ASSESSMENT

6.1 Introduction

This chapter contains figures from Matlab showing the results from the work described in the previous chapters. The sections are divided into the six management options described in Chapter 5. Both simulation models described in Chapter 3 were applied to each management option for the Schaefer model and Fox model. For each management option there are four figures - two for each of the simulation models, with 1000 simulations for each of the species. The simulations are coloured according to the behaviour of the simulation based on whether they are stable and converge to a positive number (green), oscillating indefinitely (red), or are decreasing towards 0 (blue). For each run, the number of simulations which ended above the Maximum Sustainable Yield (MSY) were recorded (above $0.5K$ for the Schaefer model, and above $0.386K$ for the Fox model), as well as those which ended below 10% and 20% of the starting biomass. The results are described in this chapter, and analysed in the following chapters.

6.2 Option 1

The Matlab code for $m = 1$ and $m = 2$ was implemented with $catch = 2681$. The results are summarized in Table 6.1 as well as in Figures 6.1, 6.2, 6.3, 6.4.

Table 6.1: Summary of results for option 1

Species	Type	Simulation Model 1		Simulation Model 2	
		Schaefer	Fox	Schaefer	Fox
ESO	Above 0.5K	97.5	84.2	98.2	88.4
	Above 0.368K	97.6	85.6	98.6	89.9
	Less than 20%	2.4	12.8	1.2	8.6
	Less than 10%	2.4	12.4	1.2	8.1
LSO	Above 0.5K	95.7	83.0	97.5	75.7
	Above 0.368K	96.3	85.3	98.6	80.5
	Less than 20%	3.3	12.2	1.2	15.6
	Less than 10%	3.3	12.2	1.2	14.9
SFL	Above 0.5K	98.1	88.5	98.1	81.7
	Above 0.368K	98.1	89.6	98.4	85.7
	Less than 20%	1.8	8.0	1.4	10.6
	Less than 10%	1.8	8.0	1.4	10.1

Figures in the table represent the probability of the simulations ending above 0.5K (B_{MSY} for Schaefer model), above 0.368K (B_{MSY} for Fox model), below 10% of the starting (virgin) biomass, and below 20% of the starting biomass.

6.2.1 Schaefer Model

Using the Schaefer model the management strategy is low risk with a very low percentage (less than 5%) of the simulations going below 10% of the virgin biomass for each of the three species for both simulation types.

6.2.2 Fox Model

Using the current catch quota, the management strategy is also a low risk option for the Fox model. The percentage of simulations which go below 20% of the virgin biomass is relatively low (below 15%) for ESO and LSO and low (below 10%) for SFL for the first simulation type. This behaviour is expected for this simulation type since the fishers will continue to catch a higher amount of ESO and LSO than SFL. For the second simulation type, however, the percentage of simulations which go below 20% of the virgin biomass is higher for LSO (just above 15%), and more even for ESO and SFL (around 10% for each). This is expected since fishers will begin to catch more of the less abundant species when the population of the most abundant species begins to decrease.

The following three figures are for the Schaefer model:

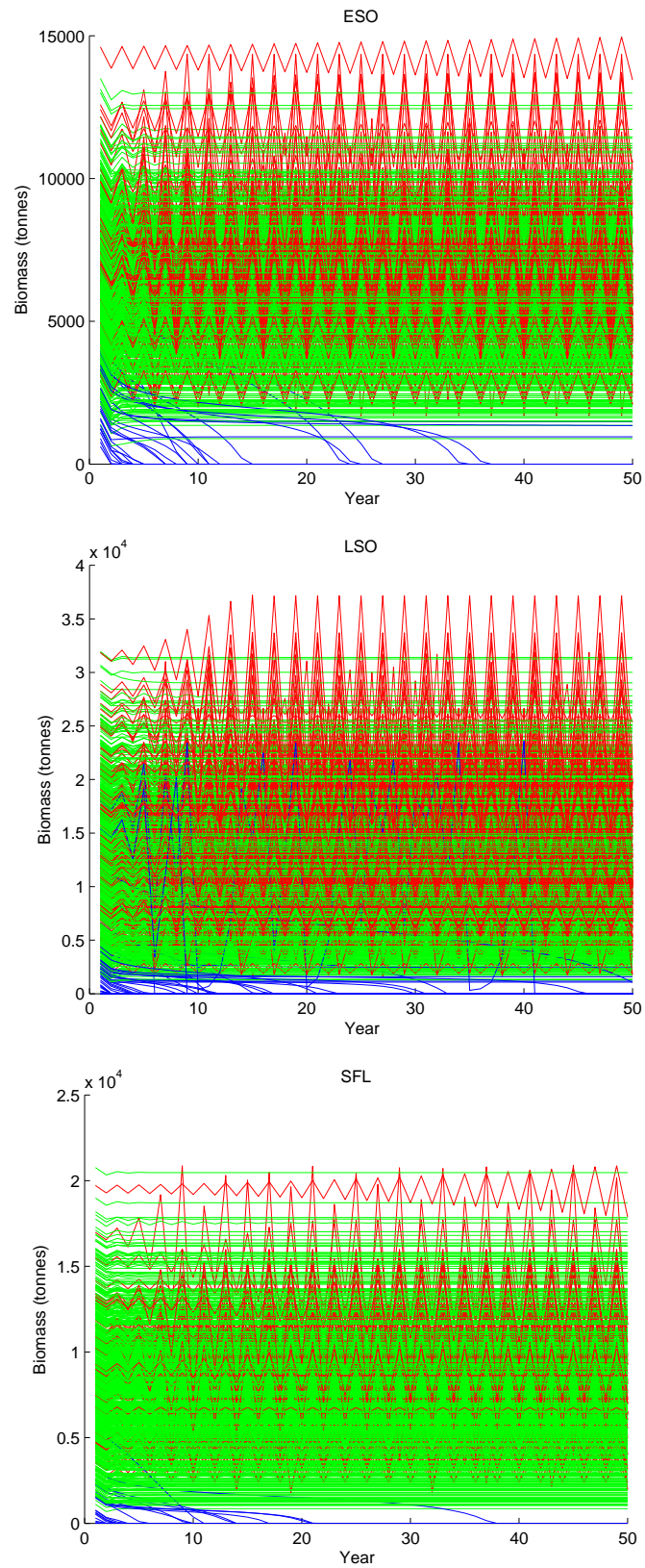


Figure 6.1: Option 1 - Simulation Model 1 (green line: stable converging, blue: decreasing towards zero, red: oscillating)

The following three figures are for the Fox model:

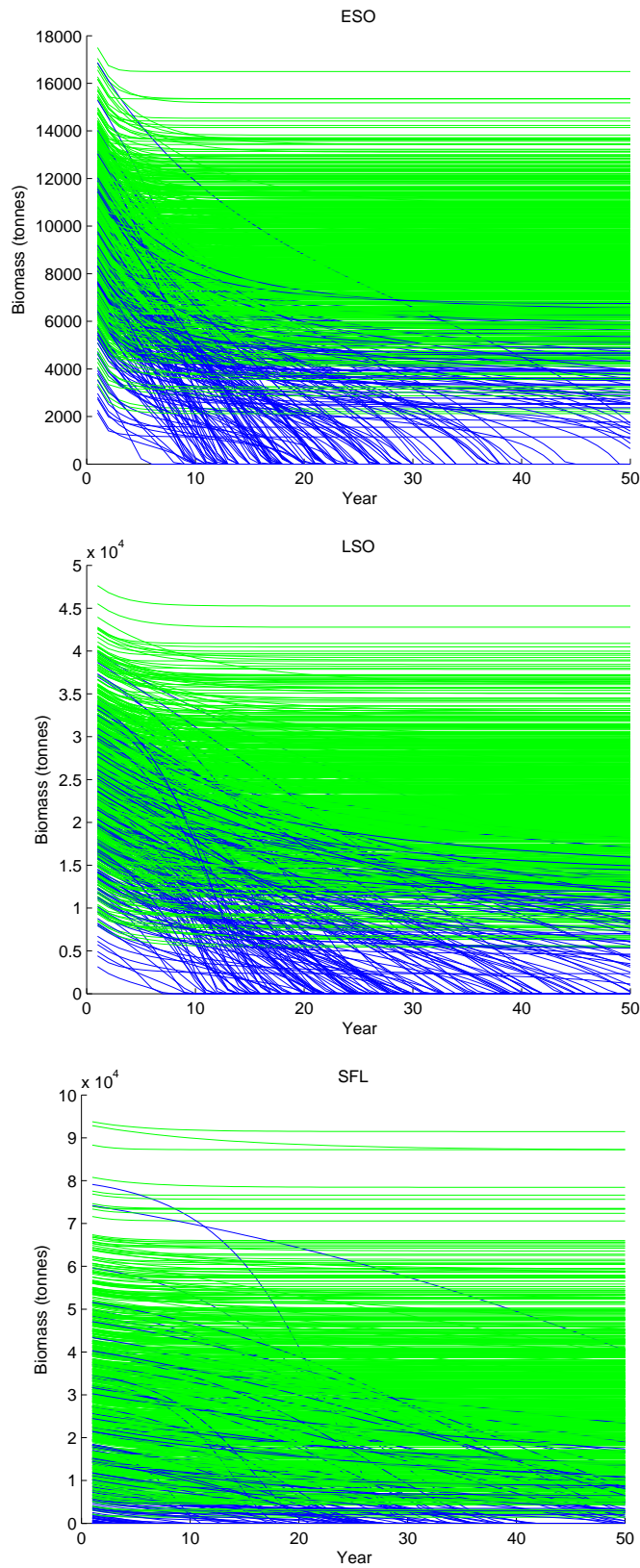


Figure 6.2: Option 1 - Simulation Model 1 (green line: stable converging, blue: decreasing towards zero, red: oscillating)

The following three figures are for the Schaefer model:

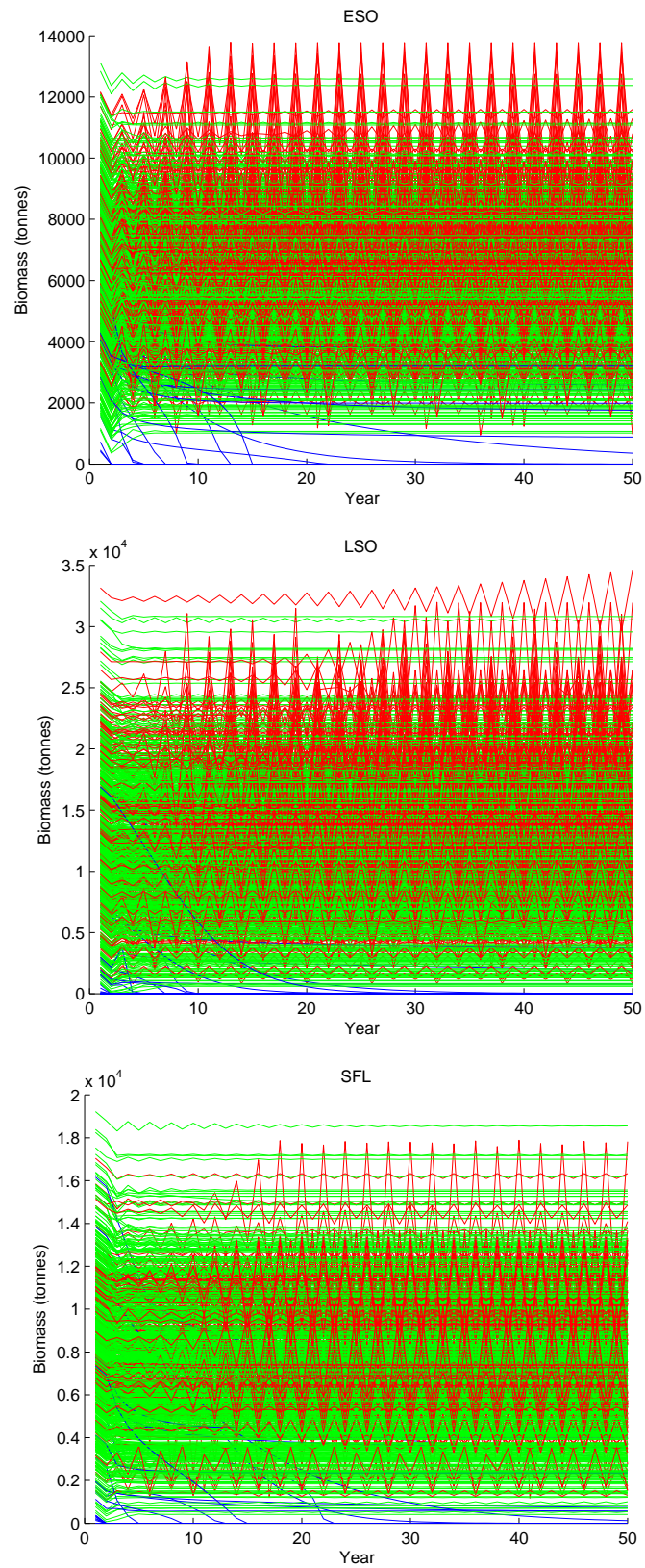


Figure 6.3: Option 1 - Simulation Model 2 (green line: stable converging, blue: decreasing towards zero, red: oscillating)

The following three figures are for the Fox model:

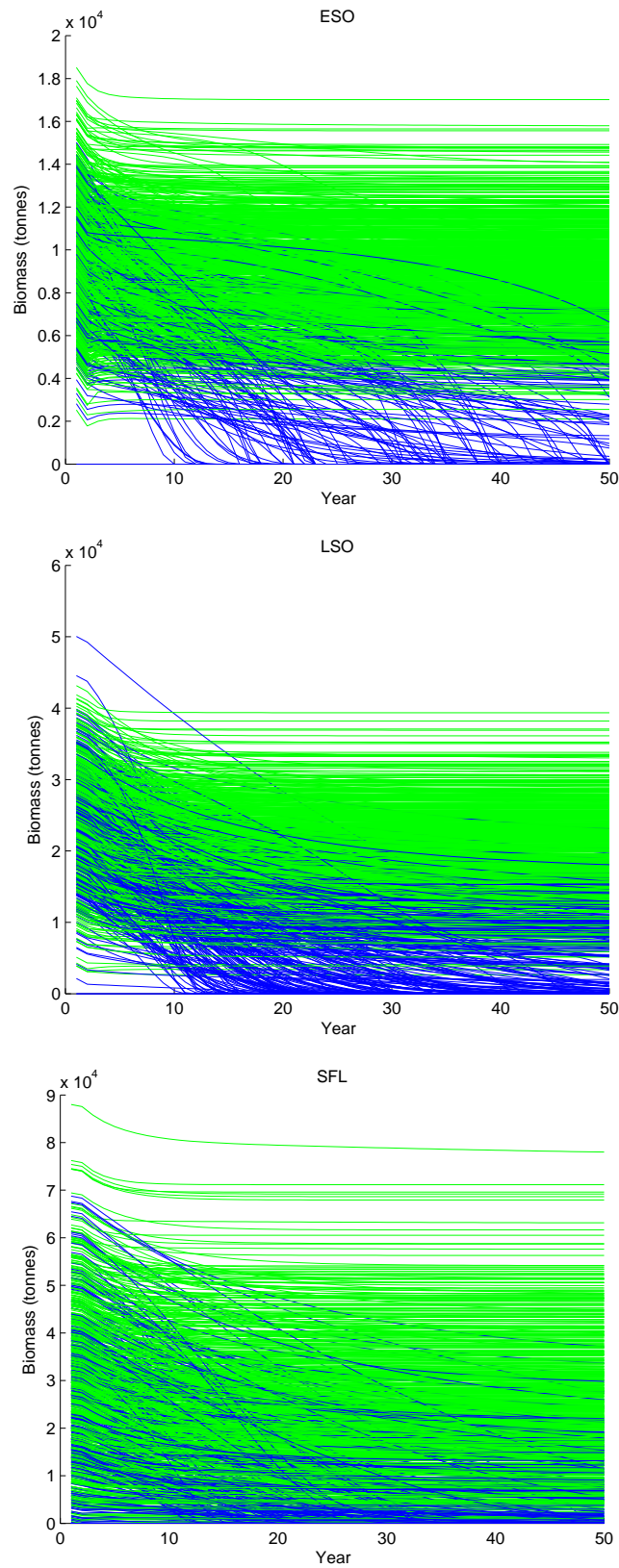


Figure 6.4: Option 1 - Simulation Model 2 (green line: stable converging, blue: decreasing towards zero, red: oscillating)

6.3 Option 2

The Matlab code for $m = 1$ and $m = 2$ was implemented with $catch = 1780$. The results for option 2 are summarized in Table 6.2 and in Figures 6.5, 6.6, 6.7, 6.8.

Table 6.2: Summary of results for option 2

Species	Type	Simulation Model 1		Simulation Model 2	
		Schaefer	Fox	Schaefer	Fox
ESO	Above 0.5K	98.8	90.9	99.0	93.8
	Above 0.368K	98.8	92.7	99.3	94.4
	Less than 20%	1.2	6.3	0.5	4.7
	Less than 10%	1.2	6.2	0.5	4.7
LSO	Above 0.5K	97.5	87.5	98.8	85.0
	Above 0.368K	98.2	89.5	99.0	86.6
	Less than 20%	1.8	7.4	0.7	10.1
	Less than 10%	1.8	7.4	0.6	9.3
SFL	Above 0.5K	97.8	91.7	99.2	89.3
	Above 0.368K	97.9	92.7	99.3	91.0
	Less than 20%	2.0	6.4	0.7	6.7
	Less than 10%	2.0	6.4	0.5	6.2

Figures in the table represent the probability of the simulations ending above 0.5K (B_{MSY} for Schaefer model), above 0.368K (B_{MSY} for Fox model), below 10% of the starting (virgin) biomass, and below 20% of the starting biomass.

6.3.1 Schaefer Model

This management is a low risk option for all three species, with less than 5% of simulations going below 10% of the virgin biomass, and over 95% of simulations remaining above the MSY for all of the three species and for both simulation types.

6.3.2 Fox Model

This management strategy for the Fox model is also a low risk strategy, since less than 10% of simulations ended below 10% of the virgin biomass of each of the three species. For both simulation models over 85% of simulations remain above the MSY for the Fox model (above 0.368K).

The following three figures are for the Schaefer model:

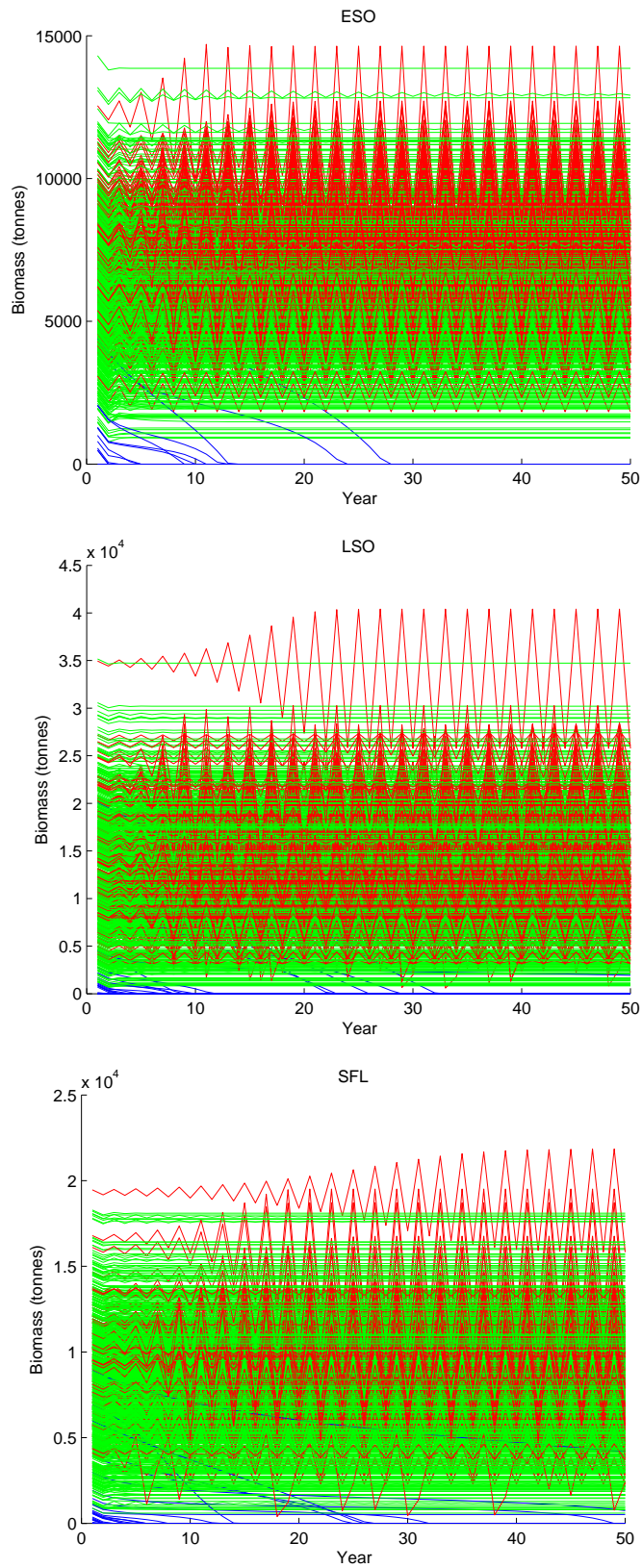


Figure 6.5: Option 2 - Simulation Model 1 (green line: stable converging, blue: decreasing towards zero, red: oscillating)

The following three figures are for the Fox model:

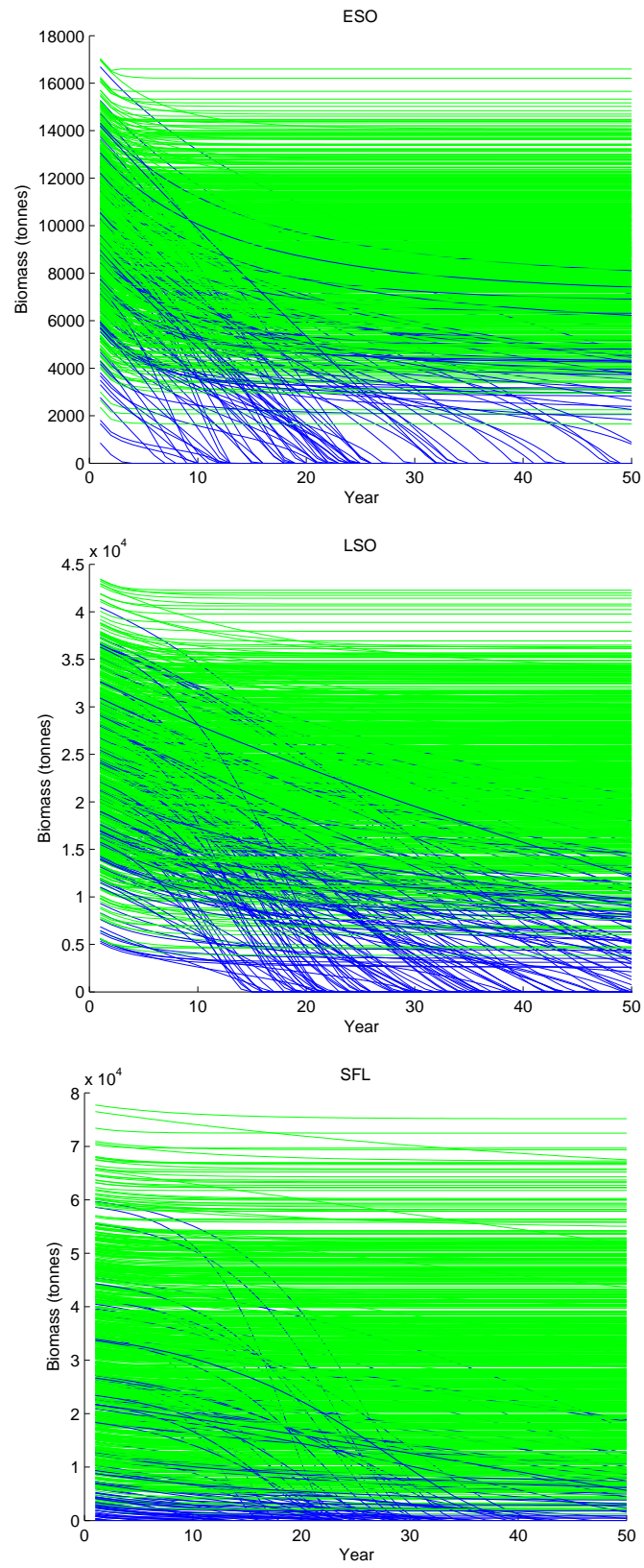


Figure 6.6: Option 2 - Simulation Model 1 (green line: stable converging, blue: decreasing towards zero, red: oscillating)

The following three figures are for the Schaefer model:

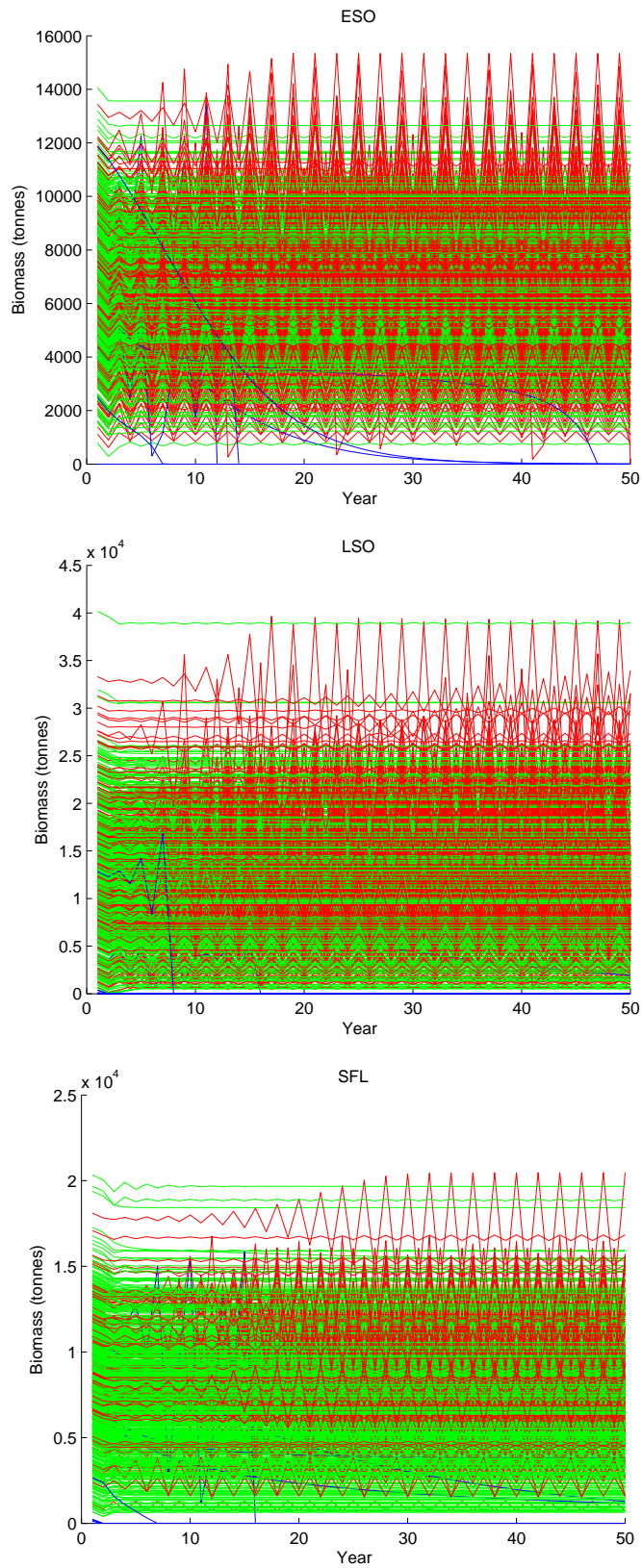


Figure 6.7: Option 2 - Simulation Model 2 (green line: stable converging, blue: decreasing towards zero, red: oscillating)

The following three figures are for the Fox model:

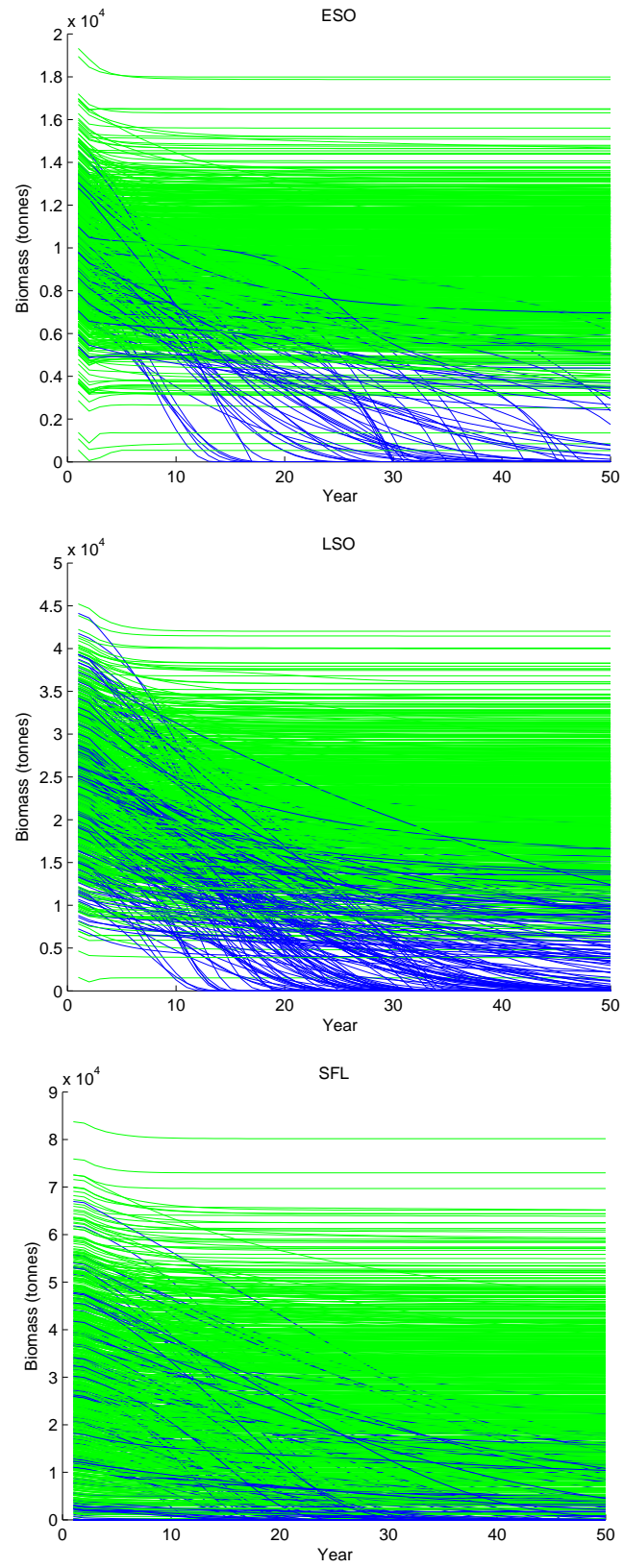


Figure 6.8: Option 2 - Simulation Model 2 (green line: stable converging, blue: decreasing towards zero, red: oscillating)

6.4 Option 3

Implement Matlab code for $m = 1$, and $m = 2$, with $catch = 1430$. The results are summarized in Table 6.3 below along with Figures 6.9, 6.10, 6.11, 6.12 in the following pages.

Table 6.3: Summary of results for option 3

Species	Type	Simulation Model 1		Simulation Model 2	
		Schaefer	Fox	Schaefer	Fox
ESO	Above 0.5K	98.7	93.5	99.6	94.6
	Above 0.368K	98.7	94.7	99.9	95.6
	Less than 20%	1.3	4.6	0.1	3.5
	Less than 10%	1.3	4.6	0.1	3.4
LSO	Above 0.5K	97.8	90.3	97.6	86.2
	Above 0.368K	98.4	90.9	97.8	88.0
	Less than 20%	1.5	6.8	1.9	8.5
	Less than 10%	1.5	6.8	1.8	7.7
SFL	Above 0.5K	98.8	91.9	99.1	90.6
	Above 0.368K	99.0	93.2	99.3	92.0
	Less than 20%	1.0	4.7	0.6	5.4
	Less than 10%	1.0	4.6	0.5	4.8

Figures in the table represent the probability of the simulations ending above 0.5K (B_{MSY} for Schaefer model), above 0.368K (B_{MSY} for Fox model), below 10% of the starting (virgin) biomass, and below 20% of the starting biomass.

6.4.1 Schaefer Model

This management option is a low risk option for the Schaefer model since both simulation types result in less than 2% of simulations ending below 10% of the virgin biomass for each of the three species.

6.4.2 Fox Model

For the Fox model, this is also a very low risk management option. For both simulation models, over 85% of simulations remain above the MSY, meaning the stock is likely to remain at sustainable levels under this management option. This option has the lowest catch amount of the six management options proposed in this study, and is the least risky option.

The following three figures are for the Schaefer model:

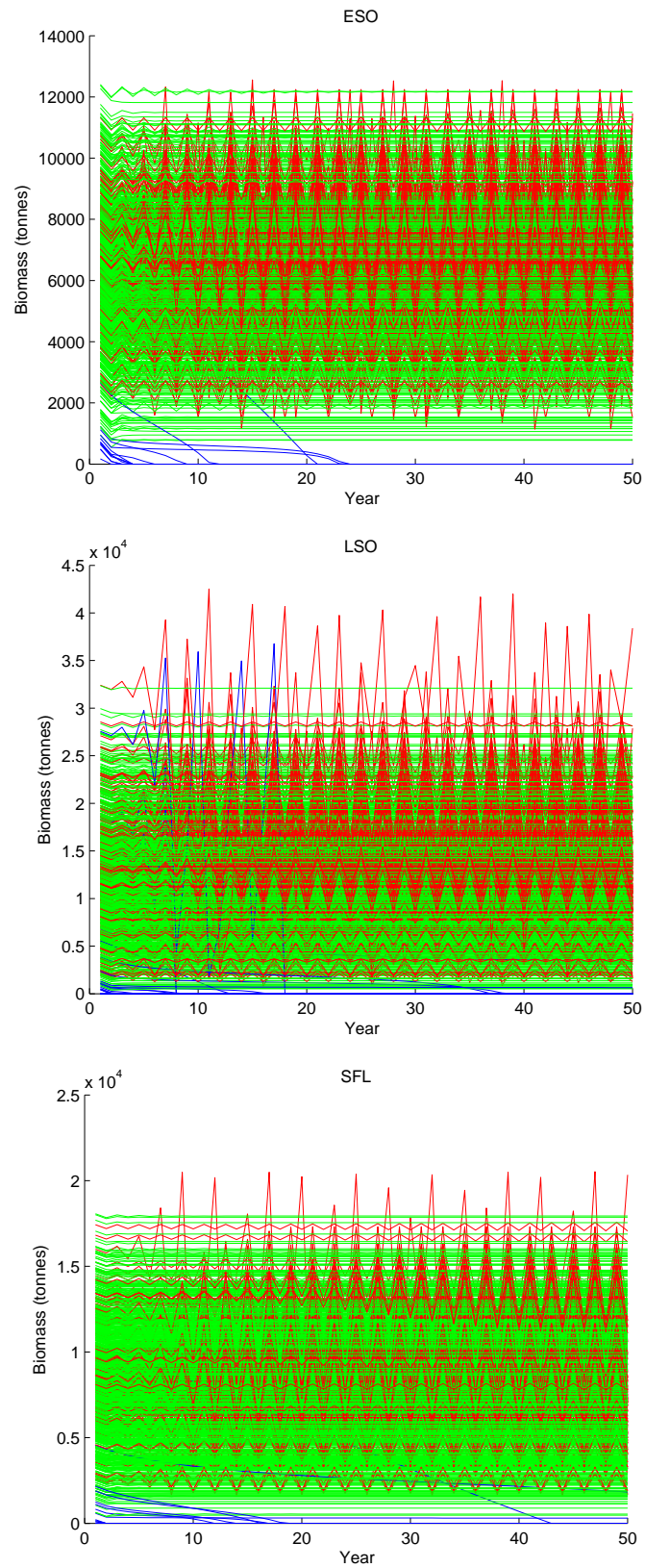


Figure 6.9: Option 3 - Simulation Model 1 (green line: stable converging, blue: decreasing towards zero, red: oscillating)

The following three figures are for the Fox model:

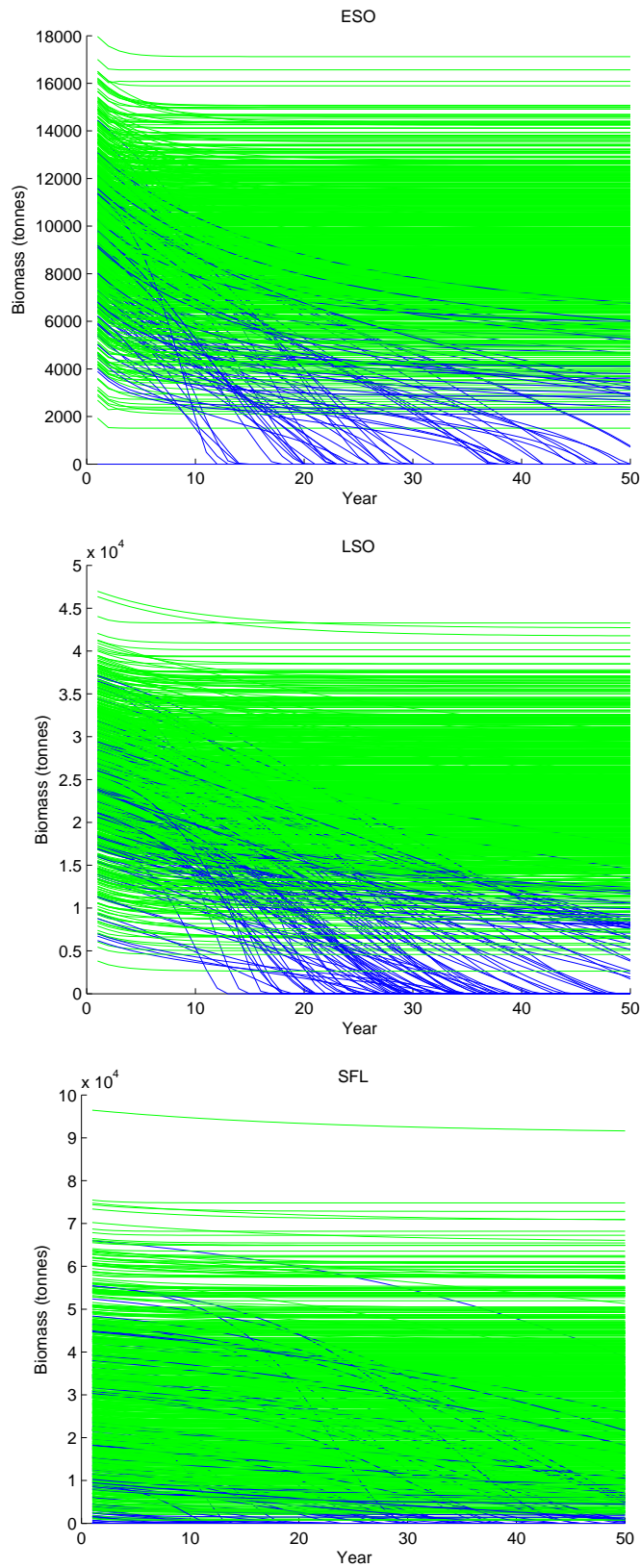


Figure 6.10: Option 3 - Simulation Model 1 (green line: stable converging, blue: decreasing towards zero, red: oscillating)

The following three figures are for the Schaefer model:

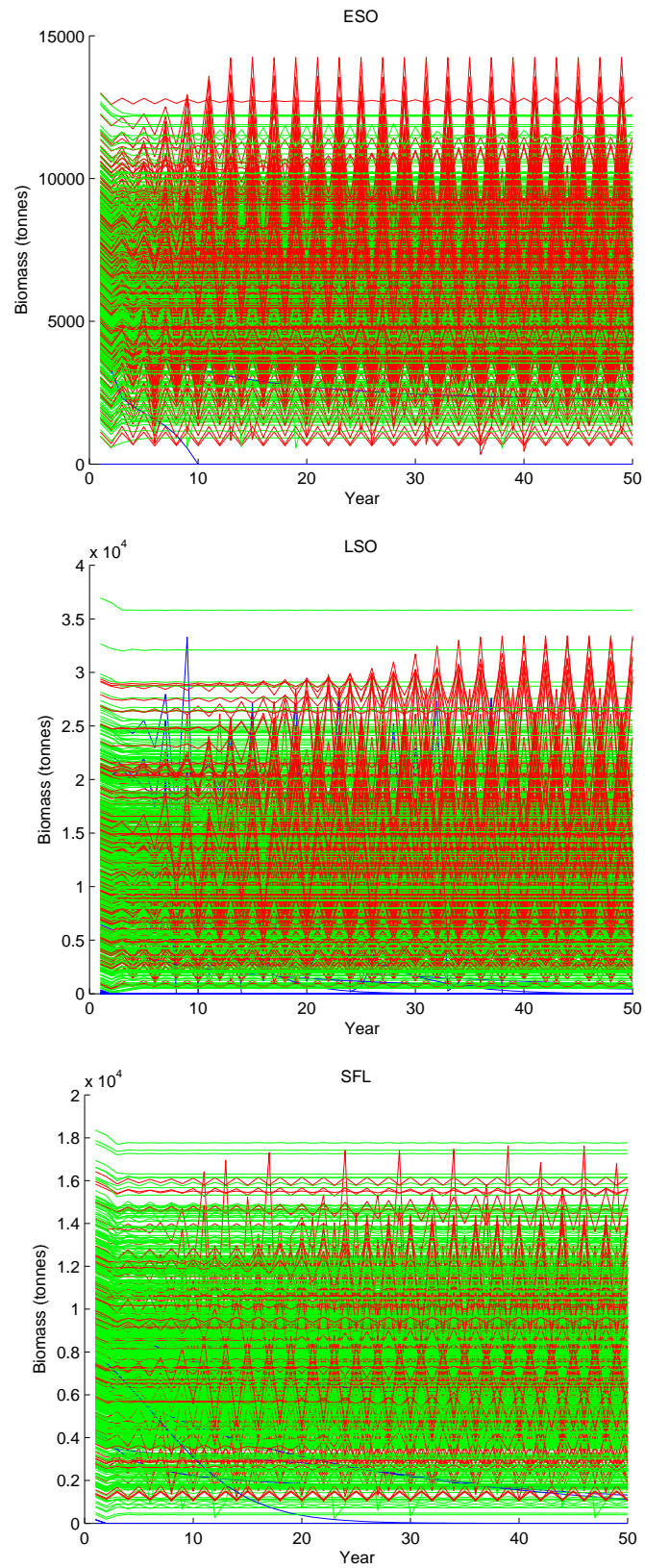


Figure 6.11: Option 3 - Simulation Model 2 (green line: stable converging, blue: decreasing towards zero, red: oscillating)

The following three figures are for the Fox model:

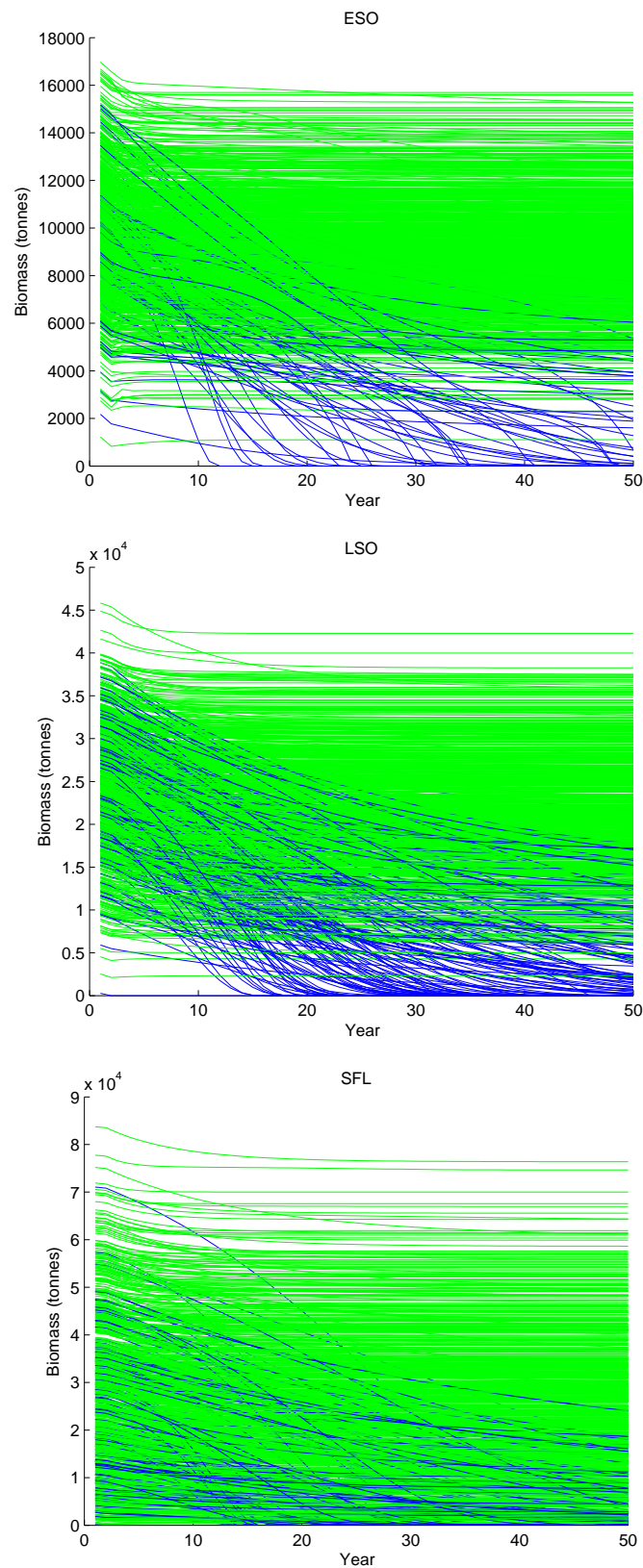


Figure 6.12: Option 3 - Simulation Model 2 (green line: stable converging, blue: decreasing towards zero, red: oscillating)

6.5 Option 4

Implement Matlab code for $m = 1$ and $m = 2$, with $catch = 14902$ for the Schaefer model and $catch = 7572$ for the Fox model. The results are summarized in Table 6.4 and in Figures 6.13, 6.14, 6.15, 6.16 in the following pages.

Table 6.4: Summary of results for option 4

Species	Type	Simulation Model 1		Simulation Model 2	
		Schaefer	Fox	Schaefer	Fox
ESO	Above 0.5K	11.1	29.7	8.0	27.1
	Above 0.368K	11.3	33.7	9.2	29.4
	Less than 20%	88.7	65.6	90.5	67.5
	Less than 10%	88.7	65.6	90.5	66.9
LSO	Above 0.5K	57.0	45.5	12.6	18.9
	Above 0.368K	57.1	49.6	12.9	26.3
	Less than 20%	42.8	45.9	86.9	69.4
	Less than 10%	42.8	45.9	86.9	68.2
SFL	Above 0.5K	58.6	74.1	8.2	29.5
	Above 0.368K	58.6	76.3	9.5	35.3
	Less than 20%	41.2	20.9	89.9	59.4
	Less than 10%	41.2	20.7	89.8	59.0

Figures in the table represent the probability of the simulations ending above 0.5K (B_{MSY} for Schaefer model), above 0.368K (B_{MSY} for Fox model), below 10% of the starting (virgin) biomass, and below 20% of the starting biomass.

6.5.1 Schaefer Model

For simulation model 1 this management strategy has high risk for ESO (less than 15% of simulations ending above MSY) and medium risk for LSO and SFL (less than 60% of simulations ending above MSY). However, using the second simulation model, this strategy is high risk for all of the three species.

6.5.2 Fox Model

For the first simulation model, the risk is reasonably high for ESO with less than 25% of simulations ending above the MSY, less risky for LSO, and even less risky for SFL. However, for the second simulation model, this method has medium risk for all three species with less than 40% of simulations ending above the MSY.

The following three figures are for the Schaefer model:

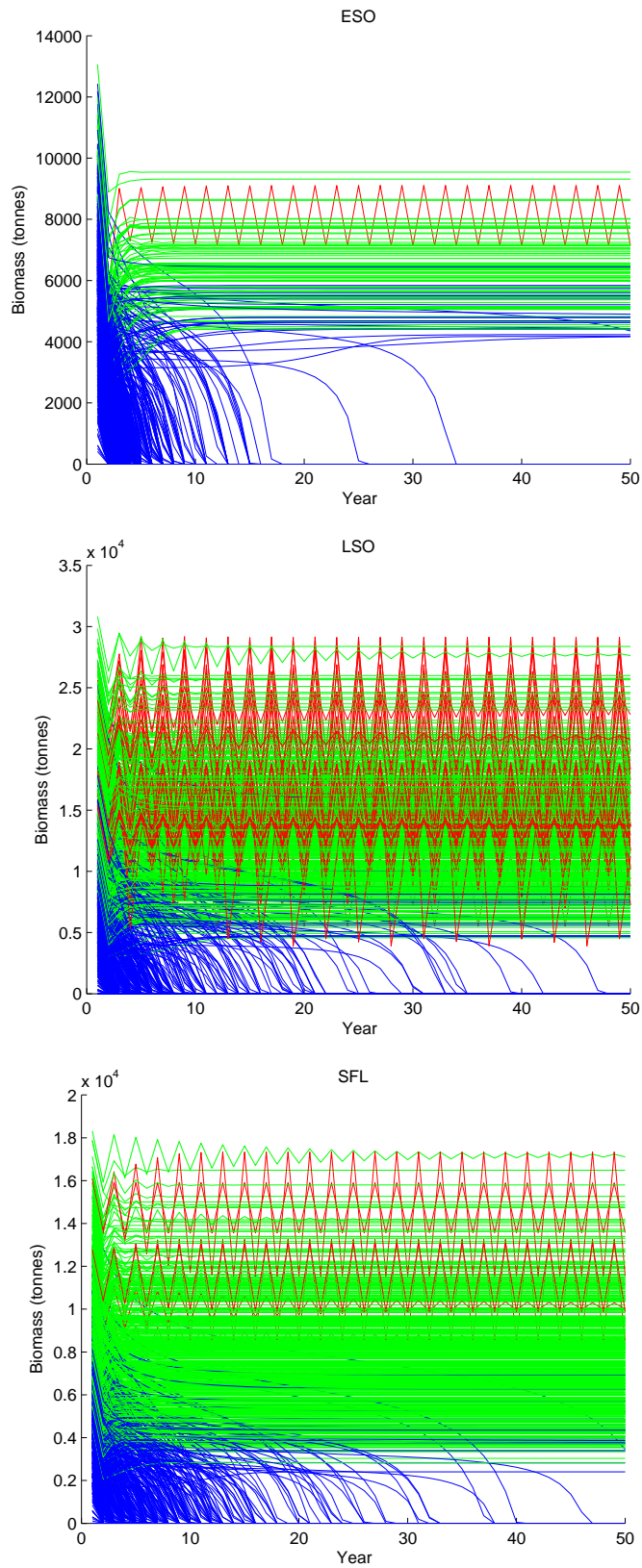


Figure 6.13: Option 4 - Simulation Model 1 (green line: stable converging, blue: decreasing towards zero, red: oscillating)

The following three figures are for the Fox model:

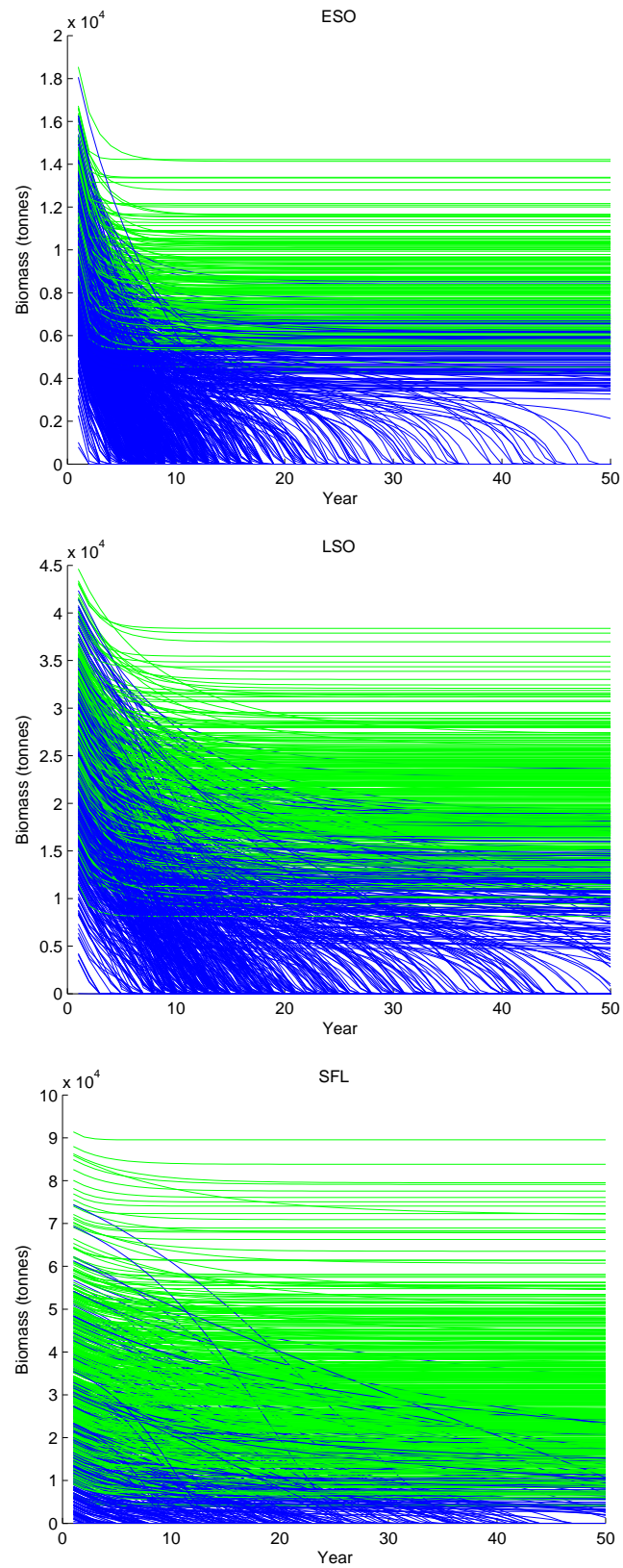


Figure 6.14: Option 4 - Simulation Model 1 (green line: stable converging, blue: decreasing towards zero, red: oscillating)

The following three figures are for the Schaefer model:

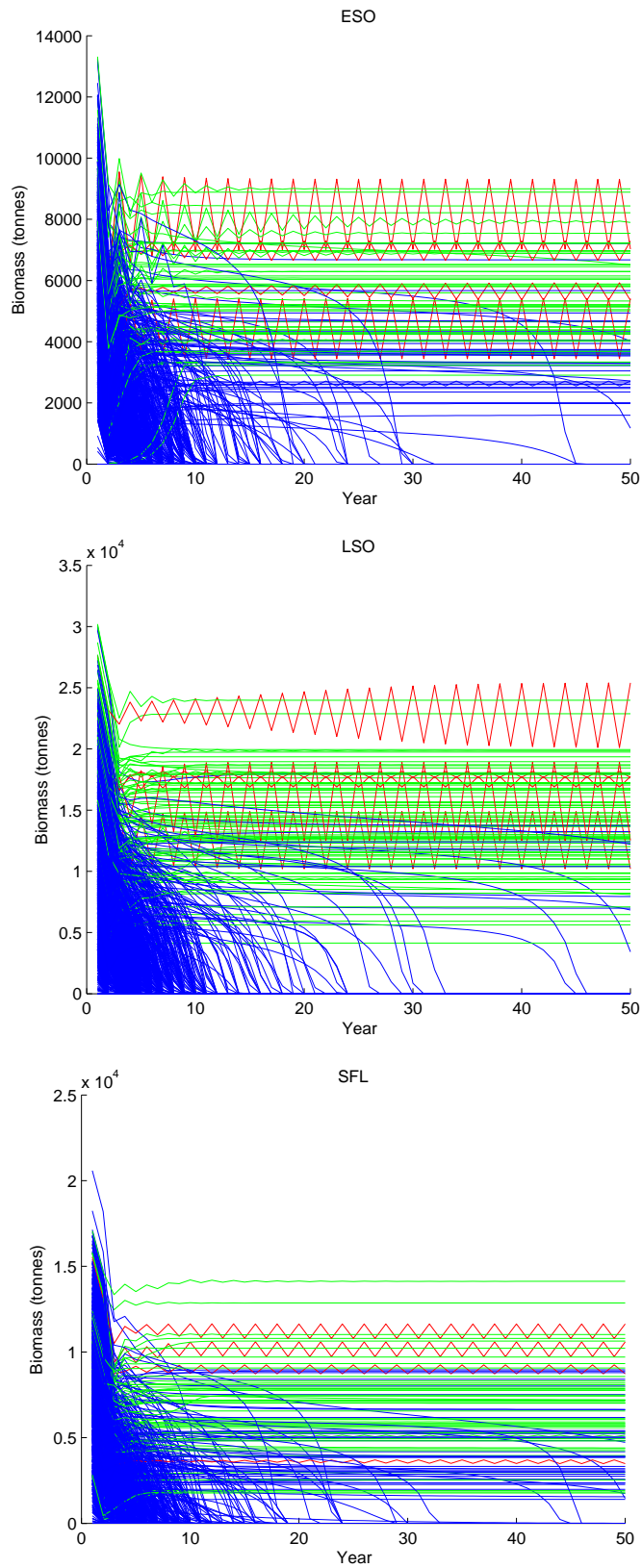


Figure 6.15: Option 4 - Simulation Model 2 (green line: stable converging, blue: decreasing towards zero, red: oscillating)

The following three figures are for the Fox model:

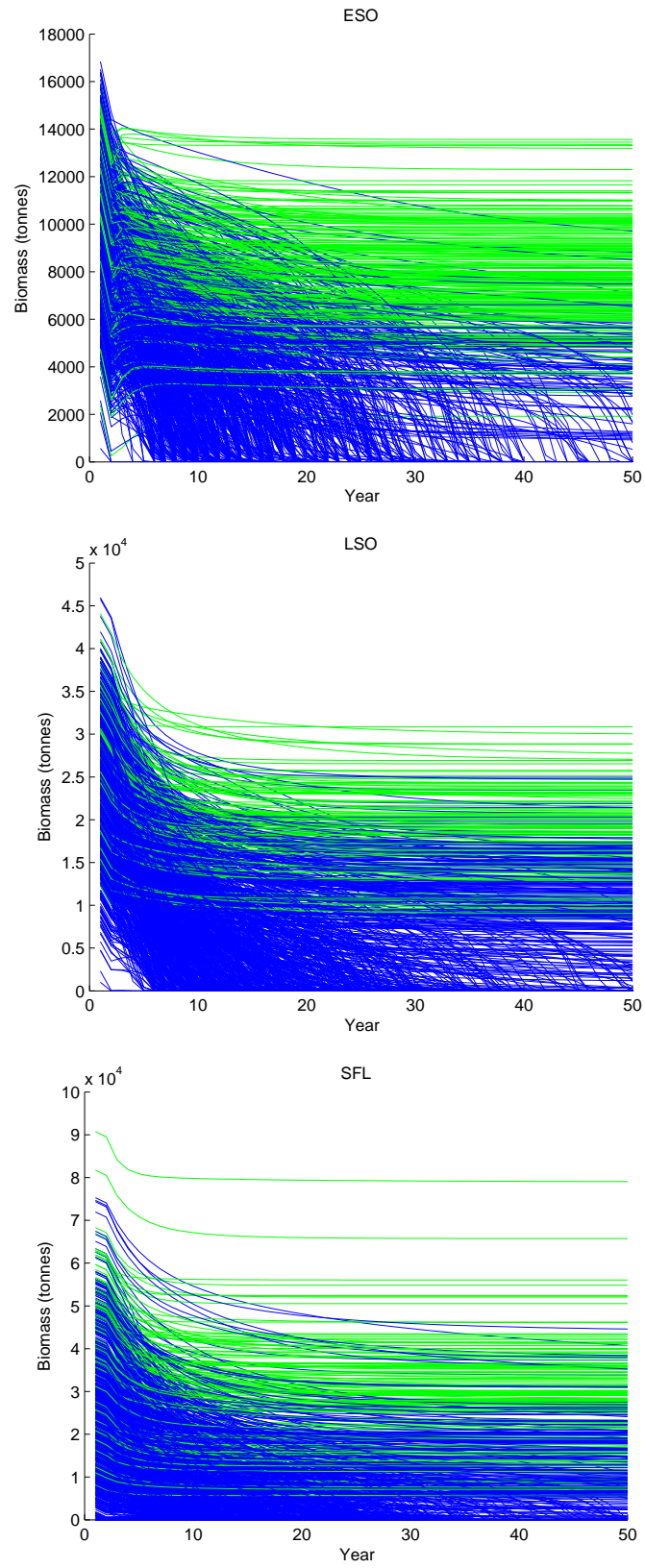


Figure 6.16: Option 4 - Simulation Model 2 (green line: stable converging, blue: decreasing towards zero, red: oscillating)

6.6 Option 5

Implement Matlab code for $m = 1$ and $m = 2$, with $catch = 8738$ for the Schaefer model and $catch = 5394$ for the Fox model. The results are summarized in Table 6.5 below as well as Figures 6.17, 6.18, 6.19, 6.20 in the following pages.

Table 6.5: Summary of results for option 5

Species	Type	Simulation Model 1		Simulation Model 2	
		Schaefer	Fox	Schaefer	Fox
ESO	Above 0.5K	55.0	55.0	59.8	55.8
	Above 0.368K	60.4	59.5	60.9	60.0
	Less than 20%	38.7	39.1	38.7	37.0
	Less than 10%	38.6	39.1	38.7	36.4
LSO	Above 0.5K	62.6	62.4	63.9	43.6
	Above 0.368K	65.9	66.8	65.1	51.5
	Less than 20%	30.3	29.2	34.4	40.5
	Less than 10%	30.3	29.2	34.4	38.9
SFL	Above 0.5K	77.8	81.2	57.7	51.4
	Above 0.368K	80.5	83.3	60.0	58.9
	Less than 20%	14.4	45.0	38.8	34.5
	Less than 10%	14.4	42.5	38.3	33.1

Figures in the table represent the probability of the simulations ending above 0.5K (B_{MSY} for Schaefer model), above 0.368K (B_{MSY} for Fox model), below 10% of the starting (virgin) biomass, and below 20% of the starting biomass.

6.6.1 Schaefer Model

This management option is a medium to low risk for each of the species using the Schaefer model, with more than 50% of the simulations ending above the MSY for both simulation models and less than 40% of simulations ending below 10% of the virgin biomass.

6.6.2 Fox Model

Using the Fox model this management strategy is also a medium to low risk option, with more than 55% of the simulations for the first simulation model ending above the MSY, and more than 50% of the simulations ending above the MSY for the second simulation model.

The following three figures are for the Schaefer model:

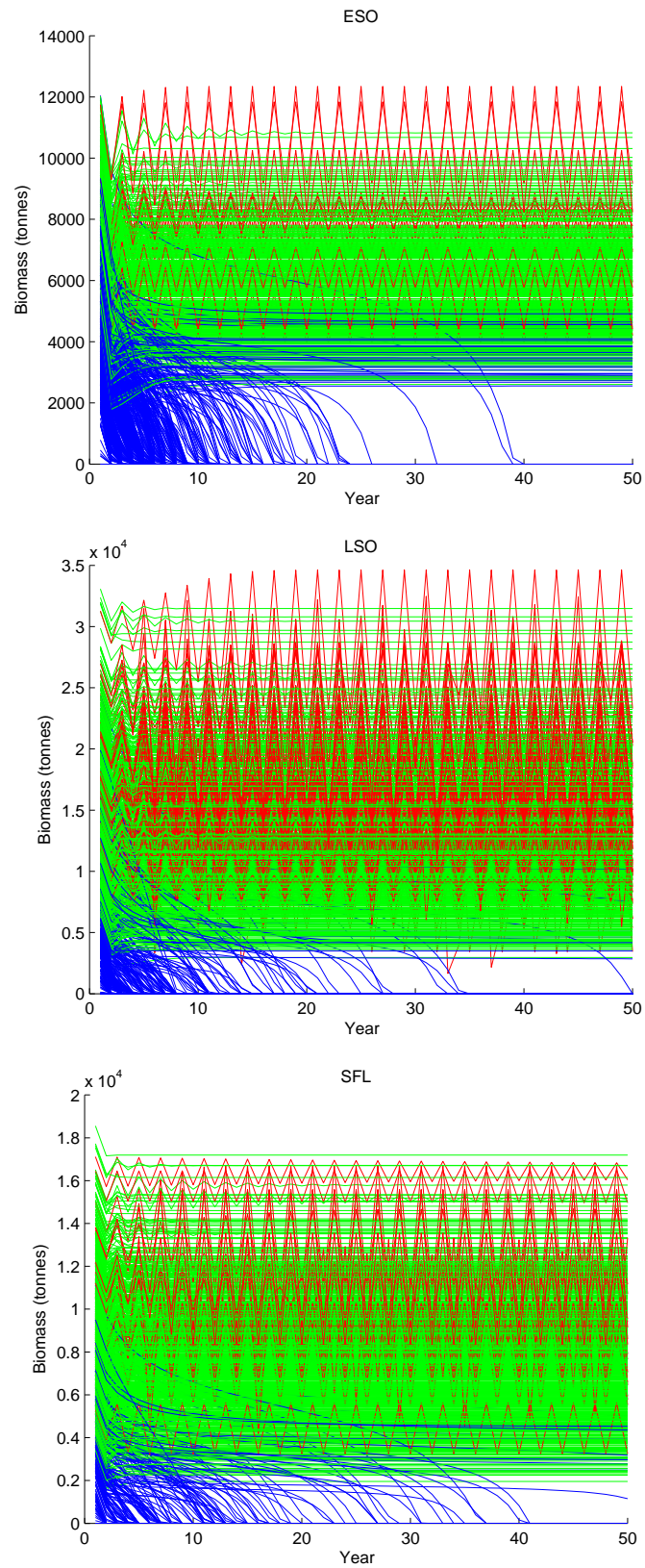


Figure 6.17: Option 5 - Simulation Model 1 (green line: stable converging, blue: decreasing towards zero, red: oscillating)

The following three figures are for the Fox model:

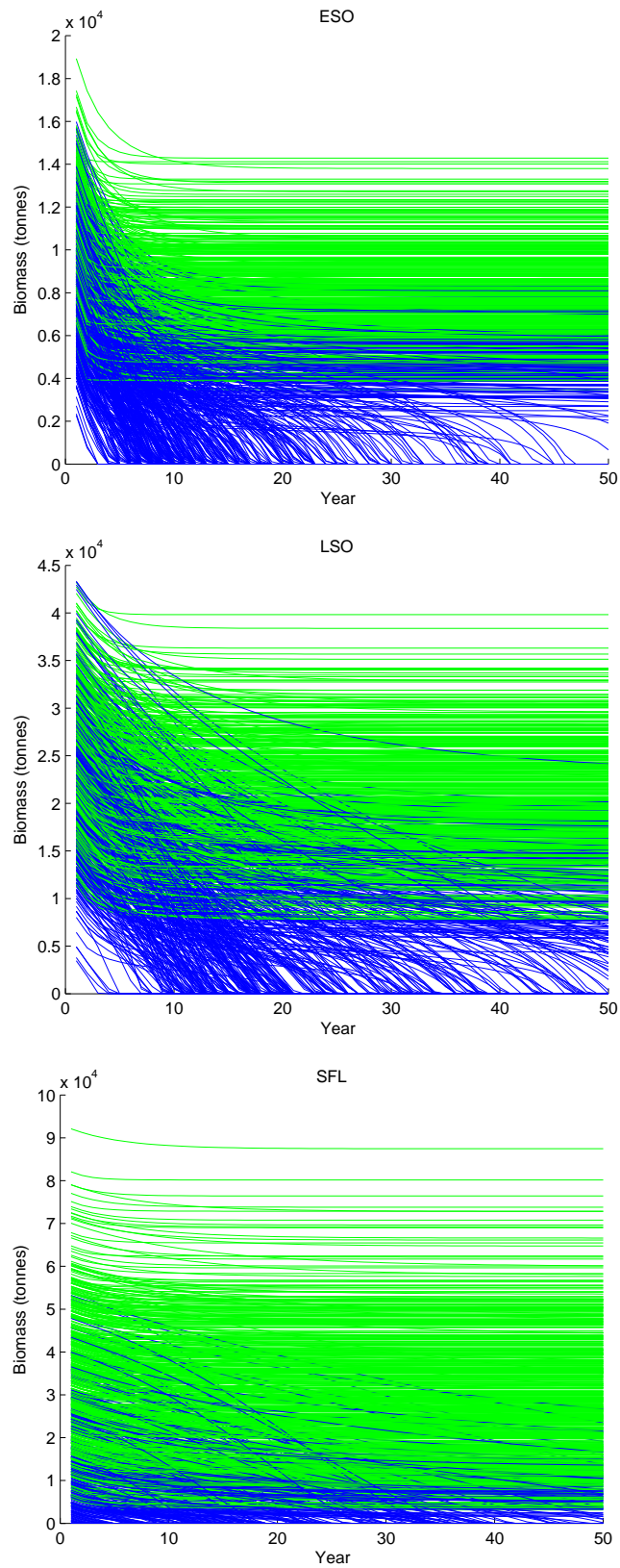


Figure 6.18: Option 5 - Simulation Model 1 (green line: stable converging, blue: decreasing towards zero, red: oscillating)

The following three figures are for the Schaefer model:

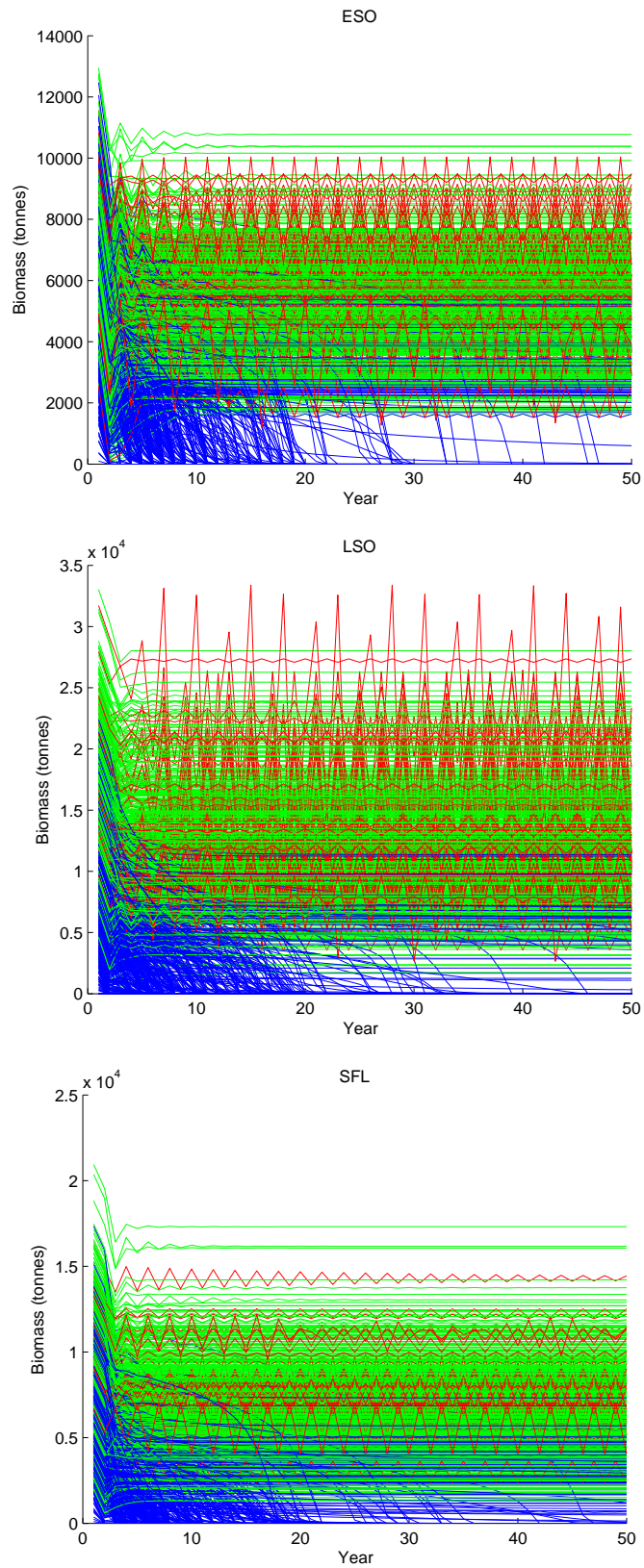


Figure 6.19: Option 5 - Simulation Model 2 (green line: stable converging, blue: decreasing towards zero, red: oscillating)

The following three figures are for the Fox model:

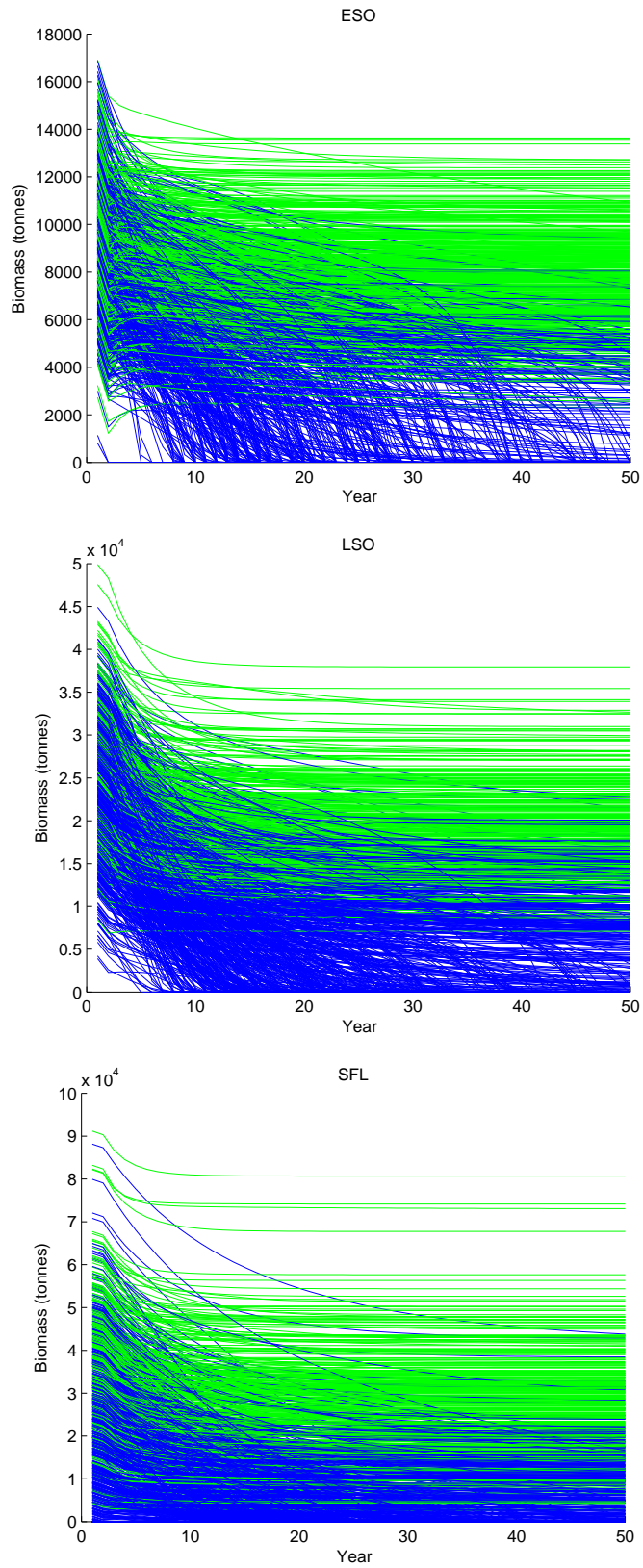


Figure 6.20: Option 5 - Simulation Model 2 (green line: stable converging, blue: decreasing towards zero, red: oscillating)

6.7 Option 6

Implement Matlab code for $m = 1$ and $m = 2$, with $catch = 10568$ for the Schaefer model and $catch = 6647$ for the Fox model. The results are summarized in Table 6.6 below along with Figures 6.21, 6.22, 6.23, 6.24 in the following pages.

Table 6.6: Summary of results for option 6

Species	Type	Simulation Model 1		Simulation Model 2	
		Schaefer	Fox	Schaefer	Fox
ESO	Above 0.5K	36.7	37.5	39.1	34.6
	Above 0.368K	36.8	43.1	40.0	38.9
	Less than 20%	62.9	56.0	59.2	58.0
	Less than 10%	62.9	55.9	59.0	57.2
LSO	Above 0.5K	72.6	47.8	42.7	26.5
	Above 0.368K	72.8	52.8	44.1	34.4
	Less than 20%	27.2	43.5	55.5	59.4
	Less than 10%	27.2	43.5	55.5	57.8
SFL	Above 0.5K	77.2	73.8	38.0	35.7
	Above 0.368K	77.3	76.7	40.3	42.3
	Less than 20%	22.5	19.8	58.7	51.8
	Less than 10%	22.5	19.8	58.4	50.7

Figures in the table represent the probability of the simulations ending above 0.5K (B_{MSY} for Schaefer model), above 0.368K (B_{MSY} for Fox model), below 10% of the starting (virgin) biomass, and below 20% of the starting biomass.

6.7.1 Schaefer Model

This management strategy is medium to high risk for ESO for the first simulation model and low risk for LSO and SFL for the Schaefer model. For the second simulation model, the strategy is medium risk for the three species with over 50% of simulations falling below 10% of the virgin biomass.

6.7.2 Fox Model

For the Fox model this strategy is low risk for SFL and medium risk for ESO and LSO for the first simulation model. For the second simulation model, this method is medium risk for all three species with more than 50% of the simulations ending below 10% of the virgin biomass.

The following three figures are for the Schaefer model:

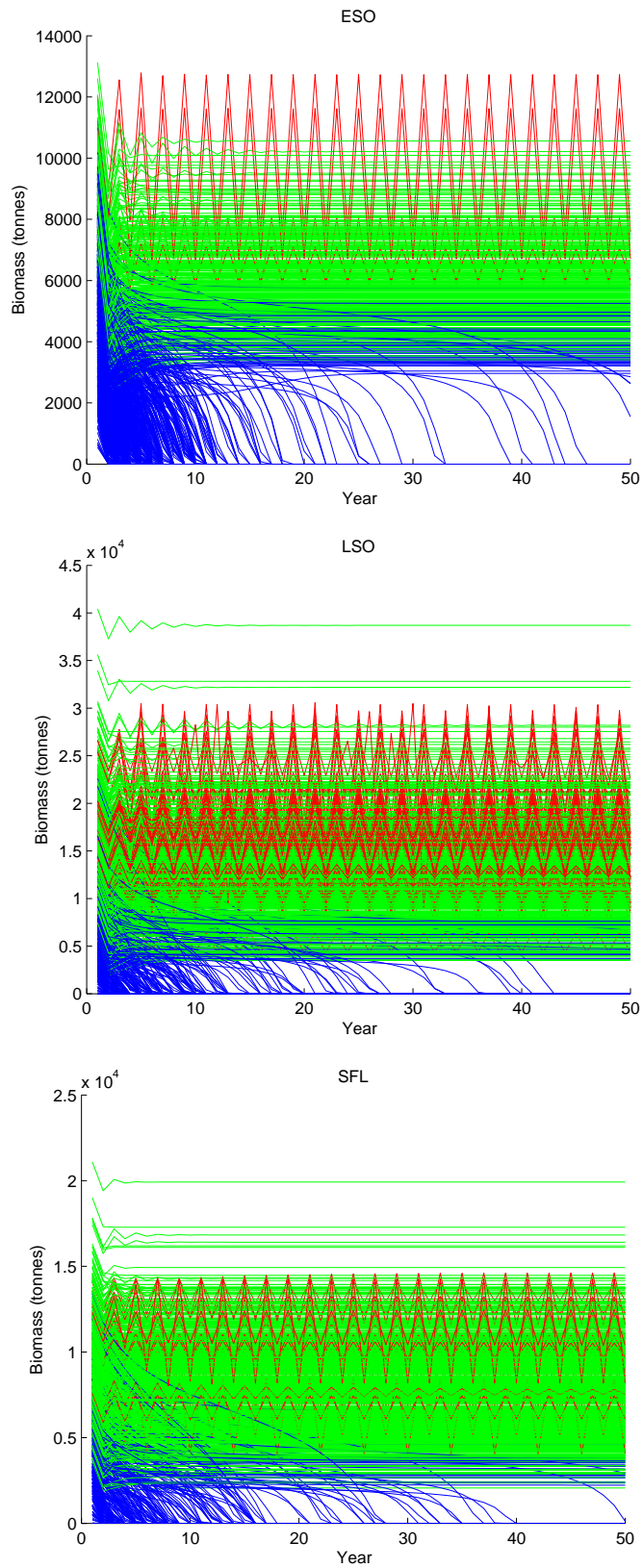


Figure 6.21: Option 6 - Simulation Model 1 (green line: stable converging, blue: decreasing towards zero, red: oscillating)

The following three figures are for the Fox model:

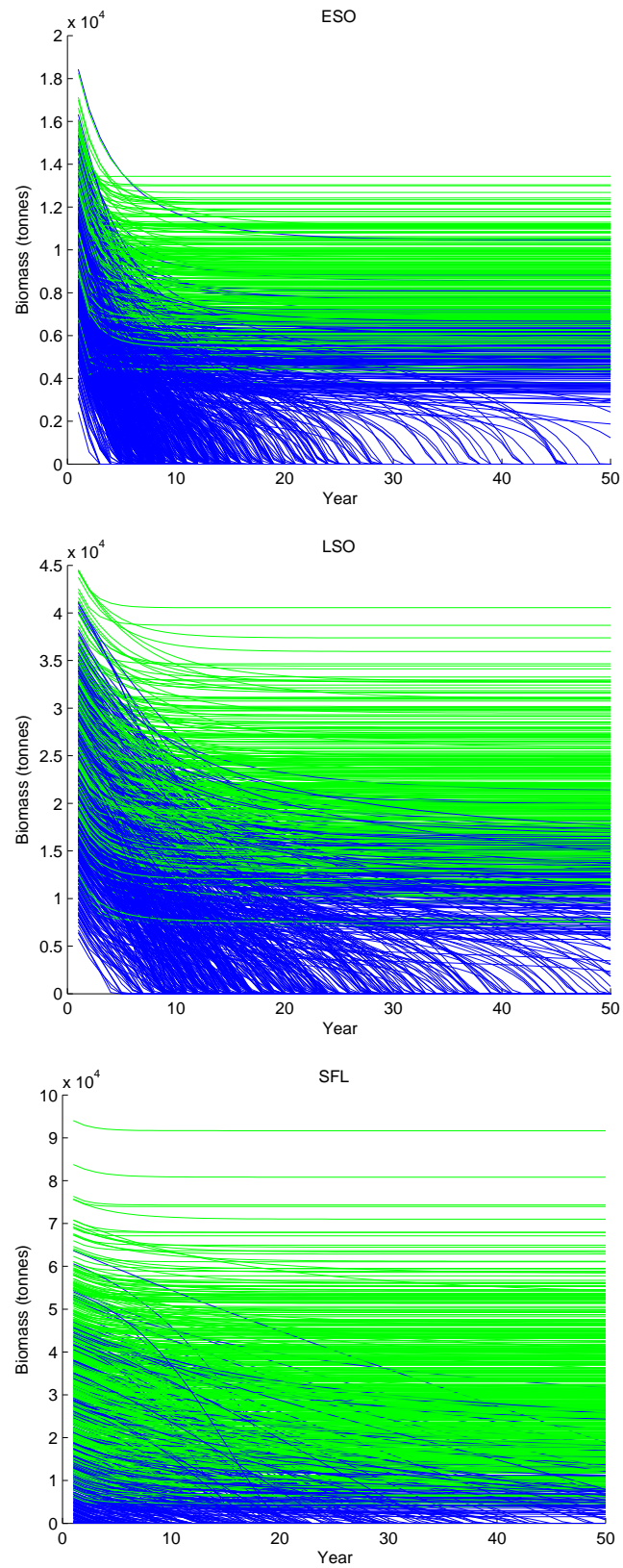


Figure 6.22: Option 6 - Simulation Model 1 (green line: stable converging, blue: decreasing towards zero, red: oscillating)

The following three figures are for the Schaefer model:

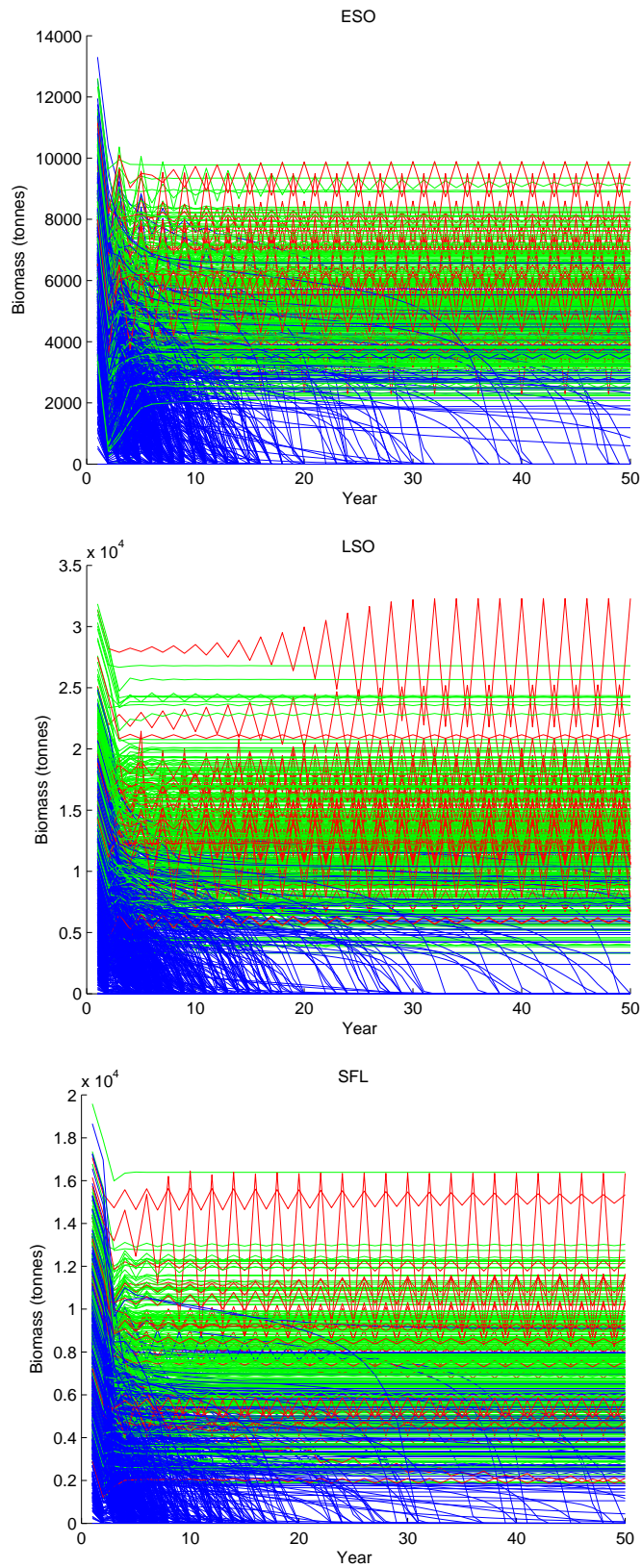


Figure 6.23: Option 6 - Simulation Model 2 (green line: stable converging, blue: decreasing towards zero, red: oscillating)

The following three figures are for the Fox model:

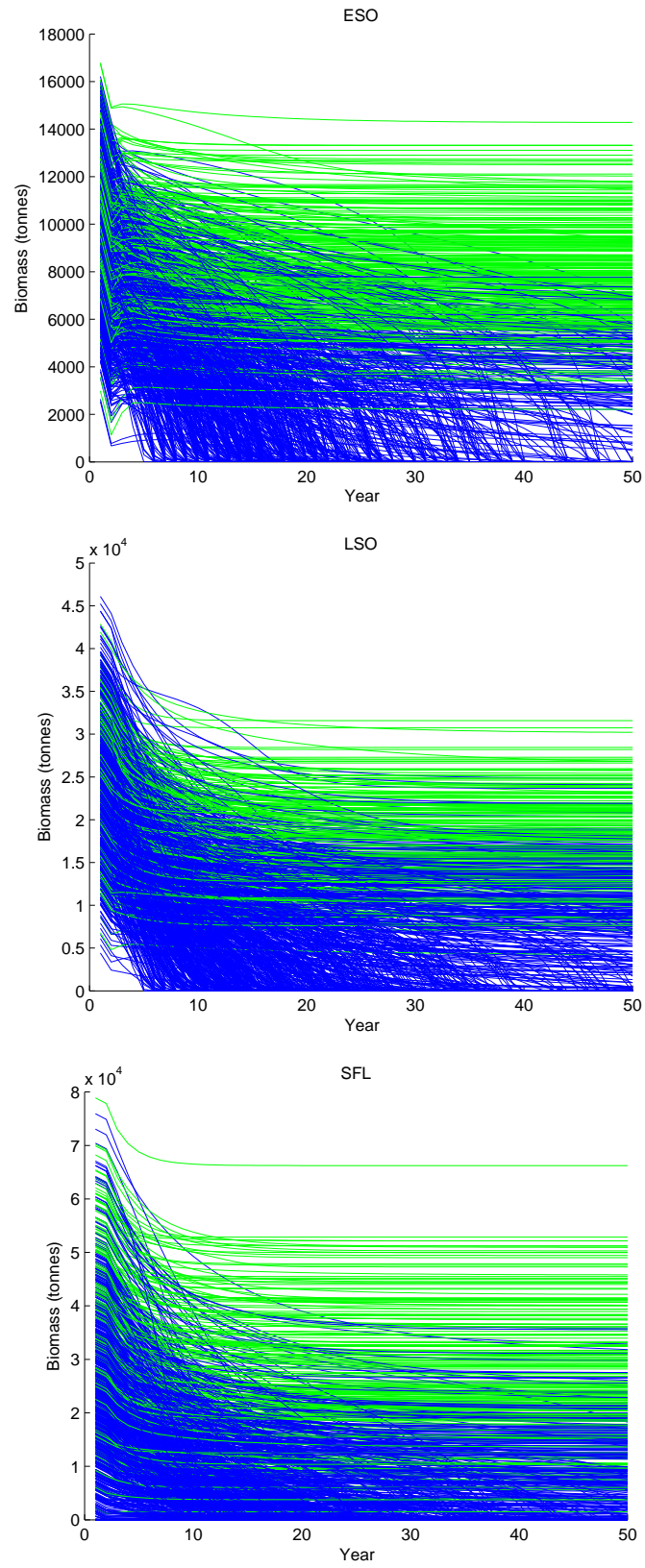


Figure 6.24: Option 6 - Simulation Model 2 (green line: stable converging, blue: decreasing towards zero, red: oscillating)

Chapter 7

CONCLUSION

It is difficult to make definitive conclusions about the management options, due to the high uncertainty in the parameter estimates. In particular, the estimates for K are very uncertain, as seen in the density and history plots for the Bayesian estimates in Chapter 4. The history plots show that the values are not converging for K for each of the three species, even for a large number of iterations. Therefore, more information is needed to make the estimates more certain. However, for the r estimates, the density and history plots show that the values are converging and are reasonably certain, because of the prior. The estimated values of r are also reasonably close to the estimated values from Fish Base as well as the regression because of the prior. With no information from the observations the prior will have a large influence on the estimate.

As discussed in Chapter 3, the non-zero fixed point for the Schaefer model is unstable for $q < r < 2 + q$. While the optimized values for r for each of the species using the Bayesian method are less than $2 + q$, the values used in the simulation models ranged widely in the Monte Carlo simulation, due to the high level of uncertainty in the parameter estimates. Consequently, a large number of simulations were run with $r > 2 + q$ and these simulations oscillate for long periods (marked in red in the figures). For simulations of this type, the population may be over-estimated or wrong.

With respect to the simulation models, the second type of model with non-constant proportions of catch is probably more realistic than the first type of model with constant catch proportions. In particular, when the population of the species

becomes relatively low, it is unlikely that fishers will be able to catch the same number as when the populations are abundant, or that the fishers will be able to target a specific species. It is more likely that the fishers will target flatfish in general, and the proportion of catch will be based on the abundance of the species. These models (type 2) are less pessimistic in general, and result in a more balanced level of depletion than type 1 simulates. Though, if the fishers can target specific species, then the simulations indicate that the initially less abundant species will be relatively unaffected, whilst the initially most abundant species will become relatively depleted. The results of model 1 (constant proportion) and model 2 (variable) were very different for options 4-6.

Due to the short-falls of the Pella-Tomlinson model with $m = 3$, the Schaefer and Fox models are the most appropriate model for this problem, along with the second simulation type (with varying catch proportions). From the results in Chapter 6, the Fox model shows that the current management strategy is a reasonably low risk strategy for all three species, with most simulations ending above the MSY's. This indicates that the populations of each of the key species are likely to remain at sustainable levels, based on the parameters used for the estimation.

From the figures and the tables in the risk assessment chapter, the safest (lowest risk) management option is the third option with TACC of 1430t. In this study, the preferred risk is the risk adverse options that minimise the chance of any simulations going below 10% or 20% of K . This conclusion is obvious since this strategy has the lowest catch allowance. However, the current management strategy (option 1), maintains sustainable levels while at higher catch rates. Therefore, the simulations indicate that this option is the optimal strategy for this area. The last three management options with TACC's based on the parameter estimates in this study may be all unrealistically high. Since there is concern for these species at the current level of catch, it is unlikely that implementing a TACC higher than the current allowance would be a suitable option. The high level of the MSY's for each of the three species may be due to the high levels of the estimated K values, compared with the current level of catches. These estimates for the MSY's are very uncertain since the MSY is calculated using r and K for each of the species, and all the estimates for these parameters are very uncertain. The figures for options 4, 5 and 6 show a number of

simulations remaining at good levels. This is due to the nature of the models, where the MSY's are derived from the models themselves, and taking catch below the MSY for each species will result in sustainable levels in the simulations. Those simulations which go below 10% of the virgin biomass are the simulations which have a MSY lower than the average MSY (calculated from the mean parameter estimates).

The key question for this problem was whether the management of these species using a single catch quota will result in some of the individual species being under or over-fished. Figures 6.1, 6.2, 6.3 and 6.4 indicate that all species remain at sustainable levels, including ESO which is the least abundant species. The figures for options 2 and 3 also show that all species are remaining at sustainable levels. However, for the first simulation type, the options with higher catch quotas (options 4-6) show that the combined catch quota has a negative effect on ESO, which has only 11.1% of simulations ending above the MSY for option 4 using the Schaefer model, and only 33.3% for option 4 using the Fox model. For the second simulation type, the simulations ending above the MSY's are reasonably even for each of the species. Since the second simulation type is considered to be more realistic, the simulations indicate that managing these species using a single catch quota will not result in the individual species being over-fished. However, from the simulations no conclusions can be made about whether some of the individual species may be under-fished.

Since the invalid assumption was made that the initial biomass was equal to the biomass that fish would tend to in absence of fishing (K), no inferences can be made for these species on suitable management decisions. This study is an initial analysis of the stock, and should be treated purely as an academic exercise in fisheries modelling.

Chapter 8

DISCUSSION

Due to the fact that this study was based around the catch and CPUE data for flatfish, it is worthwhile commenting on the validity of this data. The catch data comes from fishers and processors, and the data from these sources can have some biases. Fishers can catch flatfish when targeting other species, and this catch can go unrecorded. Fish which are caught below the minimum size limits can be discarded, which may contribute to the mortality rate of these species. The CPUE data used in this study was based on data provided from a study commissioned by the Ministry of Fisheries, which has not yet been published. Therefore the findings from the study are only preliminary findings, and the results have not yet been critically reviewed by the Ministry of Fisheries inshore working group.

While CPUE was used as the index of abundance in this study, this may not be the best index to use. In some cases, CPUE can over-estimate the abundance of the fishery, especially in cases where the fish school together. In this instance, the CPUE can remain at the same level regardless of the population size, since fishers will be able to continue catching the same amounts (providing they are fishing in an area which includes some fish schools). CPUE for flatfish might change as fishers change their target species (e.g. from flatfish to snapper). CPUE would then change, but this has nothing to do with flatfish abundance. Therefore, the assumption that CPUE provides a valid index of abundance can be a strong assumption to make.

In fisheries, the Maximum Sustainable Yield (MSY) can be used as a basis for setting a catch quota. This choice is based on the assumption that the MSY is a good estimate of the sustainable amounts of catch. However, this method has been

highly criticized in the past due to the fact that the MSY can be an over-estimate of the sustainable level of catch, and can ultimately result in populations becoming depleted [22].

The prior estimate for the r parameters was based on information obtained from the Fish Base website, using the life-history tool. However, the method used to estimate these parameters is based on correlates, and therefore the validity of these estimates for the species in this study is unknown.

Chapter 9

FURTHER RESEARCH

As the parameter estimates for K for each of the three species have a high level of uncertainty, the first option for improving the results is to give an informed prior estimate for these parameters in the Bayesian parameter estimation. One of the ways to create such a prior is to have some experts give their opinion on what the median or mean may be for each K , as well as the upper and lower quartiles, or the 5% and 95% confidence bounds. In fact, for these species, some experts provided some opinions on the K 's. One expert estimates that the median values for the K 's are $60000t$, $85000t$, and $20000t$ for ESO, LSO and SFL respectively with the 90% confidence bounds of $15000t$, $20000t$ and 5000 for the lower bounds and $120000t$, $170000t$ and $40000t$ for the upper bounds. Another expert estimated that the combined current biomass for all three species is $10000t$. Another expert estimated that the current biomass for ESO is approximately $2200t$, with 90% lower confidence bound of $450t$ and upper confidence bound $27000t$, for LSO the current $3200t$, with 90% lower of $650t$ and the upper confidence bound $10000t$, and for SFL the current $750t$, the 90% lower confidence bound of $150t$ and upper confidence bound $2300t$. A fourth expert estimated the current biomasses as $1350t$, $1950t$ and $450t$ for ESO, LSO and SFL respectively, and the 90% confidence bounds as $675t$, $975t$ and $225t$ for the lower bounds and $9000t$, $13000t$ and $3000t$ for the upper bounds. Using the estimates for the current biomass for each species, the models can be iterated backwards in time to give estimates for the virgin biomass, and the estimate for the virgin biomass can be incorporated into the prior distribution for K making it a log-normal or gamma distribution for example rather than the uniform

distribution used in this study. These estimates were obtained after completing the simulations for this study, though it would be worthwhile to incorporate them in later research. Comparing the estimates for the K 's from the first expert, the estimated values from the Bayesian goodness of fit are much smaller than these values, which may indicate that the values used in the simulation model's may be too small (in that expert's opinion).

The methods and computer codes used in this study can be applied to other fish species in New Zealand. For flatfish in particular, the FLA1 area currently has catch and CPUE data from previous years which can be directly inputted into the WinBUGS and Matlab codes. Once CPUE analyses have been completed on the other management areas of New Zealand for flatfish, the methods described in this study can also be applied. In particular, more studies have been conducted in the FLA1 management area, around the Kaipara harbour, so this data can be incorporated into the priors for the Bayesian estimations.

Another useful suggestion for further research would be to conduct further biological studies aimed specifically at flatfish, such as trawl surveys, tagging studies or age distribution studies. Though these are known to be very costly, biological studies are the best way to improve the certainty of the parameter estimates and increase the validity of the results. Once more biological data is available, different types of models can be used such as age-structured models, or dynamic pool models.

The down-side of re-estimating the r and K 's using the expert-opinion prior on K is that the r values from the estimations would be largely determined from the (Fish Base) prior, and the K values from this expert-opinion prior, making them both just educated guesses rather than determined by real data. Therefore, getting more and better real data should be a priority and further investigation into this would be worthwhile in future research.

Given further resources and data, it could be worthwhile to assess the suitability of other models for these species. If the initial biomass could be estimated independent of the K , the parameter estimates, and hence the risk analysis, may be more informative.

Appendix A

Matlab code for Simulation Model 1

```
1 %%%%%%%%%%%%%%%%%%%%%%%%%%%%%%%%%%%%%%%%%%%%%%%%%%%%%%%%%%%%%%%%%%%%%%%%%%
2 %                               Simulation Model 1                               %
3 %%%%%%%%%%%%%%%%%%%%%%%%%%%%%%%%%%%%%%%%%%%%%%%%%%%%%%%%%%%%%%%%%%%%%%%%%%
4
5 clear all
6 %Number of years to simulate
7 t = 50;
8 %Input to determine model type (m=1: Fox model,m=2 or m=3: Pella -
9 %Tomlinson with parameter m)
10 m = input('m=');
11 %Input constant catch amount
12 Catch = input('Catch=');
13 %Optimal (r,K) for species 1 as calculated using bayesian goodness
14 %of fit in WinBUGS with covariance matrix for Schaefer model
15 mu1 = [6528; 1.647];
16 cov1 = 1.0e+006 * [4.65085548767833  -0.00033883424605;
17                   -0.00033883424605   0.00000023214346];
18 MSY1 = (mu1(2)*mu1(1))/4;
19 %Optimal (r,K) for species 1 as calculated using bayesian goodness
20 %of fit in WinBUGS with covariance matrix for Fox model
21 mu1Fox = [9986; 4.508];
22 cov1Fox = 1.0e+006 * [6.49208658715848  -0.00336698817548;
23                     -0.00336698817548   0.00000672736319];
24 MSY1Fox = (mu1Fox(2)*mu1Fox(1))*(exp(-1)/log(mu1Fox(1)));
25 %Optimal (r,K) for species 2 as calculated using bayesian goodness
26 %of fit in WinBUGS with covariance matrix for Schaefer model
27 mu2 = [12160; 1.634];
```

```

28 cov2 = 1.0e+007 * [4.44854913999548  -0.00005244794830;
29      -0.00005244794830    0.00000002890212];
30 MSY2 = (mu2(2)*mu2(1))/4;
31 %Optimal (r,K) for species 2 as calculated using bayesian goodness
32 %of fit in WinBUGS with covariance matrix for Fox model
33 mu2Fox = [24360; 2.621];
34 cov2Fox = 1.0e+007 * [4.84484371766459  -0.00015766626091;
35      -0.00015766626091    0.00000032586628];
36 MSY2Fox = (mu2Fox(2)*mu2Fox(1))*(exp(-1)/log(mu2Fox(1)));
37 %Optimal (r,K) for species 3 as calculated using bayesian goodness
38 %of fit in WinBUGS with covariance matrix for Schaefer model
39 mu3 = [8079; 1.442];
40 cov3 =1.0e+007 * [1.21937741550840  -0.00000543468431;
41      -0.00000543468431    0.00000002050719];
42 MSY3 = (mu3(2)*mu3(1))/4;
43 %Optimal (r,K) for species 3 as calculated using bayesian goodness
44 %of fit in WinBUGS with covariance matrix for Fox model
45 mu3Fox = [25070; 2.772];
46 cov3Fox =1.0e+008 * [3.47895766612056  -0.00004665388342;
47      -0.00004665388342    0.00000003341849];
48 MSY3Fox = (mu3Fox(2)*mu3Fox(1))*(exp(-1)/log(mu3Fox(1)));
49 %Initialise biomass for monte carlo simulation (Schaefer)
50 B1=mul(1)*ones(t,1000); M1 = chol(cov1);
51 %B1 = Population of species 1
52 B2=mu2(2)*ones(t,1000); M2 = chol(cov2);
53 %B2 = Population of species 2
54 B3=mu3(2)*ones(t,1000); M3 = chol(cov3);
55 %B3 = Population of species 3
56 %Initialise biomass for monte carlo simulation (Fox)
57 B1Fox=mulFox(1)*ones(t,1000); M1Fox = chol(cov1Fox);
58 B2Fox=mu2Fox(2)*ones(t,1000); M2Fox = chol(cov2Fox);
59 B3Fox=mu3Fox(2)*ones(t,1000); M3Fox = chol(cov3Fox);
60 %Initial proportions based on previous data
61 B1P = 28/100;          %B1P = proportion of species 1 in FLA3
62 B2P = 30/100;          %B2P = proportion of species 2 in FLA3
63 B3P = 16/100;          %B3P = proportion of species 3 in FLA3
64 %Initial values for dividing into respective types
65 B1Type1 = 0; B1Type2 = 0; B1Type3 = 0; B1Type4 = 0;
66 B2Type1 = 0; B2Type2 = 0; B2Type3 = 0; B2Type4 = 0;

```

```

67 B3Type1 = 0; B3Type2 = 0; B3Type3 = 0; B3Type4 = 0;
68 %Tolerance for absolute differences from last 5 iterations
69 tol = 1000;
70 %Initial values for risk analysis
71 Lessthan20percentB1 = 0; Lessthan10percentB1 = 0;
72 Lessthan20percentB2 = 0; Lessthan10percentB2 = 0;
73 Lessthan20percentB3 = 0; Lessthan10percentB3 = 0;
74 Above501 = zeros(1,1000); Above502 = zeros(1,1000);
75 Above503 = zeros(1,1000);
76 Above3681 = zeros(1,1000); Above3682 = zeros(1,1000);
77 Above3683 = zeros(1,1000);
78 DifferenceMSY1 = zeros(1,1000); DifferenceMSY2 = zeros(1,1000);
79 DifferenceMSY3 = zeros(1,1000);
80 DifferenceMSY1Fox = zeros(1,1000); DifferenceMSY2Fox = zeros(1,1000);
81 DifferenceMSY3Fox = zeros(1,1000);
82 %%%%%%%%%%%%%%%%%%%%%%%%%%%%%%%%%%%%%%%%%%%%%%%%%%%%%%%%%%%%%%%%%%%%%%%%%
83 %SPECIES 1 – ESO
84
85 %Plot simulations for species 1 (ESO)
86 figure
87 hold on
88 title('ESO');
89 xlabel('Year');
90 ylabel('Biomass (tonnes)');
91 %Biomass for species 1 (ESO)
92 for j = 1:1000
93     if m == 1
94         %MC simulation to account for error in parameter estimation
95         %for Fox model
96         hat1 = mulFox + M1Fox* randn(2,1);
97         r1(j) = hat1(2);
98         K1(j) = hat1(1);
99         K1t = K1(j);
100        if K1t ≤ 0
101            K1(j) = 0;
102        end
103        B1(1,j) = K1(j);
104        MSY1 = MSY1Fox;
105

```

```

106     %Loop to calculate biomass for t years
107     %Fox model
108
109     for i = 1:t-1
110         B1(i+1,j)=B1(i,j) + ((r1(j) * B1(i,j))*(1-log(B1(i,j))/
111         log(K1(j)))) - (Catch*B1P); B1j = B1(i+1,j);
112         if B1j > 0
113             B1(i+1,j)=B1(i,j) + ((r1(j) * B1(i,j))*(1-
114             log(B1(i,j))/log(K1(j)))) - (Catch*B1P);
115         else
116             B1(i+1,j)=0;
117         end
118     end
119
120     %Pella-Tomlinson with m=2
121     elseif m > 1
122         %MC simulation to account for error in parameter estimation
123         %for Schaefer model
124         hat1 = mul + M1* randn(2,1);
125         r1(j) = hat1(2);
126         K1(j) = hat1(1);
127         K1t = K1(j);
128         if K1t ≤ 0
129             K1(j) = 0;
130         end
131         B1(1,j) = K1(j);
132         MSY1 = MSY1m2;
133
134         for i = 1:t-1
135             B1(i+1,j)=B1(i,j) + r1(j) * B1(i,j) - (r1(j)/K1(j))*
136             ((B1(i,j))^m) - (Catch*B1P); B1j = B1(i+1,j);
137             if B1j > 0
138                 B1(i+1,j)=B1(i,j) + r1(j) * B1(i,j) - (r1(j)/K1(j))*
139                 ((B1(i,j))^m) - (Catch*B1P);
140             else
141                 B1(i+1,j)=0;
142             end
143         end
144     end

```

```

145
146 %Divide each simulation into respective type
147 B1ta(j) = B1(50,j); B1t = B1ta(j);
148 XB1t(j) = abs(B1(46,j) - B1(45,j))+abs(B1(47,j) - B1(46,j))+
149 abs(B1(48,j) - B1(47,j))+abs(B1(49,j) - B1(48,j))+abs(B1(50,j)
150 - B1(49,j)); XB1 = XB1t(j);
151 B1gradt(j) = B1(49,j) - B1(50,j); B1grad = B1gradt(j);
152 B1gradtminus1(j) = B1(48,j) - B1(49,j);
153 B1gradminus1 = B1gradtminus1(j);
154 B1gradtminus2(j) = B1(47,j) - B1(48,j);
155 B1gradminus2 = B1gradtminus2(j);
156 FinalProportion1(j) = B1t/K1(j); x1 = FinalProportion1(j);
157
158 %Type 1 - Oscillating
159 if ((XB1 > tol) & (B1grad > 0) & (B1gradminus1 < 0))
160     B1Type1 = B1Type1 + 1;
161     B1(51,j) = 1;
162     plot(B1(1:50,j), 'Color', 'red', 'MarkerSize', 8)
163 elseif ((XB1 > tol) & (B1grad < 0) & (B1gradminus1 > 0))
164     B1Type1 = B1Type1 + 1;
165     B1(51,j) = 1;
166     plot(B1(1:50,j), 'Color', 'red', 'MarkerSize', 8)
167 elseif ((XB1 > tol) & (B1t ≠ 0) & (B1grad < 0) &
168 (B1gradminus2 > 0))
169     B1Type1 = B1Type1 + 1;
170     B1(51,j) = 1;
171     plot(B1(1:50,j), 'Color', 'red', 'MarkerSize', 8)
172 elseif ((XB1 > tol) & (B1t ≠ 0) & (B1grad > 0) &
173 (B1gradminus2 < 0))
174     B1Type1 = B1Type1 + 1;
175     B1(51,j) = 1;
176     plot(B1(1:50,j), 'Color', 'red', 'MarkerSize', 8)
177
178 %Type 2 - Decreasing towards zero
179 elseif (B1t == 0)
180     B1Type2 = B1Type2 + 1;
181     B1(51,j) = 2;
182     plot(B1(1:50,j), 'Color', 'blue', 'MarkerSize', 8)
183 elseif ((B1t ≠ 0) & (x1 ≤ 0.6))

```

```

184         B1Type2 = B1Type2 + 1;
185         B1(51,j) = 2;
186         plot(B1(1:50,j), 'Color', 'blue', 'MarkerSize', 8)
187
188         %Type 3 – Stable converging
189         else B1Type3 = B1Type3 + 1;
190             B1(51,j) = 3;
191             plot(B1(1:50,j), 'Color', 'green', 'MarkerSize', 8)
192         end
193
194         %Risk Analysis
195         if (x1 < 0.2) & (XB1 ≤ tol)
196             Lessthan20percentB1 = Lessthan20percentB1 + 1;
197         end
198         if (x1 < 0.1) & (XB1 ≤ tol)
199             Lessthan10percentB1 = Lessthan10percentB1 + 1;
200         end
201         if (B1t ≥ 0.5*K1t)
202             Above501(j) = 1;
203             DifferenceMSY1(j) = B1t - 0.5*K1t;
204         elseif (B1t < 0.5*K1t)
205             Above501(j) = 0;
206             DifferenceMSY1(j) = B1t - 0.5*K1t;
207         end
208         if (B1t ≥ 0.368*K1t)
209             Above3681(j) = 1;
210             DifferenceMSY1Fox(j) = B1t - 0.368*K1t;
211         elseif (B1t < 0.368*K1t)
212             Above3681(j) = 0;
213             DifferenceMSY1Fox(j) = B1t - 0.368*K1t;
214         end
215     end
216     %%%%%%%%%%%%%%%%%%%%%%%%%%%%%%%%%%%%%%%%%%%%%%%%%%%%%%%%%%%%%%%%%%%%%%%%%
217     %SPECIES 2 – LSO
218
219     %Plot simulations for species 2 (LSO)
220     figure
221     hold on
222     title('LSO');

```



```

223 xlabel('Year');
224 ylabel('Biomass (tonnes)');
225 %Biomass for species 2 (LSO)
226 for j = 1:1000
227     %Fox model
228     if m == 1
229         %MC simulation to account for error in parameter estimation
230         hat2 = mu2Fox + M2Fox* randn(2,1);
231         r2(j) = hat2(2);
232         K2(j) = hat2(1);
233         K2t = K2(j);
234         if K2t ≤ 0
235             K2(j) = 0;
236         end
237         B2(1,j) = K2(j);
238         MSY2 = MSY2Fox;
239
240         %Loop to calculate biomass for t years
241         for i = 1:t-1
242             B2(i+1,j)=B2(i,j) + ((r2(j) * B2(i,j))*(1-log(B2(i,j))/
243             log(K2(j)))) - (Catch*B2P); B2j = B2(i+1,j);
244             if B2j > 0
245                 B2(i+1,j)=B2(i,j) + ((r2(j) * B2(i,j))*(1-
246                 log(B2(i,j))/log(K2(j)))) - (Catch*B2P);
247             else
248                 B2(i+1,j)=0;
249             end
250         end
251
252         %Pella-Tomlinson with m=2
253     elseif m > 1
254         %MC simulation to account for error in parameter estimation
255         hat2 = mu2 + M2* randn(2,1);
256         r2(j) = hat2(2);
257         K2(j) = hat2(1);
258         K2t = K2(j);
259         if K2t ≤ 0
260             K2(j) = 0;
261         end

```

```

262     B2(1,j) = K2(j);
263     MSY2 = MSY2m2;
264
265     %Loop to calculate biomass for t years
266     for i = 1:t-1
267         B2(i+1,j)=B2(i,j) + r2(j) * B2(i,j) - (r2(j)/K2(j))*
268             ((B2(i,j))^m) - (Catch*B2P); B2j = B2(i+1,j);
269         if B2j > 0
270             B2(i+1,j)=B2(i,j) + r2(j) * B2(i,j) - (r2(j)/K2(j))*
271                 ((B2(i,j))^m) - (Catch*B2P);
272         else
273             B2(i+1,j)=0;
274         end
275     end
276 end
277 %Divide each simulation into respective type
278 B2ta(j) = B2(50,j); B2t = B2ta(j);
279 XB2t(j) = abs(B2(46,j) - B2(45,j))+abs(B2(47,j) - B2(46,j))+
280     abs(B2(48,j) - B2(47,j))+abs(B2(49,j) - B2(48,j))+abs(B2(50,j) -
281     B2(49,j)); XB2 = XB2t(j);
282 B2gradt(j) = B2(49,j) - B2(50,j); B2grad = B2gradt(j);
283 B2gradtminus1(j) = B2(48,j) - B2(49,j);
284 B2gradminus1 = B2gradtminus1(j);
285 B2gradtminus2(j) = B2(47,j) - B2(48,j);
286 B2gradminus2 = B2gradtminus2(j);
287 FinalProportion2(j) = B2t/K2(j); x2 = FinalProportion2(j);
288
289 %Type 1 - Oscillating
290 if ((XB2 > tol) & (B2grad > 0) & (B2gradminus1 < 0))
291     B2Type1 = B2Type1 + 1;
292     B2(51,j) = 1;
293     plot(B2(1:50,j),'Color','red','MarkerSize',8)
294 elseif ((XB2 > tol) & (B2grad < 0) & (B2gradminus1 > 0))
295     B2Type1 = B2Type1 + 1;
296     B2(51,j) = 1;
297     plot(B2(1:50,j),'Color','red','MarkerSize',8)
298 elseif ((XB2 > tol) & (B2t ≠ 0) & (B2grad < 0) &
299     (B2gradminus2 > 0))
300     B2Type1 = B2Type1 + 1;

```

```

301         B2(51,j) = 1;
302         plot(B2(1:50,j), 'Color', 'red', 'MarkerSize', 8)
303     elseif ((XB2 > tol) & (B2t ≠ 0) & (B2grad > 0) &
304         (B2gradminus2 < 0))
305         B2Type1 = B2Type1 + 1;
306         B2(51,j) = 1;
307         plot(B2(1:50,j), 'Color', 'red', 'MarkerSize', 8)
308
309     %Type 2 – Decreasing towards zero
310     elseif (B2t == 0)
311         B2Type2 = B2Type2 + 1;
312         B2(51,j) = 2;
313         plot(B2(1:50,j), 'Color', 'blue', 'MarkerSize', 8)
314     elseif ((B2t ≠ 0) & (x2 ≤ 0.6))
315         B2Type2 = B2Type2 + 1;
316         B2(51,j) = 2;
317         plot(B2(1:50,j), 'Color', 'blue', 'MarkerSize', 8)
318
319     %Type 3 – Stable converging
320     else B2Type3 = B2Type3 + 1;
321         B2(51,j) = 3;
322         plot(B2(1:50,j), 'Color', 'green', 'MarkerSize', 8)
323     end
324
325     %Risk Analysis
326     if (x2 < 0.2) & (XB2 ≤ tol)
327         Lessthan20percentB2 = Lessthan20percentB2 + 1;
328     end
329     if (x2 < 0.1) & (XB2 ≤ tol)
330         Lessthan10percentB2 = Lessthan10percentB2 + 1;
331     end
332     if (B2t ≥ 0.5*K2t)
333         Above502(j) = 1;
334         DifferenceMSY2(j) = B2t - 0.5*K2t;
335     elseif (B2t < 0.5*K2t)
336         Above502(j) = 0;
337         DifferenceMSY2(j) = B2t - 0.5*K2t;
338     end
339     if (B2t ≥ 0.368*K2t)

```

```

340     Above3682(j) = 1;
341     DifferenceMSY2Fox(j) = B2t - 0.368*K2t;
342 elseif (B2t < 0.368*K2t)
343     Above3682(j) = 0;
344     DifferenceMSY2Fox(j) = B2t - 0.368*K2t;
345 end
346 end
347 %%%%%%%%%%%%%%%%%%%%%%%%%%%%%%%%%%%%%%%%%%%%%%%%%%%%%%%%%%%%%%%%%%%%%%%%%
348 %SPECIES 3 - SFL
349
350 %Plot simulations for species 3 (SFL)
351 figure
352 hold on
353 title('SFL');
354 xlabel('Year');
355 ylabel('Biomass (tonnes)');
356 %Biomass for species 3 (SFL)
357 for j = 1:1000
358
359     %Loop to calculate biomass for t years
360     %Fox model
361     if m == 1
362         %MC simulation to account for error in parameter estimation
363         hat3 = mu3Fox + M3Fox* randn(2,1);
364         r3(j) = hat3(2);
365         K3(j) = hat3(1);
366         K3t = K3(j);
367         if K3t <= 0
368             K3(j) = 0;
369         end
370         B3(1,j) = K3(j);
371         MSY3 = MSY3Fox;
372
373         for i = 1:t-1
374             B3(i+1,j)=B3(i,j) + ((r3(j) * B3(i,j))*(1-log(B3(i,j))/
375             log(K3(j)))) - (Catch*B3P); B3j = B3(i+1,j);
376             if B3j > 0
377                 B3(i+1,j)=B3(i,j) + ((r3(j) * B3(i,j))*(1-
378                 log(B3(i,j))/log(K3(j)))) - (Catch*B3P);

```

```

379         else
380             B3(i+1,j)=0;
381         end
382     end
383
384     %Pella-Tomlinson with m=2 or m=3
385     elseif m > 1
386         %MC simulation to account for error in parameter estimation
387         hat3 = mu3 + M3* randn(2,1);
388         r3(j) = hat3(2);
389         K3(j) = hat3(1);
390         K3t = K3(j);
391         if K3t ≤ 0
392             K3(j) = 0;
393         end
394         B3(1,j) = K3(j);
395         MSY3 = MSY3m2;
396
397         for i = 1:t-1
398             B3(i+1,j)=B3(i,j) + r3(j) * B3(i,j) - (r3(j)/K3(j))*
399             ((B3(i,j))^m) - (Catch*B3P); B3j = B3(i+1,j);
400             if B3j > 0
401                 B3(i+1,j)=B3(i,j) + r3(j) * B3(i,j) - (r3(j)/K3(j))*
402                 ((B3(i,j))^m) - (Catch*B3P);
403             else
404                 B3(i+1,j)=0;
405             end
406         end
407     end
408
409     %Divide each simulation into respective type
410     B3ta(j) = B3(50,j); B3t = B3ta(j);
411     XB3t(j) = abs(B3(46,j) - B3(45,j))+abs(B3(47,j) - B3(46,j))+
412     abs(B3(48,j) - B3(47,j))+abs(B3(49,j) - B3(48,j))+abs(B3(50,j) -
413     B3(49,j)); XB3 = XB3t(j);
414     B3gradt(j) = B3(49,j) - B3(50,j); B3grad = B3gradt(j);
415     B3gradtminus1(j) = B3(48,j) - B3(49,j);
416     B3gradminus1 = B3gradtminus1(j);
417     B3gradtminus2(j) = B3(47,j) - B3(48,j);

```

```

418 B3gradminus2 = B3gradtminus2(j);
419 FinalProportion3(j) = B3t/K3(j); x3 = FinalProportion3(j);
420
421 %Type 1 – Oscillating
422 if ((XB3 > tol) & (B3grad > 0) & (B3gradminus1 < 0))
423     B3Type1 = B3Type1 + 1;
424     B3(51,j) = 1;
425     plot(B3(1:50,j),'Color','red','MarkerSize',8)
426 elseif ((XB3 > tol) & (B3grad < 0) & (B3gradminus1 > 0))
427     B3Type1 = B3Type1 + 1;
428     B3(51,j) = 1;
429     plot(B3(1:50,j),'Color','red','MarkerSize',8)
430 elseif ((XB3 > tol) & (B3t ≠ 0) & (B3grad < 0) &
431         (B3gradminus2 > 0))
432     B3Type1 = B3Type1 + 1;
433     B3(51,j) = 1;
434     plot(B3(1:50,j),'Color','red','MarkerSize',8)
435 elseif ((XB3 > tol) & (B3t ≠ 0) & (B3grad > 0) &
436         (B3gradminus2 < 0))
437     B3Type1 = B3Type1 + 1;
438     B3(51,j) = 1;
439     plot(B3(1:50,j),'Color','red','MarkerSize',8)
440
441 %Type 2 – Decreasing towards zero
442 elseif (B3t == 0)
443     B3Type2 = B3Type2 + 1;
444     B3(51,j) = 2;
445     plot(B3(1:50,j),'Color','blue','MarkerSize',8)
446 elseif ((B3t ≠ 0) & (x3 ≤ 0.6))
447     B3Type2 = B3Type2 + 1;
448     B3(51,j) = 2;
449     plot(B3(1:50,j),'Color','blue','MarkerSize',8)
450
451 %Type 3 – Stable converging
452 else B3Type3 = B3Type3 + 1;
453     B3(51,j) = 3;
454     plot(B3(1:50,j),'Color','green','MarkerSize',8)
455 end
456

```

```

457     %Risk Analysis
458     if (x3 < 0.2) & (XB3 ≤ tol)
459         Lessthan20percentB3 = Lessthan20percentB3 + 1;
460     end
461     if (x3 < 0.1) & (XB3 ≤ tol)
462         Lessthan10percentB3 = Lessthan10percentB3 + 1;
463     end
464     if (B3t ≥ 0.5*K3t)
465         Above503(j) = 1;
466         DifferenceMSY3(j) = B3t - 0.5*K3t;
467     elseif (B3t < 0.5*K3t)
468         Above503(j) = 0;
469         DifferenceMSY3(j) = B3t - 0.5*K3t;
470     end
471     if (B3t ≥ 0.368*K3t)
472         Above3683(j) = 1;
473         DifferenceMSY3Fox(j) = B3t - 0.368*K3t;
474     elseif (B3t < 0.368*K3t)
475         Above3683(j) = 0;
476         DifferenceMSY3Fox(j) = B3t - 0.368*K3t;
477     end
478 end
479 %%%%%%%%%%%%%%%%%%%%%%%%%%%%%%%%%%%%%%%%%%%%%%%%%%%%%%%%%%%%%%%%%%%%%%%%%

```

Matlab code for Simulation Model 2

```

1  %%%%%%%%%%%%%%%%%%%%%%%%%%%%%%%%%%%%%%%%%%%%%%%%%%%%%%%%%%%%%%%%%%%%%%%%%
2  %                               Simulation Model 2                               %
3  %%%%%%%%%%%%%%%%%%%%%%%%%%%%%%%%%%%%%%%%%%%%%%%%%%%%%%%%%%%%%%%%%%%%%%%%%
4
5  clear all
6  %Number of years to simulate
7  t = 50;
8  %Input to determine model type (m=1: Fox model,m=2 or m=3: Pella –
9  %Tomlinson with parameter m)
10 m = input('m=');
11 %Input constant catch amount
12 Catch = input('Catch=');
13 %Optimal (r,K) for species 1 as calculated using bayesian goodness
14 %of fit in WinBUGS with covariance matrix for Schaefer model
15 mu1 = [6528; 1.647];
16 cov1 = 1.0e+006 * [4.65085548767833  -0.00033883424605;
17  -0.00033883424605  0.00000023214346];
18 MSY1m2 = (mu1(2)*mu1(1))/4;
19 %Optimal (r,K) for species 1 as calculated using bayesian goodness
20 %of fit in WinBUGS with covariance matrix for Fox model
21 mu1Fox = [9986; 4.508];
22 cov1Fox = 1.0e+006 * [6.49208658715848  -0.00336698817548;
23  -0.00336698817548  0.00000672736319];
24 MSY1Fox = (mu1Fox(2)*mu1Fox(1))*(exp(-1)/log(mu1Fox(1)));
25 %Optimal (r,K) for species 2 as calculated using bayesian goodness
26 %of fit in WinBUGS with covariance matrix for Schaefer model
27 mu2 = [12160; 1.634];
28 cov2 = 1.0e+007 * [4.44854913999548  -0.00005244794830;
29  -0.00005244794830  0.00000002890212];
30 MSY2m2 = (mu2(2)*mu2(1))/4;
31 %Optimal (r,K) for species 2 as calculated using bayesian goodness
32 %of fit in WinBUGS with covariance matrix for Fox model
33 mu2Fox = [24360; 2.621];
34 cov2Fox = 1.0e+007 * [4.84484371766459  -0.00015766626091;
35  -0.00015766626091  0.00000032586628];
36 MSY2Fox = (mu2Fox(2)*mu2Fox(1))*(exp(-1)/log(mu2Fox(1)));

```



```

37 %Optimal (r,K) for species 3 as calculated using bayesian goodness
38 %of fit in WinBUGS with covariance matrix for Schaefer model
39 mu3 = [8079; 1.442];
40 cov3 =1.0e+007 * [1.21937741550840 -0.00000543468431;
41 -0.00000543468431 0.00000002050719];
42 MSY3m3 = (mu3(2)*mu3(1))/4;
43 %Optimal (r,K) for species 3 as calculated using bayesian goodness
44 %of fit in WinBUGS with covariance matrix for Fox model
45 mu3Fox = [25070; 2.772];
46 cov3Fox =1.0e+008 * [3.47895766612056 -0.00004665388342;
47 -0.00004665388342 0.00000003341849];
48 MSY3Fox = (mu3(2)*mu3(1))/exp(1);
49 %Initialise biomass for monte carlo simulation (Schaefer)
50 B1=mu1(1)*ones(t,1000); M1 = chol(cov1);
51 %B1 = Population of species 1
52 B2=mu2(2)*ones(t,1000); M2 = chol(cov2);
53 %B2 = Population of species 2
54 B3=mu3(2)*ones(t,1000); M3 = chol(cov3);
55 %B3 = Population of species 3
56 %Initialise biomass for monte carlo simulation (Fox)
57 B1Fox=mu1Fox(1)*ones(t,1000); M1Fox = chol(cov1Fox);
58 B2Fox=mu2Fox(2)*ones(t,1000); M2Fox = chol(cov2Fox);
59 B3Fox=mu3Fox(2)*ones(t,1000); M3Fox = chol(cov3Fox);
60 %Initial proportions based on previous data
61 B1P0 = 28/100; B1P=B1P0*ones(t,1000);
62 B2P0 = 30/100; B2P=B2P0*ones(t,1000);
63 B3P0 = 16/100; B3P=B3P0*ones(t,1000);
64 %Initial values for dividing into respective types
65 B1Type1 = 0; B1Type2 = 0; B1Type3 = 0; B1Type4 = 0;
66 B2Type1 = 0; B2Type2 = 0; B2Type3 = 0; B2Type4 = 0;
67 B3Type1 = 0; B3Type2 = 0; B3Type3 = 0; B3Type4 = 0;
68 %Tolerance for absolute differences from last 5 iterations
69 tol = 1000;
70 %Initial values for risk analysis
71 Lessthan20percentB1 = 0; Lessthan10percentB1 = 0;
72 Lessthan20percentB2 = 0; Lessthan10percentB2 = 0;
73 Lessthan20percentB3 = 0; Lessthan10percentB3 = 0;
74 Above501 = zeros(1,1000); Above502 = zeros(1,1000);
75 Above503 = zeros(1,1000);

```

```

76 Above3681 = zeros(1,1000); Above3682 = zeros(1,1000);
77 Above3683 = zeros(1,1000);
78 DifferenceMSY1 = zeros(1,1000); DifferenceMSY2 = zeros(1,1000);
79 DifferenceMSY3 = zeros(1,1000);
80 DifferenceMSY1Fox = zeros(1,1000); DifferenceMSY2Fox = zeros(1,1000);
81 DifferenceMSY3Fox = zeros(1,1000);
82 %%%%%%%%%%%%%%%%%%%%%%%%%%%%%%%%%%%%%%%%%%%%%%%%%%%%%%%%%%%%%%%%%%%%%%%%%
83 %MC simulation to account for error in parameter estimation
84 for j = 1:1000
85     %Loop to calculate biomass for t years
86     %Fox model
87     if m == 1
88         %Monte Carlo simulation for species 1
89         hat1 = mulFox + M1Fox* randn(2,1);
90         r1(j) = hat1(2);
91         K1(j) = hat1(1);
92         K1t = K1(j);
93         if K1t ≤ 0
94             K1(j) = 0;
95         end
96         B1(1,j) = K1(j);
97         %Monte Carlo simulation for species 2
98         hat2 = mu2Fox + M2Fox* randn(2,1);
99         r2(j) = hat2(2);
100        K2(j) = hat2(1);
101        K2t = K2(j);
102        if K2t ≤ 0
103            K2(j) = 0;
104        end
105        B2(1,j) = K2(j);
106        %Monte Carlo simulation for species 3
107        hat3 = mu3Fox + M3Fox* randn(2,1);
108        r3(j) = hat3(2);
109        K3(j) = hat3(1);
110        K3t = K3(j);
111        if K3t ≤ 0
112            K3(j) = 0;
113        end
114        B3(1,j) = K3(j);

```

```

115     MSY1 = MSY1Fox;
116     MSY2 = MSY2Fox;
117     MSY3 = MSY3Fox;
118
119     for i = 1:t-1
120         B1(i+1,j)=B1(i,j) + ((r1(j) * B1(i,j))*(1-log(B1(i,j))/
121             log(K1(j)))) - (Catch*B1P(i,j)); B1j = B1(i+1,j);
122         B2(i+1,j)=B2(i,j) + ((r2(j) * B2(i,j))*(1-log(B2(i,j))/
123             log(K2(j)))) - (Catch*B2P(i,j)); B2j = B2(i+1,j);
124         B3(i+1,j)=B3(i,j) + ((r3(j) * B3(i,j))*(1-log(B3(i,j))/
125             log(K3(j)))) - (Catch*B3P(i,j)); B3j = B3(i+1,j);
126         if B1j > 0
127             B1(i+1,j)=B1(i,j) + ((r1(j) * B1(i,j))*(1-
128                 log(B1(i,j))/log(K1(j)))) - (Catch*B1P(i,j));
129         else
130             B1(i+1,j)=0;
131         end
132         if B2j > 0
133             B2(i+1,j)=B2(i,j) + ((r2(j) * B2(i,j))*(1-
134                 log(B2(i,j))/log(K2(j)))) - (Catch*B2P(i,j));
135         else
136             B2(i+1,j)=0;
137         end
138         if B3j > 0
139             B3(i+1,j)=B3(i,j) + ((r3(j) * B3(i,j))*(1-
140                 log(B3(i,j))/log(K3(j)))) - (Catch*B3P(i,j));
141         else
142             B3(i+1,j)=0;
143         end
144         %Loop to calculate new proportions
145         if (B1(i+1,j)+B2(i+1,j)+B3(i+1,j)) > 0
146             B1P(i+1,j) = B1(i+1,j)/(B1(i+1,j)+B2(i+1,j)+B3(i+1,j));
147             B2P(i+1,j) = B2(i+1,j)/(B1(i+1,j)+B2(i+1,j)+B3(i+1,j));
148             B3P(i+1,j) = B3(i+1,j)/(B1(i+1,j)+B2(i+1,j)+B3(i+1,j));
149         else
150             B1P(i+1,j) = 0;
151             B2P(i+1,j) = 0;
152             B3P(i+1,j) = 0;
153         end

```

```

154         end
155
156         %Pella-Tomlinson with m=2 or m=3
157     elseif m > 1
158         %Monte Carlo simulation for species 1
159         hat1 = mu1 + M1* randn(2,1);
160         r1(j) = hat1(2);
161         K1(j) = hat1(1);
162         K1t = K1(j);
163         if K1t ≤ 0
164             K1(j) = 0;
165         end
166         B1(1,j) = K1(j);
167         %Monte Carlo simulation for species 2
168         hat2 = mu2 + M2* randn(2,1);
169         r2(j) = hat2(2);
170         K2(j) = hat2(1);
171         K2t = K2(j);
172         if K2t ≤ 0
173             K2(j) = 0;
174         end
175         B2(1,j) = K2(j);
176         %Monte Carlo simulation for species 3
177         hat3 = mu3 + M3* randn(2,1);
178         r3(j) = hat3(2);
179         K3(j) = hat3(1);
180         K3t = K3(j);
181         if K3t ≤ 0
182             K3(j) = 0;
183         end
184         B3(1,j) = K3(j);
185         MSY1 = MSY1m2;
186         MSY2 = MSY2m2;
187         MSY3 = MSY3m2;
188
189         for i = 1:t-1
190             B1(i+1,j)=B1(i,j) + r1(j) * B1(i,j) - (r1(j)/K1(j))*
191             ((B1(i,j))^m) - (Catch*B1P(i,j)); B1j = B1(i+1,j);
192             B2(i+1,j)=B2(i,j) + r2(j) * B2(i,j) - (r2(j)/K2(j))*

```

```

193         ((B2(i,j))^m) - (Catch*B2P(i,j)); B2j = B2(i+1,j);
194         B3(i+1,j)=B3(i,j) + r3(j) * B3(i,j) - (r3(j)/K3(j))*
195         ((B3(i,j))^m) - (Catch*B3P(i,j)); B3j = B3(i+1,j);
196         if B1j > 0
197             B1(i+1,j)=B1(i,j) + r1(j) * B1(i,j) - (r1(j)/K1(j))*
198             ((B1(i,j))^m) - (Catch*B1P(i,j));
199         else
200             B1(i+1,j)=0;
201         end
202         if B2j > 0
203             B2(i+1,j)=B2(i,j) + r2(j) * B2(i,j) - (r2(j)/K2(j))*
204             ((B2(i,j))^m) - (Catch*B2P(i,j));
205         else
206             B2(i+1,j)=0;
207         end
208         if B3j > 0
209             B3(i+1,j)=B3(i,j) + r3(j) * B3(i,j) - (r3(j)/K3(j))*
210             ((B3(i,j))^m) - (Catch*B3P(i,j));
211         else
212             B3(i+1,j)=0;
213         end
214         %Loop to calculate new proportions
215         if (B1(i+1,j)+B2(i+1,j)+B3(i+1,j)) > 0
216             B1P(i+1,j) = B1(i+1,j)/(B1(i+1,j)+B2(i+1,j)+B3(i+1,j));
217             B2P(i+1,j) = B2(i+1,j)/(B1(i+1,j)+B2(i+1,j)+B3(i+1,j));
218             B3P(i+1,j) = B3(i+1,j)/(B1(i+1,j)+B2(i+1,j)+B3(i+1,j));
219         else
220             B1P(i+1,j) = 0;
221             B2P(i+1,j) = 0;
222             B3P(i+1,j) = 0;
223         end
224     end
225 end
226
227 %SPECIES 1 - ESO
228 % Divide each simulation into respective type
229 B1ta(j) = B1(50,j); B1t = B1ta(j);
230 XB1t(j) = abs(B1(46,j) - B1(45,j))+abs(B1(47,j) - B1(46,j))+
231 abs(B1(48,j) - B1(47,j))+abs(B1(49,j) - B1(48,j))+abs(B1(50,j) -

```

```

232     B1(49,j)); XB1 = XB1t(j);
233     Blgradt(j) = B1(49,j) - B1(50,j); Blgrad = Blgradt(j);
234     Blgradtminus1(j) = B1(48,j) - B1(49,j);
235     Blgradminus1 = Blgradtminus1(j);
236     Blgradtminus2(j) = B1(47,j) - B1(48,j);
237     Blgradminus2 = Blgradtminus2(j);
238     FinalProportion1(j) = B1t/K1(j); x1 = FinalProportion1(j);
239
240     %Type 1 - Oscillating
241     if ((XB1 > tol) & (Blgrad > 0) & (Blgradminus1 < 0))
242         B1Type1 = B1Type1 + 1;
243         B1(51,j) = 1;
244     elseif ((XB1 > tol) & (Blgrad < 0) & (Blgradminus1 > 0))
245         B1Type1 = B1Type1 + 1;
246         B1(51,j) = 1;
247     elseif ((XB1 > tol) & (B1t ≠ 0) & (Blgrad < 0) &
248         (Blgradminus2 > 0))
249         B1Type1 = B1Type1 + 1;
250         B1(51,j) = 1;
251     elseif ((XB1 > tol) & (B1t ≠ 0) & (Blgrad > 0) &
252         (Blgradminus2 < 0))
253         B1Type1 = B1Type1 + 1;
254         B1(51,j) = 1;
255
256     %Type 2 - Decreasing towards zero
257     elseif (B1t == 0)
258         B1Type2 = B1Type2 + 1;
259         B1(51,j) = 2;
260     elseif ((B1t ≠ 0) & (x1 ≤ 0.6))
261         B1Type2 = B1Type2 + 1;
262         B1(51,j) = 2;
263
264     %Type 3 - Stable converging
265     else B1Type3 = B1Type3 + 1;
266         B1(51,j) = 3;
267     end
268
269     %Risk Analysis
270     if (x1 < 0.2) & (XB1 ≤ tol)

```

```

271         Lessthan20percentB1 = Lessthan20percentB1 + 1;
272     end
273     if (x1 < 0.1) & (XB1 ≤ tol)
274         Lessthan10percentB1 = Lessthan10percentB1 + 1;
275     end
276     if (B1t ≥ 0.5*K1t)
277         Above501(j) = 1;
278         DifferenceMSY1(j) = B1t - 0.5*K1t;
279     elseif (B1t < 0.5*K1t)
280         Above501(j) = 0;
281         DifferenceMSY1(j) = B1t - 0.5*K1t;
282     end
283     if (B1t ≥ 0.368*K1t)
284         Above3681(j) = 1;
285         DifferenceMSY1Fox(j) = B1t - 0.368*K1t;
286     elseif (B1t < 0.368*K1t)
287         Above3681(j) = 0;
288         DifferenceMSY1Fox(j) = B1t - 0.368*K1t;
289     end
290
291
292     %SPECIES 2 – LSO
293     %Divide each simulation into respective type
294     B2ta(j) = B2(50,j); B2t = B2ta(j);
295     XB2t(j) = abs(B2(46,j) - B2(45,j))+abs(B2(47,j) - B2(46,j))+
296     abs(B2(48,j) - B2(47,j))+abs(B2(49,j) - B2(48,j))+abs(B2(50,j) -
297     B2(49,j)); XB2 = XB2t(j);
298     B2gradt(j) = B2(49,j) - B2(50,j); B2grad = B2gradt(j);
299     B2gradtminus1(j) = B2(48,j) - B2(49,j);
300     B2gradminus1 = B2gradtminus1(j);
301     B2gradtminus2(j) = B2(47,j) - B2(48,j);
302     B2gradminus2 = B2gradtminus2(j);
303     FinalProportion2(j) = B2t/K2(j); x2 = FinalProportion2(j);
304
305     %Type 1 – Oscillating
306     if ((XB2 > tol) & (B2grad > 0) & (B2gradminus1 < 0))
307         B2Type1 = B2Type1 + 1;
308         B2(51,j) = 1;
309     elseif ((XB2 > tol) & (B2grad < 0) & (B2gradminus1 > 0))

```

```

310         B2Type1 = B2Type1 + 1;
311         B2(51,j) = 1;
312     elseif ((XB2 > tol) & (B2t ≠ 0) & (B2grad < 0) &
313         (B2gradminus2 > 0))
314         B2Type1 = B2Type1 + 1;
315         B2(51,j) = 1;
316     elseif ((XB2 > tol) & (B2t ≠ 0) & (B2grad > 0) &
317         (B2gradminus2 < 0))
318         B2Type1 = B2Type1 + 1;
319         B2(51,j) = 1;
320
321     %Type 2 – Decreasing towards zero
322     elseif (B2t == 0)
323         B2Type2 = B2Type2 + 1;
324         B2(51,j) = 2;
325     elseif ((B2t ≠ 0) & (x2 ≤ 0.6))
326         B2Type2 = B2Type2 + 1;
327         B2(51,j) = 2;
328
329     %Type 3 – Stable converging
330     else B2Type3 = B2Type3 + 1;
331         B2(51,j) = 3;
332     end
333
334     %Risk Analysis
335     if (x2 < 0.2) & (XB2 ≤ tol)
336         Lessthan20percentB2 = Lessthan20percentB2 + 1;
337     end
338     if (x2 < 0.1) & (XB2 ≤ tol)
339         Lessthan10percentB2 = Lessthan10percentB2 + 1;
340     end
341     if (B2t ≥ 0.5*K2t)
342         Above502(j) = 1;
343         DifferenceMSY2(j) = B2t - 0.5*K2t;
344     elseif (B2t < 0.5*K2t)
345         Above502(j) = 0;
346         DifferenceMSY2(j) = B2t - 0.5*K2t;
347     end
348     if (B2t ≥ 0.368*K2t)

```



```

349         Above3682(j) = 1;
350         DifferenceMSY2Fox(j) = B2t - 0.368*K2t;
351     elseif (B2t < 0.368*K2t)
352         Above3682(j) = 0;
353         DifferenceMSY2Fox(j) = B2t - 0.368*K2t;
354     end
355
356     %SPECIES 3 - SFL
357     % Divide each simulation into respective type
358     B3ta(j) = B3(50,j); B3t = B3ta(j);
359     XB3t(j) = abs(B3(46,j) - B3(45,j))+abs(B3(47,j) - B3(46,j))+
360     abs(B3(48,j) - B3(47,j))+abs(B3(49,j) - B3(48,j))+abs(B3(50,j) -
361     B3(49,j)); XB3 = XB3t(j);
362     B3gradt(j) = B3(49,j) - B3(50,j); B3grad = B3gradt(j);
363     B3gradtminus1(j) = B3(48,j) - B3(49,j);
364     B3gradminus1 = B3gradtminus1(j);
365     B3gradtminus2(j) = B3(47,j) - B3(48,j);
366     B3gradminus2 = B3gradtminus2(j);
367     FinalProportion3(j) = B3t/K3(j); x3 = FinalProportion3(j);
368
369     %Type 1 - Oscillating
370     if ((XB3 > tol) & (B3grad > 0) & (B3gradminus1 < 0))
371         B3Type1 = B3Type1 + 1;
372         B3(51,j) = 1;
373     elseif ((XB3 > tol) & (B3grad < 0) & (B3gradminus1 > 0))
374         B3Type1 = B3Type1 + 1;
375         B3(51,j) = 1;
376     elseif ((XB3 > tol) & (B3t ≠ 0) & (B3grad < 0) &
377         (B3gradminus2 > 0))
378         B3Type1 = B3Type1 + 1;
379         B3(51,j) = 1;
380     elseif ((XB3 > tol) & (B3t ≠ 0) & (B3grad > 0) &
381         (B3gradminus2 < 0))
382         B3Type1 = B3Type1 + 1;
383         B3(51,j) = 1;
384
385     %Type 2 - Decreasing towards zero
386     elseif (B3t == 0)
387         B3Type2 = B3Type2 + 1;

```

```

388         B3(51,j) = 2;
389     elseif ((B3t ≠ 0) & (x3 ≤ 0.6))
390         B3Type2 = B3Type2 + 1;
391         B3(51,j) = 2;
392
393     %Type 3 – Stable converging
394     else B3Type3 = B3Type3 + 1;
395         B3(51,j) = 3;
396     end
397
398     %Risk Analysis
399     if (x3 < 0.2) & (XB3 ≤ tol)
400         Lessthan20percentB3 = Lessthan20percentB3 + 1;
401     end
402     if (x3 < 0.1) & (XB3 ≤ tol)
403         Lessthan10percentB3 = Lessthan10percentB3 + 1;
404     end
405     if (B3t ≥ 0.5*K3t)
406         Above503(j) = 1;
407         DifferenceMSY3(j) = B3t - 0.5*K3t;
408     elseif (B3t < 0.5*K3t)
409         Above503(j) = 0;
410         DifferenceMSY3(j) = B3t - 0.5*K3t;
411     end
412     if (B3t ≥ 0.368*K3t)
413         Above3683(j) = 1;
414         DifferenceMSY3Fox(j) = B3t - 0.368*K3t;
415     elseif (B3t < 0.368*K3t)
416         Above3683(j) = 0;
417         DifferenceMSY3Fox(j) = B3t - 0.368*K3t;
418     end
419 end
420 %%%%%%%%%%%%%%%%%%%%%%%%%%%%%%%%%%%%%%%%%%%%%%%%%%%%%%%%%%%%%%%%%%%%%%%%%
421 %Plot for species 1 (ESO)
422 figure
423 hold on
424 title('ESO');
425 xlabel('Year');
426 ylabel('Biomass (tonnes)');

```

```

427 for i = 1:1000
428     B151 = B1(51,i);
429     if B151 == 1
430         plot(B1(1:50,i), 'Color', 'red', 'MarkerSize', 8)
431     elseif B151 == 2
432         plot(B1(1:50,i), 'Color', 'blue', 'MarkerSize', 8)
433     elseif B151 == 3
434         plot(B1(1:50,i), 'Color', 'green', 'MarkerSize', 8)
435     end
436 end
437
438 %Plot for species 2 (LSO)
439 figure
440 hold on
441 title('LSO');
442 xlabel('Year');
443 ylabel('Biomass (tonnes)');
444 for i = 1:1000
445     B251 = B2(51,i);
446     if B251 == 1
447         plot(B2(1:50,i), 'Color', 'red', 'MarkerSize', 8)
448     elseif B251 == 2
449         plot(B2(1:50,i), 'Color', 'blue', 'MarkerSize', 8)
450     elseif B251 == 3
451         plot(B2(1:50,i), 'Color', 'green', 'MarkerSize', 8)
452     end
453 end
454
455 %Plot for species 3 (SFL)
456 figure
457 hold on
458 title('SFL');
459 xlabel('Year');
460 ylabel('Biomass (tonnes)');
461 for i = 1:1000
462     B351 = B3(51,i);
463     if B351 == 1
464         plot(B3(1:50,i), 'Color', 'red', 'MarkerSize', 8)
465     elseif B351 == 2

```

```

466         plot(B3(1:50,i), 'Color', 'blue', 'MarkerSize', 8)
467     elseif B351 == 3
468         plot(B3(1:50,i), 'Color', 'green', 'MarkerSize', 8)
469     end
470 end
471
472 %%%%%%%%%%%%%%%%%%%%%%%%%%%%%%%%%%%%%%%%%%%%%%%%%%%%%%%%%%%

```

Appendix B

R code for maximum likelihood estimation for ESO (similar for LSO, SFL, FLA-ALL)

```
1 #####
2 #                                                                 #
3 #   Fitting a Schaefer model to CPUE and Catch data for FLA 3 ESO #
4 #                                                                 #
5 #####
6
7 rm(list=ls(all=TRUE))
8 # function to replace a number (x, in this problem x=K) with a
9 #small number (in a smooth way so the
10 # gradient minimiser doesn't get stuck) – this prevents K from
11 #being negative
12
13 v<- 0.00001
14 z<- function(x,v){
15   ifelse(x>=v,x,v/((2-x)/v))}
16
17 # initial parameter estimates, in order K,r,q,sigma
18 y<-c(10000, 1, 0.001, 0.1)
19
20
21 # the catch and cpue indices
22 CPUE<-c(0.9,0.93,1.15,1.05,1.22,1.33,1.07,0.97,1.09,1.1,1.5,1.13)
23 catch<-c(381,462,697,751,650,673,796,518,359,431,567,592)
24
25
26 # function returning negative log likelihood for each set of
```

```

27 # parameters
28 fr<-function(y) {
29   K<-y[1]
30   r<-y[2]
31   q<-y[3]
32   sigma<-y[4]
33   Biomass<-rep(K,length(CPUE))
34   for(i in 1:(length(Biomass)-1)) {
35     Biomass[i+1]<- Biomass[i]+r*Biomass[i]*(1-(Biomass[i]/
36       z(K,v)))- catch[i]
37   }
38   LogLik<-(log(z(sigma,v))+0.5*(log(2*pi))+((log(z(q,v)*
39     z(Biomass,v))-log(CPUE))^2)/(2*(z(sigma,v))^2))
40   sumLL<-(sum(LogLik,na.rm=T))
41 }
42
43 # optimise function
44 result1<- optim(y,fr, method="SANN", control=list(maxit=100000,
45   parscale=c(y[1]/10,y[2]/10,y[3]/10,y[4]/10)))
46 result1
47
48 w<-c(result1$par[1], result1$par[2], result1$par[3],result1$par[4])
49 # function returning negative log likelihood for each set of
50 # parameters
51 fn<-function(w) {
52   K1<-w[1]
53   r1<-w[2]
54   q1<-w[3]
55   sigma1<-w[4]
56   Biomass1<-rep(K1,length(CPUE))
57   for(i in 1:(length(Biomass1)-1)) {
58     Biomass1[i+1]<- Biomass1[i]+r1*Biomass1[i]*(1-
59       (Biomass1[i]/z(K1,v)))-catch[i]
60   }
61   LogLik1<-(log(z(sigma1,v))+0.5*(log(2*pi))+((log(z(q1,v)*
62     z(Biomass1,v))-log(CPUE))^2)/(2*(z(sigma1,v))^2))
63   sumLL1<-(sum(LogLik1,na.rm=T))
64 }
65

```

```

66 # optimise function
67 FinalResult1<- optim(w,fn, control=list(maxit=100000,
68 parscale=c(w[1]/10,w[2]/10,w[3]/10,w[4]/10)), hessian = TRUE)
69 FinalResult1
70
71
72
73 # plot the CPUE and fit
74 plot(CPUE, main = "FLA 3 ESO", xlab = "", ylab = "CPUE index",
75 axes = FALSE)
76 axis(1, 1:12, 1991:2002)
77 axis(2)
78 box()
79 Biomass2<-rep(FinalResult1$par[1],length(CPUE))
80 for(i in 1:(length(Biomass2)-1)) {
81     Biomass2[i+1]<- Biomass2[i]+FinalResult1$par[2]*Biomass2[i]*
82     (1-(Biomass2[i]/FinalResult1$par[1]))-catch[i]
83 }
84 lines(FinalResult1$par[3]*Biomass2)
85
86 cov1<-solve(FinalResult1$hessian[1:2,1:2])
87 cov1
88 mul<-FinalResult1$par[1:2]
89 mul
90
91 #####

```

R code for likelihood profile for maximum likelihood estimation for ESO (similar for LSO, SFL)

```

1 #####
2 #                                                                 #
3 # Fitting a Schaefer model to CPUE and Catch data for FLA 3 ESO #
4 #                               - Likelihood Profile              #
5 #                                                                 #
6 #####
7
8 rm(list=ls(all=TRUE))
9 # function to replace a number (x, in this problem x=K) with a
10 #small number (in a smooth way so the gradient minimiser doesn't
11 #get stuck) - this prevents K from being negative
12
13 v<- 0.00001
14 z<- function(x,v){
15   ifelse(x>v,x,v/((2-x)/v))}
16
17
18 # initial parameter estimates, in order K,r,q,sigma
19 y<-c(50000, 1.000000e-05, 1.458858e-01)
20
21
22 # the catch and cpue indices
23 CPUE<-c(0.9,0.93,1.15,1.05,1.22,1.33,1.07,0.97,1.09,1.1,1.5,1.13)
24 catch<-c(466,517,730,774,681,706,830,537,374,458,602,634)
25
26 r<-2.6
27 # function returning negative log likelihood for each set of
28 # parameters
29 fr<-function(y) {
30   K<-y[1]
31   q<-y[2]
32   sigma<-y[3]
33   Biomass<-rep(K,length(CPUE))
34   for(i in 1:(length(Biomass)-1)) {
35     Biomass[i+1]<- Biomass[i]+r*Biomass[i]*(1-(Biomass[i]/

```



```

36             z(K,v))- catch[i]
37     }
38     LogLik<-(log(z(sigma,v))+0.5*(log(2*pi))+((log(z(q,v)*
39             z(Biomass,v))-log(CPUE))^2)/(2*(z(sigma,v))^2))
40     sumLL<-(sum(LogLik,na.rm=T))
41 }
42
43 # optimise function
44 result<- optim(y,fr, method="SANN", control=list(maxit=100000,
45 parscale=c(y[1]/10,y[2]/10,y[3]/10)))
46 result
47
48 w<-c(result$par[1], result$par[2], result$par[3])
49 r1<-r
50 # function returning negative log likelihood for each set of
51 # parameters
52 fn<-function(w) {
53     K1<-w[1]
54     q1<-w[2]
55     sigma1<-w[3]
56     Biomass1<-rep(K1,length(CPUE))
57     for(i in 1:(length(Biomass1)-1)) {
58         Biomass1[i+1]<- Biomass1[i]+r1*Biomass1[i]*(1-
59             (Biomass1[i]/z(K1,v)))-catch[i]
60     }
61     LogLik1<-(log(z(sigma1,v))+0.5*(log(2*pi))+((log(z(q1,v)*
62             z(Biomass1,v))-log(CPUE))^2)/(2*(z(sigma1,v))^2))
63     sumLL1<-(sum(LogLik1,na.rm=T))
64 }
65
66 # optimise function
67 FinalResult<- optim(w,fn, control=list(maxit=100000,
68 parscale=c(w[1]/10,w[2]/10,w[3]/10)))
69 FinalResult
70
71 #####

```

Appendix C

WinBUGS code used to calculate bayesian parameter estimates for ESO (similar code for LSO, SFL, FLA-ALL)

```
1 #ESO - Final
2 model
3
4 {
5   for( i in 1: Trials) {
6
7     mu[i] <- log(q*Biomass[i])
8     CPUE[i] ~ dlnorm(mu[i], tau)
9
10    muB[i+1]<-Biomass[i]+r*Biomass[i]*(1-(Biomass[i]/K))-catch[i]
11    Biomass[i+1] ~ dnorm(muB[i+1], tauB)
12  }
13
14  K ~ dunif(0,200000)
15  q ~ dgamma(1,1000)
16  r ~ dlnorm(0.73881,2.588915)
17  tau ~ dgamma(20,1)
18  tauB ~ dgamma(0.0001,0.01)
19  Biomass[1] <- K
20
21 list(Trials = 12, catch = c(381,462,697,751,650,673,796,518,359,
22    431,567,592),
23    CPUE =c(0.9,0.93,1.15,1.05,1.22,1.33,1.07,0.97,1.09,1.1,
24    1.5,1.13))
25
26 list(r = 1, K = 10000, q = 0.001, tau = 100, tauB = 0.00001)
```

Bibliography

- [1] Hilborn, R., Walters, C., *Quantitative Fisheries Stock Assessment : Choice, Dynamics and Uncertainty*. Chapman and Hall, New York, 1992.
- [2] Hilborn, R., Mangel, M., *The Ecological Detective*. Princeton University Press, New Jersey, 1997.
- [3] *Flatfish Plenary Report 2008*. Retrieved from [http](http://fpcs.fish.govt.nz/Science/Plenary.aspx) : [//fpcs.fish.govt.nz/Science/Plenary.aspx](http://fpcs.fish.govt.nz/Science/Plenary.aspx), 2009.
- [4] Beentjes, M. P., Review of flatfish catch data and species composition. *New Zealand Fisheries Assessment Report 2003/17*. Retrieved from [http](http://fpcs.fish.govt.nz/science/documents/) : [//fpcs.fish.govt.nz/science/documents/](http://fpcs.fish.govt.nz/science/documents/) on 14/3/2009.
- [5] Manikiam, J. S., A Guide to The Flatfishes (Order Heterosomata) of New Zealand. *Tuatara* 17. 1969.
- [6] Liewes, E. W., *Culture, feeding and diseases of commercial flatfish species*. CRC Press, Amsterdam, 1984.
- [7] Unknown author, *Flatfish (FLA 3)*. Retrieved from [http](http://www.fish.govt.nz/NR/rdonlyres/E8D545DD-B155-42AE-AB28-05EC73D87313/0/ipp0708fla3.pdf) : [//www.fish.govt.nz/NR/rdonlyres/E8D545DD-B155-42AE-AB28-05EC73D87313/0/ipp0708fla3.pdf](http://www.fish.govt.nz/NR/rdonlyres/E8D545DD-B155-42AE-AB28-05EC73D87313/0/ipp0708fla3.pdf) on 20/3/2009.
- [8] Kirk, P.D., *Flatfish New Zealand Fisheries Assessment Research Document 88/13*. 1988.
- [9] Haddon, M. *Modelling and Quantitative Methods in Fisheries*. Chapman and Hall CRC, New York, 2001.

- [10] Colman, J. A., Size at maturity of two species of flounders in the Hauraki Gulf, New Zealand. *New Zealand Journal of Marine and Freshwater Research* 6(3). 1972.
- [11] Colman, J.A., Spawning and fecundity of two flounder species in the Hauraki Gulf, New Zealand. *New Zealand Journal of Marine and Freshwater Research* 7(1,2). 1973.
- [12] Colman, J.A., Movements of flounders in the Hauraki Gulf, New Zealand. *New Zealand Journal of Marine and Freshwater Research* 8(1). 1974.
- [13] Hartill, B. Characterisation of the commercial flatfish, grey mullet, and rig fisheries in the Kaipara Harbour. *New Zealand Fisheries Assessment Report* 2004/1. 2004.
- [14] Ricker, W.E. Computation and interpretation of biological statistics of fish populations. *Bulletin of Fisheries Research Board of Canada* 191. 1975.
- [15] Froese, R., Pauly, D. (Ed). *FishBase World Wide Web electronic publication*. Retrieved from *www.fishbase.org*, 2009.
- [16] Fox, W.W. An exponential surplus-yield model for optimizing exploited fish populations. *Transactions of the American Fisheries Society* 99. 1970.
- [17] Schaefer, M. B. Some aspects of the dynamics of populations important to the management of the commercial marine fisheries. *Bulletin, Inter-American Tropical Tuna Commission* 2. 1954.
- [18] National Institute of Water and Atmospheric Research (NIWA). *Fish Identification - Sand Flounder*. Retrieved from *http : //www.fish.govt.nz/en - nz/Recreational/Most + Popular + Species/Fish + Identification/S + - + Z/Sand + Flounder.htm*, 2009.
- [19] National Institute of Water and Atmospheric Research (NIWA). *Fish Identification - Lemon Sole*. Retrieved from *http : //www.fish.govt.nz/en - nz/Recreational/Most + Popular + Species/Fish + Identification/L + - + R/Lemon + Sole.htm*, 2009.

- [20] Harley, S., Myers, R., Dunn, A. *Is catch per unit effort proportional to abundance*. NRC Research Press Web site, 2001.
- [21] Masters, J. *The use of surplus production models and length frequency data in stock assessments: explorations using greenland halibut observations*. Retrieved from [http : //www.unuftp.is/static/fellows/document/june07prf.pdf](http://www.unuftp.is/static/fellows/document/june07prf.pdf), 2007.
- [22] Legovic, T., Klanjcek, J., Gecek, S. *The maximum sustainable yield leads to extinction of species in most single and multispecies fisheries*. Nature Precedings. Retrieved from [http : //hdl.handle.net/10101/npre.2009.2910.1](http://hdl.handle.net/10101/npre.2009.2910.1), 2009.
- [23] Pitcher, T., Hart, P. *Fisheries Ecology*. Springer, 1983.
- [24] King, M. *Fisheries Biology, Assessment and Management*. Blackwell Publishing, 2007.
- [25] Quinn, T., Deriso, R. *Quantitative Fish Dynamics*. Oxford University Press US, 1999.
- [26] Cadima, E.L. Fish stock assessment manual. *FAO Fisheries Technical Paper No. 393*. Rome, 2003.
- [27] Coburn, R. P., Beentjes, M. P. *Abundance estimates for flatfish in FLA 1 from standardised catch per unit effort analysis of the set net fisheries, 1989-90 to 2003-04*. Retrieved from [http : //fs.fish.govt.nz/Doc/10663/200520FARs/0557_FAR.pdf.ashx](http://fs.fish.govt.nz/Doc/10663/200520FARs/0557_FAR.pdf.ashx) on 24/03/2009.
- [28] Howson, C., Urbach, P. *Scientific reasoning: the Bayesian approach*. Open Court, 1993.



Declaration Confirming Content of Digital Version of Thesis

I confirm that the content of the digital version of this thesis

Title: Risk Analysis of a Flatfish Stock Complex

is the final amended version following the examination process and is identical to this hard bound paper copy.

Student's Name: Kristin McLeod

Student's Signature:

A handwritten signature in black ink, appearing to read "K McLeod", written over a horizontal line.

Date: 10/06/2010